Characterization of human bitter taste receptor T2R1

by

Jasbir Deol Upadhyaya

A Thesis submitted to the Faculty of Graduate Studies of

The University of Manitoba

in partial fulfilment of the requirements of the degree of

MASTER OF SCIENCE

Department of Oral Biology

University of Manitoba

Winnipeg

© 2010

ABSTRACT

Humans are able to perceive five basic tastes which are sweet, umami, bitter, salty and sour. Bitter taste plays a crucial role as a warning sensor against the ingestion of toxic compounds. Bitter taste signaling, in humans, is mediated by a family of 25 G-protein coupled receptors, referred to as T2Rs. Humans prefer bitterness to some extent in certain foodstuffs and beverages, however excessive bitterness decreases their sensory quality. Fermented foods such as cheese, soy sauce, and miso contain numerous peptides derived from material proteins. Enzymatic hydrolysis during the aging process in fermented products frequently results in bitter taste, and bitter peptides formed during the fermentation process were shown to be responsible for the bitter taste of fermented food. The relationship between taste sensation and structures of peptides in fermented food have been widely investigated, however the molecular (sensory) targets of these bitter peptides remained elusive. Some of the peptides isolated from various fermented foods were identified to be inhibitors of the blood pressure regulatory protein, angiotensin-converting enzyme (ACE). A previous study showed that some of the bitter di-peptides isolated from casein hydrolysate can activate some T2Rs, with T2R1-expressing cells activated the most. However, in that study only two dipeptides were tested and the efficacy of the other food-protein derived bitter peptides towards T2Rs was not characterized. The major objective of the study presented here was to functionally characterize the human bitter taste receptor, T2R1, and to elucidate its activation with bitter tasting di- and tri-peptides. Using a heterologous expression system, T2R1 gene was transiently transfected in C6 glial cells and the gene expression was confirmed by reverse transcriptase-PCR analysis. The localization of T2R1 gene was predominantly in the cell membrane of glial cells and was confirmed by immunofluorescence microscopy.

Functional assays on T2R1 were carried out by measuring changes in intracellular calcium after stimulating the receptor with increasing concentrations of bitter di- and tri-peptides. The results showed that some of the peptides were very potent in activating T2R1 and causing changes in intracellular calcium levels. Furthermore, molecular modeling was done to elucidate the potential binding sites of these peptides on T2R1. Another objective of the study was to increase the expression of T2R1 using a codon-optimized gene and the HEK293S-TetR inducible mammalian expression system, so that biophysical studies like NMR spectroscopy could be pursued on T2R1. This expression system resulted in 7-8 fold increase in the protein level than what was observed following transient expression of T2R1. In summary, in this work we characterized *in vitro* a receptor present in the human oral cavity that is activated by some of the food protein derived bitter tasting di- and tripeptides. The results showed that some of the bitter peptides activate the human bitter receptor T2R1, at concentration ranges that humans also perceive as bitter. Among the peptides tested, the tripeptide FFF showed high efficacy with an EC_{50} in the micromolar range. Some of the peptides with ACE-inhibitory activity were also able to activate the T2R1 receptor. Results from the molecular modeling study of T2R1, identified a small number of amino acid residues in the receptor that might be important for ligand binding, and are potential targets for future structure-function studies on T2R1.

ACKNOWLEDGEMENTS

TABLE OF CONTENTS

1.   INTRODUCTION

2.   MATERIALS AND METHODS

4.   DISCUSSION

5.   REFERENCES

LIST OF TABLES

LIST OF FIGURES

.

LIST OF ABBREVIATIONS

A_{260}	Absorbance (λ260)
AA	Amino acid
APS	Ammonium persulfate
ATP	Adenosine triphosphate
Ca^{2+}	Calcium
CTP	Cytosine triphosphate
cDNA	Complementary DNA
DAG	Diacylglycerol
DM	Dodecyl-n-maltoside
DMSO	Dimethyl sulfoxide
DTT	Dithiothreitol
ECL	Extracellular loop
EDTA	Ethylenediaminetetraaceticacid
FBS	Fetal bovine serum
FFF	Phe-Phe-Phe
FL	Phe-Leu
G418	Geneticin
GAPDH	Glyceraldehyde 3-phosphate dehydrogenase
GF	Gly-Phe
GL	Gly-Leu
GDP	Guanosine 5'-diphosphate
GLL	Gly-Leu-Leu
GTP	Guanosine 5'-triphosphate
GPCR	G-protein coupled receptor
HEK	Human embryo kidney
ICL	Intracellular loop
IF	Ile-Phe
IP_3	Inositol 1,4,5 triphosphate
IQW	Ile-Gln-Trp
IRW	Ile-Arg-Trp
LKP	Leu-Lys-Pro
Na^{2+}	Sodium
ON	Overnight
PAGE	Polyacrylamide gel electrophoresis
PCR	Polymerase chain reaction
PMSF	Phenylmethylsulfonylfluoride
RT	Room temperature
SDS	Sodium dodecyl sulphate
TEMED	Tetramethylethylenediamine
TM	Transmembrane
TRC	Taste receptor cell
TTP	Thiamine triphosphate

CHAPTER ONE

Introduction

1.1. Background to the taste system

1.1.1. Introduction

Our sensory systems are responsible for generating an internal representation of the outside world, including its chemical (taste and olfaction) and physical (mechanical, sound, vision and temperature) features. The gustatory system of vertebrates consists of (i) peripheral multicellular chemoreceptors, termed taste buds, which are innervated by branches of the facial, glossopharyngeal and vagal nerves, and (ii) a series of central neural centres and pathways that mediate the sensory modality of taste. Taste or *gustation*, is a form of direct chemoreception which is involved in the choice of foods. The sense of taste is very important for the well-being and even survival of an individual, since it provides a checkpoint before the ingestion of potentially harmful substances. Along with taste sensation, food usually evokes other sensations like temperature, touch and odor. However, these nongustatory stimuli are sensed by the olfactory and somatosensory systems. In humans and many vertebrate animals, the sense of taste partners with the less direct sense of smell, resulting in the brain's perception of flavor. The concept of good taste for most people encompasses both flavor and texture of food. Taste, thus remains a powerful determinant of food selection.

1.1.2. Physiology of the Lingual Taste System

The human tongue has about 10,000 taste buds on its dorsal surface, which are distributed across different papillae. Each taste bud is oval in shape and contains 50-100 special sensory cells known as the taste receptor cells (TRCs) that mediate the sense of taste. Each TRC is again made up of dozens of individual taste receptors. Taste receptor cells project microvilli to the apical surface of the taste bud, where they form the *taste pore* (Figure 1A). The taste pore is the site of interaction with tastants; this interaction generates signals that are transmitted to the brain via branches of VII (facial), IX (glossopharyngeal) and X (vagus) cranial nerves. Taste buds are also present on the palate, back of the mouth, pharynx, epiglottis, and larynx. A substantial number of nonlingual taste papillae are also present in the soft palate, pharynx, larynx, epiglottis, uvula, and initial one-third of the esophagus.

Types of Papillae

The majority of taste buds are located on raised protrusions of the tongue surface called papillae (Figure 1B). There are four types of papillae present on the human tongue:-

1) **Fungiform papillae.** These are slightly mushroom-shaped and are present on the anterior two-thirds of the tongue, as well as at the sides. They usually contain 1-18 taste buds and are innervated by the chorda tympani branch of the facial (VII) nerve.

2) **Filiform papillae.** These are the most abundant and appear as short, V-shaped rough structures covered with thick keratinized epithelium. They do not contain taste buds and are not involved in gustation.

3) **Foliate papillae.** These lie on the lateral sides of the tongue and appear like ridges and grooves. They contain about a dozen to hundreds of taste buds and are innervated by the facial (anterior papillae) and the glossopharyngeal (posterior papillae) nerves.

4) **Circumvallate papillae.** These papillae are located on the posterior aspect of the dorsal surface of tongue, appearing as pin cushions with a surrounding trough, called a crypt. The crypt is lined by an epithelium, called the gustatory epithelium, which contains hundreds to thousands of taste buds. There are 12-15 circumvallate papillae in humans which are innervated by the glossopharyngeal (IX) nerve.

1.1.3. Anatomy of Taste Receptor Cells

The TRCs are specialized epithelial cells which are assembled into taste buds and contain the taste receptors. TRCs turn over at a fairly rapid rate in mammals with a life span of 10 days (Beidler et al, 1965). Based on morphological differences in cytoplasmic translucency, structure, and synaptic connectivity, these cells have been categorized into four types (Figure 2):-

(i) Dark Cells or Type I cells

Dark cells, so called because of their affinity for accumulating basophilic dyes, are defined by a dark cytoplasm, dense-core granules at the tip of the cell, indentations in the nuclear membrane, patches of heterochromatin (DNA) along the inner edge of the
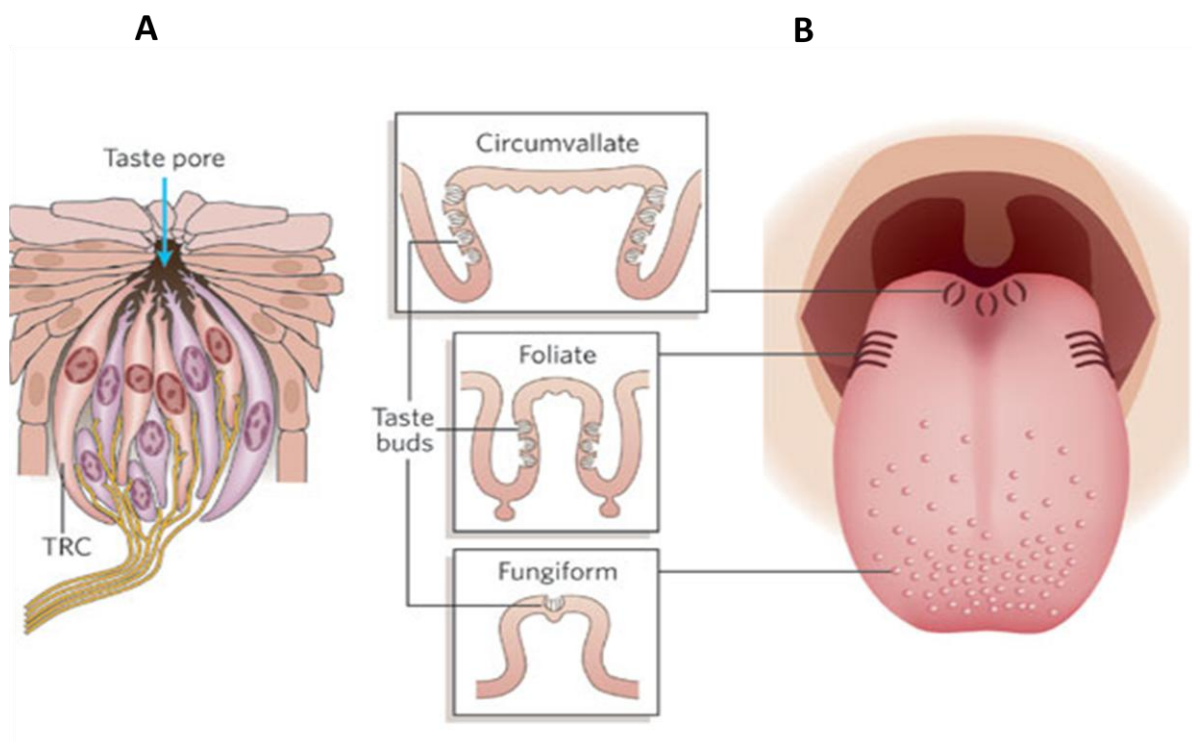
FIGURE 1. Taste-receptor cells, taste buds and papillae A. Taste bud showing the taste receptor cells and taste pore. Human taste buds are composed of 50-150 taste receptor cells (TRC), distributed across different papillae. TRCs project microvillae to the apical surface of the taste bud, where they form the taste pore, which is the site of interaction with tastants. **B.** The human tongue showing the localization and structure of different papillae. Circumvallate papillae are found at the very back of the tongue, foliate papillae are present at the posterior lateral edges of the tongue, whereas fungiform papillae are found in the anterior two-thirds of the tongue.
Used with permission from Nature Publishing Group: [Nature 444 (7117), 288-294] Chandrashekhar, J., Hoon, M.A., Ryba, N.J.P., and Zuker, C.S. The receptors and cells for mammalian taste, 2006.

nucleus, and apical structures ending into tall microvilli. These cells extend lamellate

processes around other types of taste cells and express GLAST, a glial glutamate

transporter (Lawton et al, 2000). These features suggest a glial function for Type I cells,

e.g. transmitter clearance and functional isolation of other taste cell types.

(ii) Light Cells or Type II cells

Light cells, so called because of their aversion for basophilic dyes, are

characterized by a light cytoplasm, clear vesicles and mitochondria at the tip of the cell, a

large round to oval nucleus with less heterochromatin (DNA) along the inner edge, and

their apical surface terminates into short microvilli. Type II cells express all of the

elements of taste transduction for sweet, umami and bitter tastes (Hoon et al, 1999), the

downstream transduction components, $PLC\beta_2$ and IP_3R3 (Clapp et al, 2001; Miyoshi et

al, 2001), and gustducin (Yang et al, 2000a). Type II cells are thus the transducing cells

for these taste modalities.

(iii) Intermediate or Type III cells

Type III cells are characterized by morphologically identifiable synaptic contacts

with the gustatory nerve fibres and expression of the synaptic membrane protein (Yang et

al, 2000b) SNAP25 as well as the neural cell adhesion molecule (NCAM) (Nelson and

Finger, 1993). The presence of a prominent synaptic contact, implicates these cells in

transmission of information to the nervous system. Type III cells have also been termed

as the presynaptic cells.
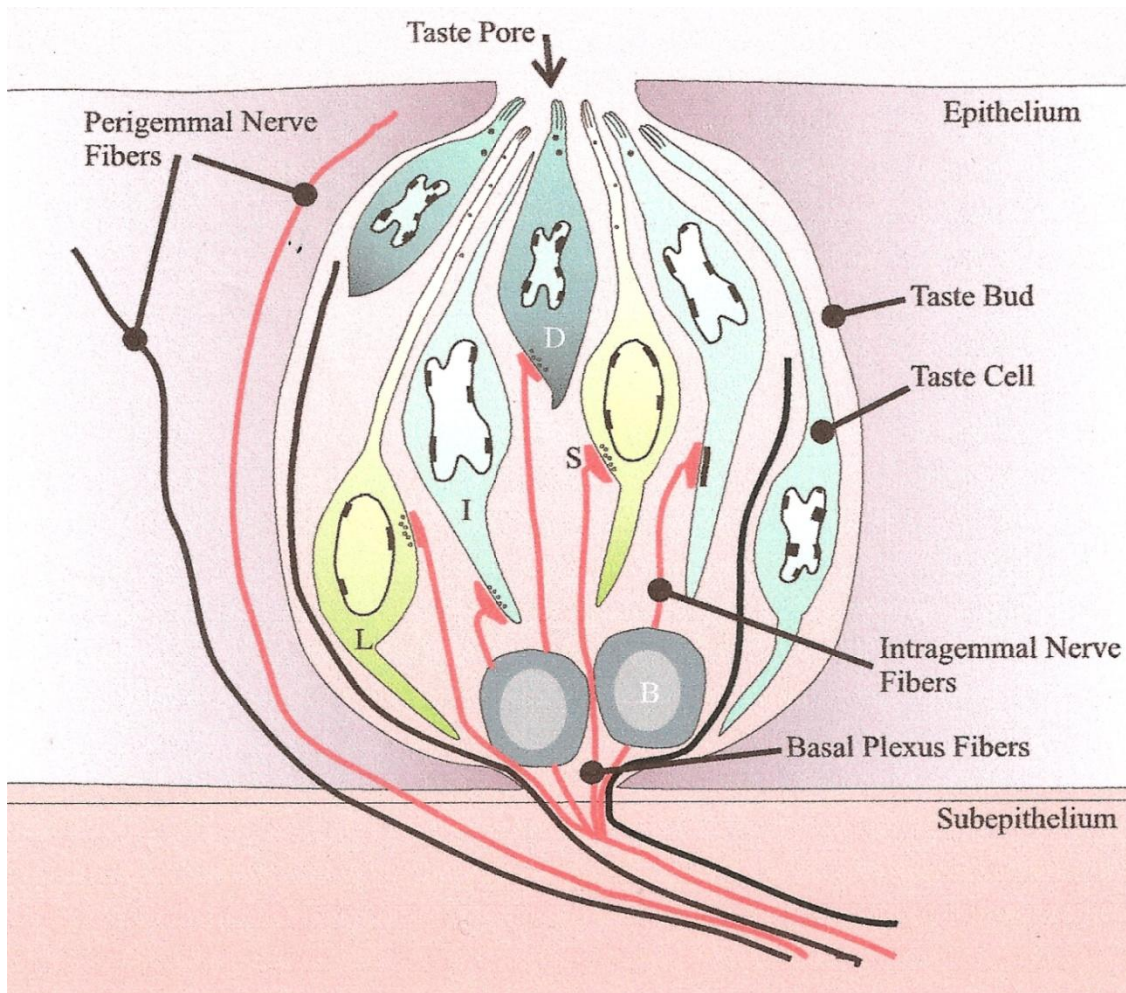
FIGURE 2. Morphology of a taste bud. The taste bud contains basal cells (B) in the lower portion of the bud, and the light cells (L), intermediate cells (I), and dark cells (D) are shown with some of the features that characterize each cell type. The latter three types of taste cells extend upward to the opening in the oral cavity, the taste pore. In addition, the intragemmal and perigemmal nerve fibers seen are present in the subepithelial connective tissue and enter each bud from the base. The red fibers represent the nerve fibers which contain synaptic vesicle proteins, and the black fibers represent nerve fibers which contain peptides. S, synapse.

(iv) Basal or Type IV cells

Basal cells are small disc-like cells which lie directly on the basement membrane of the epithelium and constitute a proliferative population of cells. They frequently come in close contact with afferent fibres.

1.1.4 Taste Modalities

For a long period, it has been commonly accepted that there are a finite number of "basic tastes" by which all foods can be grouped. Until the 1980s, this was considered to be a group of four basic tastes, i.e., sweet, bitter, sour and salty. In the late 1980s, a fifth taste, umami (the taste of monosodium glutamate) has been added to the list of basic tastes (Iwasaki et al, 1985; Kawamura et al, 1987; Kinnamon et al, 1992). Recently, it was shown that humans have an orosensory system responsible for the detection of dietary fats (Mattes et al, 2001a, 2001b; Smith et al, 2000). A plasma membrane glycoprotein, CD36, has been postulated to be a candidate fat taste receptor on the tongue (Laugerette et al, 2005). In addition to these well known taste modalities, the taste system appears to be responsive to CO_2, i.e. the taste of carbonation (Kawamura et al, 1967; Komai et al, 1994). In mammals, carbonation elicits both somatosensory and chemosensory responses, including activation of taste neurons. Studies show that the sour-sensing cells act as the taste sensors for carbonation and carbonic anhydrase 4 enzyme functions as the principal CO_2 taste sensor (Chandrashekhar et al, 2009). The five basic taste modalities sensed by humans are:-

(i) Bitter

The bitter taste is usually perceived as unpleasant or aversive, and is elicited by compounds with diverse chemical structures. Many plant alkaloids, toxins and venom are extremely bitter and can be harmful if ingested. Common bitter foods and beverages include coffee, unsweetened chocolate, bitter melon, beer, bitter olives and many plants in the *Brassicaceae* family. Bitter taste allows us to sense natural toxins.

(ii) Sweet

Sweetness is produced by the presence of sugars and is associated primarily with energy rich nutrients (carbohydrates). It is stimulated by chemicals with a number of hydrophilic molecular structures. Sucrose (table sugar) is the prototypical example of a sweet substance. Some of the amino acids like alanine, glycine and serine are sweet. A number of plant species produce glycosides that are many times sweeter than sugar.

(iii) Umami

Umami is the taste sensation produced by compounds such as glutamate, and are commonly found in fermented and aged food. Umami is a Japanese word meaning "savory", a deliciousness factor derived specifically from detection of the natural amino acid, glutamic acid, or glutamates common in meats, cheese, broth, stock and other protein-heavy foods.

(iv) Salt

Saltiness is a taste produced by the presence of sodium ions and indicates the electrolyte balance. Some potassium and ammonium salts also taste salty.

(v) Sour

The sour taste is a basic taste quality that detects the presence of acids. Acid taste may be a primarily aversive modality to monitor food spoilage and fruit ripeness, and prevent tissue damage (Lindemann B, 2001). Though sourness evokes an innate rejection response in humans and many other animals at high concentrations, weak acids however are often perceived as pleasant. Sour taste may thus play an appetitive role by signaling food safety, since many harmful bacteria cannot exist at the acidic pH associated with sour compounds (Gilbertson et al, 1992).

1.1.5. Taste Receptors

Taste receptors function as chemoreceptors that interact with taste stimuli, or ligands, to initiate an afferent signal transmitted to the brain, which results in taste perception. Electrophysiological studies suggest that sour and salty tastants depolarize TRCs by directly interacting with ion channels (Heck et al, 1984; Kinnamon et al, 1988). In contrast, sweet, umami, and bitter taste transduction is believed to be mediated by G protein-coupled receptor (GPCR) signaling pathways (Striem et al, 1989; Wong et al, 1996; Chaudhari et al, 2000).

The two best-characterized families of taste receptors, sweet-umami (T1Rs) and bitter (T2Rs) receptors, belong to the GPCR superfamily which represents one of the largest and the most diverse group of membrane proteins in the human genome (Lander et al, 2001; Venter et al, 2001; Takeda et al, 2002). GPCRs have seven transmembrane (TM) helices (H1–H7), three extracellular loops (ECLs) and three intracellular (ICLs) loops.
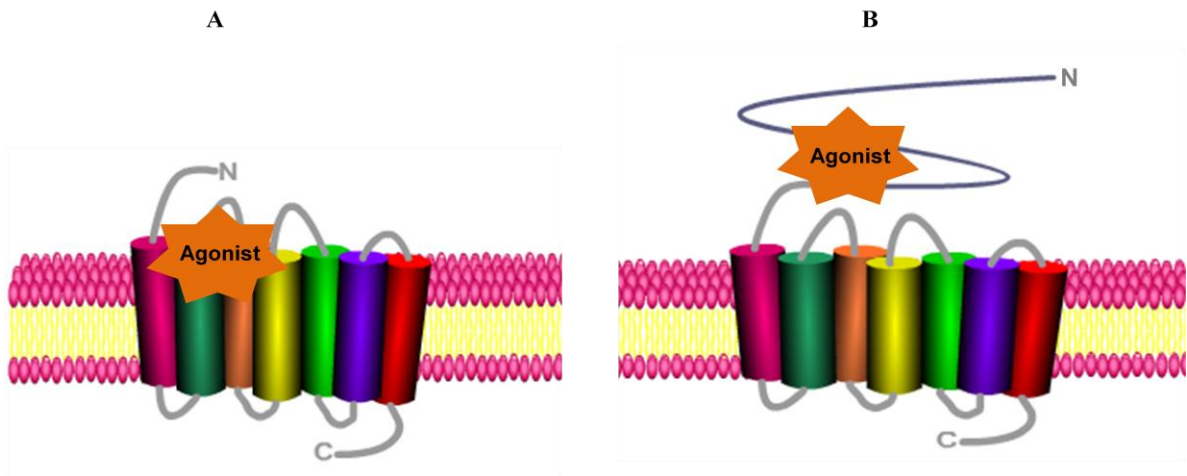
FIGURE 3. Human taste receptors. **A.** Bitter taste receptor (T2R) consists of around 300-330 amino acids, has a short extracellular N-terminus consisting of 7-19 amino acids, an intracellular C-terminus around 7-32 amino acids long, with the extracellular loops and TM regions being the likely sites of agonist binding. T2Rs are localized in clusters on human chromosomes 5, 7 and 12 **B.** Sweet/Umami taste receptor (T1R) consists of around 850 amino acids, has a long extracellular N-terminus which is believed to mediate ligand binding, and a short intracellular C-terminus.

GPCRs mediate a broad variety of physiological processes, like neurotransmission, cell metabolism, cell proliferation, and differentiation as well as sensory perception. Approximately 2% of the human genome is encoded by GPCR genes (Takeda et al, 2002; Lander et al, 2001). The ligand binding to the GPCRs on the extracellular side induces a conformational change in the receptor, leading to the activation of bound heterotrimeric G-proteins on the intracellular side. These activated heterotrimeric G-proteins trigger an intracellular signaling cascade.

Sweet and Umami taste receptors

Sweet and umami tastes are mediated by receptors referred to as T1Rs (Figure 3B). The T1R class of taste-specific receptors consists of three members, T1R1, T1R2 and T1R3, which belong to class C of the GPCR superfamily, and are characterized by a long extracellular N-terminus that is believed to mediate ligand recognition and binding (Kunishima et al, 2000).

1.1.5.1. Genomic organization

The T1R proteins consist of ~850 amino acids and they assemble into dimeric receptor complexes to form the functional receptor. T1R1 and T1R3 combine together to form a umami receptor, whereas T1R2 and T1R3 dimer functions as a sweet receptor. In humans, the three T1R genes are clustered on chromosome 1, whereas in mouse they are located on chromosome 4. Unlike the T2R genes which are intronless, the T1R genes contain six coding exons (Bachmanov et al, 2007).

1.1.5.2. Expression in lingual tissues

The main sites of expression of the T1R genes are TRCs of the taste buds. In humans, the T1R3 gene is expressed in all types of taste buds (Kitagawa et al, 2001; Montmayeur et al, 2001; Nelson et al, 2001). The T1R1 gene is predominantly expressed in the fungiform and palate taste buds, in a smaller percentage of the foliate taste buds, and is rarely expressed in the circumvallate taste buds. The T1R2 gene is expressed predominantly in the circumvallate and foliate taste buds, in a smaller percentage of palate taste buds, and rarely expressed in the fungiform taste buds (Hoon et al, 1999; Nelson et al, 2001). T1R1 and T1R2 are rarely co-expressed in the same TRC. The T1R genes are not co-expressed with the T2R genes (Nelson et al, 2001).

1.1.6.1. Taste localization on the tongue

In the 1970s, it was originally proposed that there is a "tongue map" and each of the taste modalities is localized to a discrete region on the surface of the tongue (Figure 4, Trefz B., 1972). According to the tongue map hypothesis, sweet taste is localized to the fungiform papillae of the tip of the dorsum; salt, to the fungiform papillae of the lateral aspects of the anterior two thirds of the dorsum; bitter, to the circumvallate papillae of the posterior third of the dorsum; and sour, to the foliate papillae of the lateral aspects of the posterior third of the dorsum. Recent studies show that contrary to popular belief, there is no tongue 'map' responsiveness to the five basic taste modalities - bitter, sour, sweet, salty and umami, as these tastes are sensed by all areas of the tongue (Hoon et al, 1999; Nelson et al, 2001, 2002; Adler et al, 2000; Huang et al, 2006).
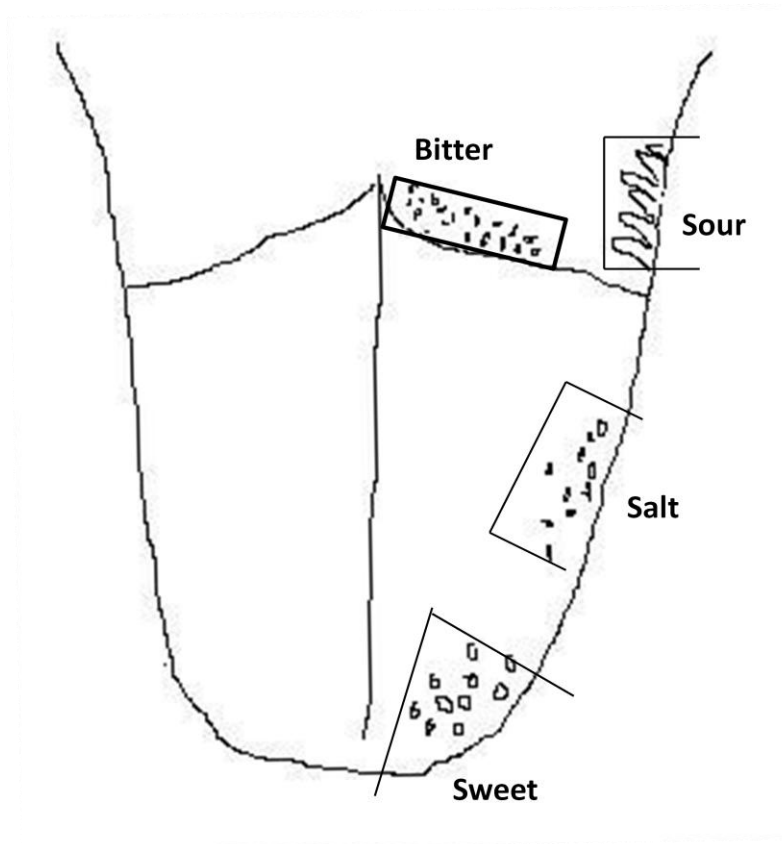
FIGURE 4. Classical taste modality localization on the human tongue. Each of the taste modalities (sweet, sour, bitter and salt) were considered to be localized to a discrete region on the surface of the tongue: sweet, to the fungiform papillae of the tip of the dorsum; salt, to the fungiform papillae of the lateral aspects of the anterior two thirds of the dorsum; bitter, to the circumvallate papillae of the posterior third of the dorsum; and sour, to the foliate papillae of the lateral aspects of the posterior third of the dorsum.
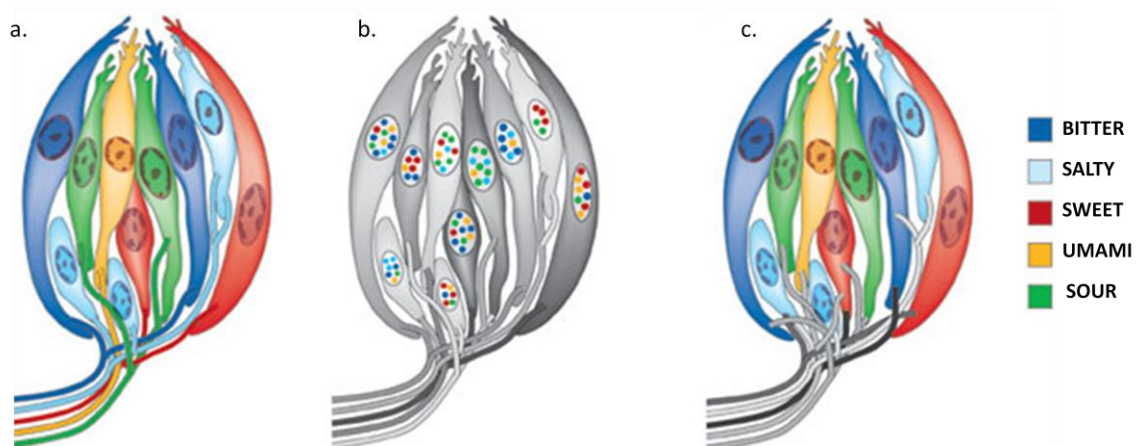
FIGURE 5. Encoding of taste qualities at the periphery (a) Labelled-line model, which states that receptor cells are tuned to respond to single taste modality – sweet, bitter, sour, salty or umami – and are innervated by individually tuned nerve fibres. **(b,c)** Two contrasting models of across-fibre pattern. Either individual TRCs are tuned to multiple taste modalities and the same afferent fibre carries information for more than one taste modality (b), or TRCs are tuned to single modality but same afferent fibre carries information for more than one taste modality (c)
Used with permission from Nature Publishing Group: [Nature 444 (7117), 288-294] Chandrashekhar, J., Hoon, M.A., Ryba, N.J.P., and Zuker, C.S. The receptors and cells for mammalian taste, 2006.

1.1.6.2. Taste Coding at the Periphery

The discovery of taste receptors led to the introduction of two new models to explain how taste is coded in the periphery. According to the '*labelled-line*' theory, TRCs are tuned to respond to single taste modalities — sweet, bitter, sour, salty or umami — and are innervated by individually tuned nerve fibres (Figure 5). In this case, each taste quality is specified by the activity of non-overlapping cells and fibres.

The '*across-fibre pattern*' states that either individual TRCs are tuned to multiple taste qualities, and consequently the same afferent fibre carries information for more than one taste modality, or that TRCs are still tuned to single taste qualities but the same afferent fibre carries information for more than one taste modality. Recent molecular and functional studies in mice have demonstrated that different TRCs define the different taste modalities, and that activation of a single type of TRC is sufficient to encode taste quality, strongly supporting the labelled-line model.

1.2. Bitter taste

Unlike sweet and umami stimuli, which indicate calorie-rich food and elicit positive behaviours, bitter substances generally cause aversive reactions. Bitter compounds are ubiquitous in plants, animals, and fungi and can also be formed during food processing (Frank and Hofmann, 2002). Organisms frequently produce bitter compounds as part of their chemical defense mechanisms, and hence many of them are toxic (Biere et al, 2004). Bitter taste is considered of importance as it is believed to have evolved as a defence mechanism against the ingestion of toxic substances, a crucial response for survival.

In humans, bitter taste is perceived by a family of 25 GPCRs, referred to as T2Rs. Based on sequence conservation, the GPCR family is subdivided into several subfamilies. T2Rs, according to the A through F classification system, are described either as a separate putative family (GPCRDB, 2007) or as distantly related to class A (rhodopsin-like) GPCRs (Adler et al, 2000). In the more recently developed GRAFTS (glutamate-rhodopsin-adhesion-frizzled/taste2-secretin) classification system, which is based on phylogenetic analysis of transmembrane regions of human GPCRs (Fredriksson et al, 2003), T2Rs form a distinct cluster within the frizzled/taste2 family.

1.2.1. Bitter Taste Receptors

1.2.1.1. Discovery

The T2R genes in humans and rodents were discovered in 2000 by two different groups, Charles S. Zuker and Nicholas J.P. Ryba; and Linda B. Buck (Adler et al, 2000; Matsunami et al, 2000). Adler et al examined a region of human chromosome 5 linked to perception of a bitter compound 6-n-propyl-2-thiouracil (PROP) and discovered a novel GPCR, *T2R1*. Homology search of human genomic DNA revealed additional related genes on human chromosomes 7 and 12. Matsunami et al examined a region of human chromosome 12 with conserved synteny to a region of mouse chromosome 6 containing the sucrose octaacetate aversion (*Soa*) locus and discovered the T2R genes.

1.2.1.2. Genomic Organization

T2R genes are organized in the genome in clusters (Adler et al, 2000; Matsunami et al, 2000) and are genetically linked to loci that influence bitter perception in

mice and humans. T2R1 gene is mapped to chromosome 5p15, the location of a genetic locus that controls the detection of the bitter compound, PROP. All other T2R sequences are organized in clusters on chromosomes 7 and 12 (Conte et el, 2002). In the mouse, with the exception of T2R34 and T2R19, located on chromosomes 2 and 15 respectively, all T2R genes are located on chromosome 6.

One of the most conspicuous features of the genomic organization of T2R genes is the absence of introns. The T2R genes encode 300-330 amino acids and contain seven transmembrane domains, short N-terminal extracellular and C-terminal intracellular domains (Figure 3A). Despite substantial sequence diversity, these receptors contain conserved sequence motifs in the first (FIxxVN), second (LxxSR), third (LxxFY) and seventh (HxxILI) transmembrane domains, and in the second intracellular loop (KIA, FxxLK) (Kim et al, 2004; Maehashi et al, 2009).

1.2.1.3. Expression in lingual tissues

T2R genes in mammals are selectively expressed in subsets of TRCs of the circumvallate, foliate, fungiform, palate, and epiglottis taste buds (Adler et al, 2000; Behrens et al, 2004; Bufe et al, 2002). A single TRC expresses a large repertoire of T2Rs (Adler et al, 2000), suggesting that each taste cell may be capable of recognizing multiple bitter tastants. This implies that individual T2R-expressing cells may function as broadly tuned sensors for all bitter chemicals but might have very limited, if any, discrimination for them. The T2R genes have been shown to be invariably expressed in TRCs that contain α-gustducin, (Adler et al, 2000; Matsunami et al, 2000) a G-protein subunit implicated in the transduction of bitter taste (Wong et al, 1996).

1.2.1.4. Expression in non-lingual tissues

Some non-gustatory tissues also express T2R genes, indicating that these receptors have additional roles apart from taste sensation. Chemosensory cells expressing T2R genes, together with α-gustducin, were identified within the respiratory epithelium of the nasal cavity (Finger et al, 2003). Another site of T2R gene expression is the gastrointestinal tract. T2R genes were detected in the stomach and duodenum of mice and rats. Moreover, the enteroendocrine cell line STC-1 shows rapid transient increases in intracellular calcium levels after stimulation with different bitter compounds, indicating that these cells might represent true sensors for bitter compounds (Wu et al, 2002). Recently, T2R receptors were found to be expressed in the motile cilia of the airway epithelial cells (Shah et al, 2009). The T2Rs in cilia might be playing a role in sensing noxious substances entering airways, and the cilia helping in initiating a defensive mechanical mechanism to eliminate the offending compounds.

1.2.1.5. Ligands

The number of compounds perceived by humans as bitter is much larger than the number of human T2R genes, implying that each human T2R responds to more than one bitter ligand (Behrens et al, 2006). Bitter compounds are not only numerous but also structurally diverse, ranging from hydroxyl fatty acids, peptides, amino acids, amines, ureas, thioureas, carbamides, esters, carbonyl compounds, phenols, terpenoids, alkaloids, glycosides to flavonoids and steroids (Belitz and Wieser 1985). Although T2R1 gene is a candidate for the PROP sensitivity locus, which suggests that this should be a bitter taste receptor for PROP, it does not hold true. Recent studies show that T2R1 receptor

responds to many structurally diverse bitter compounds and a few synthetic dipeptides (Meyerhof et al, 2010, Maehashi et al, 2008). Table I represents some of the recently characterized agonists that activate T2R1.

TABLE I. Agonists of T2R1 receptor

Receptor	Bitter ligands
T2R1	Peptides (GF, GL)
	Amarogentin
	Arborescin
	Cascarillin
	Chloramphenicol
	Dextromethorphan
	Diphenidol
	Isohumulone
	Parthenolide
	Picrotoxinin
	Sodium cyclamate
	Sodium thiocyanate
	Thiamine
	Yohimbine

1.2.2. Bitter taste signal transduction

The molecular events in the perception of bitter taste start with the binding of specific water-soluble tastants or ligands to the TM domains of bitter receptors initiating a neural signaling via activation of the intracellular Gα subunit, gustducin (Adler et al, 2000; Chandrashekhar et al, 2000). Bitter signal transduction pathway involves the IP_3-

mediated release of intracellular Ca^{2+} (Figure 6). The extracellular loops and transmembrane domains that vary considerably from receptor to receptor within the family of bitter receptors are the likely regions for agonist binding sites (Brockhoff et al, 2006).

In the trimeric state, the G-protein is inactive with GDP bound to its α-subunit (Figure 6, *step 1*). The interaction of a taste molecule with bitter taste receptor is presumed to induce a conformational change in the receptor, enabling it to activate heterotrimeric GTP-binding proteins (G proteins). When stimulated by an activated receptor, the G-α subunit exchanges its bound GDP for GTP (*step 2*). This exchange causes the dissociation of the α and βγ subunits. Thus, in the active state, G-protein consists of G-α bound to GTP, dissociated from the G-βγ dimer. The G-protein involved in bitter taste perception is gustducin, which is comprised of α-gustducin, Gβ3 and Gγ13 (Adler et al, 2000; Wong et al, 1996). The G-αq activates the plasma membrane bound enzyme, PLC-β2 (*step 3*). This hydrolyzes inositol phospholipid, PIP_2, to produce two intracellular messengers; IP_3 and diacylglycerol, DAG (*step 4*). IP_3 activates the type-III IP_3 receptors which open the Ca^{2+} release channels from intracellular stores (*step 5,6*). Rapid increase in $[Ca^{2+}]_i$ opens TRPM5 channels, leading to the Na^+ influx and membrane depolarization (*step 7*), and thus neurotransmitter release (*step 8*). To date, serotonin (5HT) has been one of the best studied transmitters of taste buds and has been identified with high-performance liquid chromatography (HPLC) in mammalian taste tissues (Zancanaro et al, 1995).

Histochemical and immunocytochemical techniques have demonstrated that 5HT is present in a subset of Type III taste cells in circumvallate and foliate papillae of

mouse, rat, rabbit and monkey (Yee et al, 2001; Kim et al, 1995). Studies show that ATP

is also a likely transmitter released by taste buds in response to gustatory stimulation

(Finger et al, 2005b). The sensory afferent fibres innervating the receptor cells transmit

the taste signal to the neurons in the solitary tract nuclei of the medulla. From the solitary

tract nuclei, taste information is transferred to the neurons in the pontine parabrachial

nuclei, then to the thalamus, and then to the gustatory cortex of the brain. The second

intracellular messenger, DAG, on the other hand activates a serine/threonine protein

kinase called protein kinase C (PKC) which phosphorylates other target proteins.
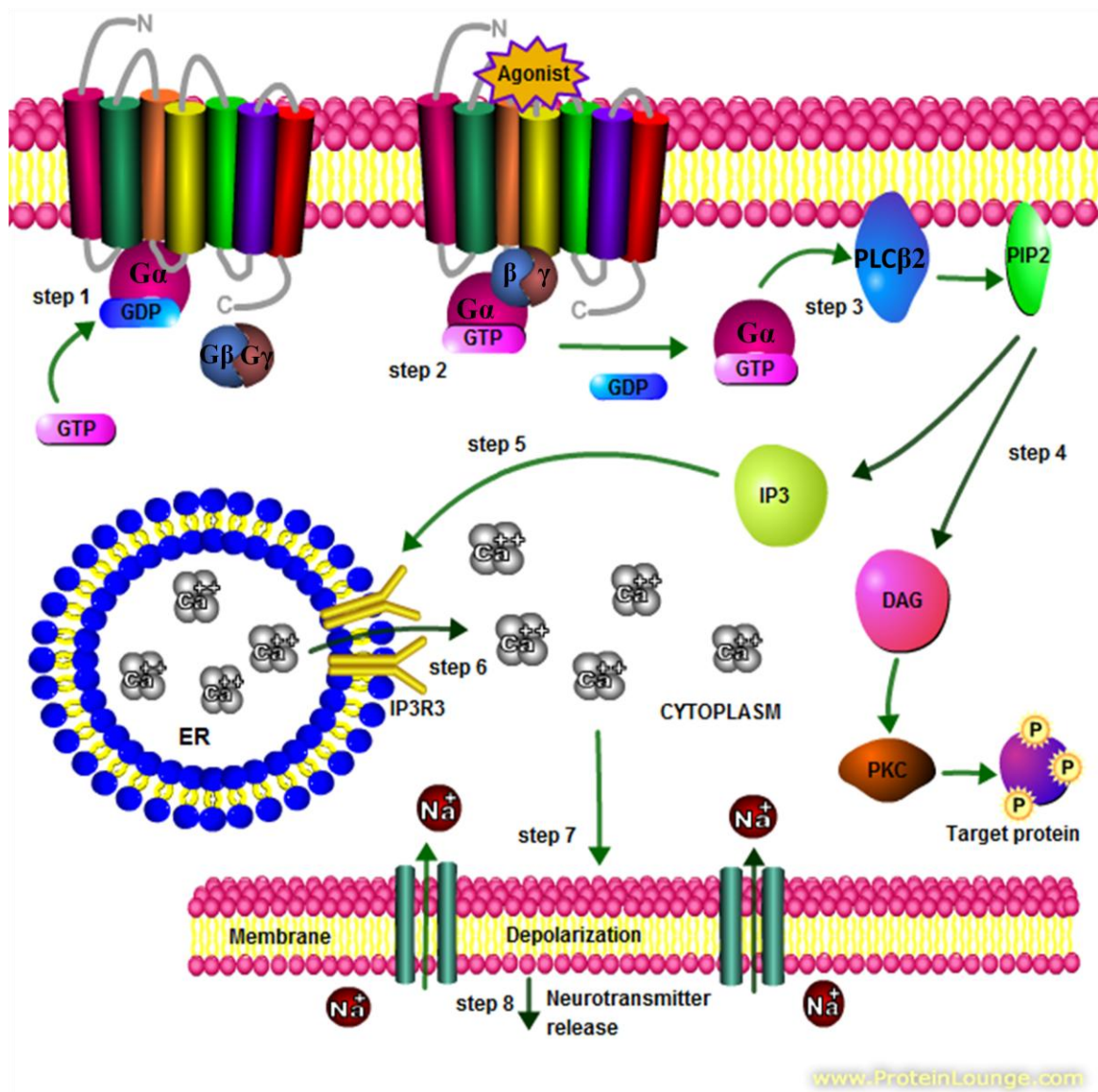
FIGURE 6. Bitter taste signaling pathway (IP$_3$ pathway) Abbreviations: PLCβ2, phospholipase C β2; PIP$_2$, phospatidyl-inositol-biphosphate; DAG, diacylglycerol; IP$_3$, inositol triphosphate; PKC, protein kinase C; ER, endoplasmic reticulum; Ca^{2+}, calcium; Na$^+$, sodium; P, phosphorus. Reactions are explained in text as referred to by step numbers in brackets.

1.3 <u>HYPOTHESIS</u>

This study has two hypothesis:-

1) T2Rs, like most GPCRs, are poorly expressed at the surface of heterologous cells. To successfully target these receptors to the cell surface for proper functional responses, the first 20-38 amino acids of rhodopsin are placed in frame to the N-termini of T2Rs. We hypothesized that alternative methods of improving GPCR expression, like optimization of the most frequently used codons, will also be able to increase the expression of T2R1. Thus, a codon-optimized synthetic T2R1-rho1D4 gene construct which has a bovine rhodopsin epitope tag at the C-terminus to facilitate its detection was used in the study.

2) A wide variety of bitter peptides isolated from dietary-proteins are found in various foods and fermented products. Many of these food-derived peptides possess various health related physiological activities. A recent study showed that human bitter taste receptor T2R1 is activated by bitter dipeptides Gly-Phe (GF) and Gly-Leu (GL). Our hypothesis was that other potent bitter di- as well as tri-peptides should also be able to activate T2R1 receptor.

CHAPTER TWO

Materials and Methods

2.1. Materials

Synthetic oligonucleotides and geneticin were purchased from Invitrogen (Burlington, ON, Canada). The detergent n-dodecyl-β-D-maltoside (DM) was purchased from Anatrace (Maumee, OH, USA). The mouse monoclonal anti-rhodopsin antibody, rho-1D4, was prepared by the Cell Culture Center (Minneapolis, MN, USA) from a cell line provided by R.S. Molday (University of British Columbia, Vancouver, Canada), rabbit polyclonal anti-Cadherin antibody (Cat#ab6529) was from Abcam Inc. (Cambridge, MA, USA), goat polyclonal rho S-17 primary antibody (Cat#sc14355) and donkey anti-goat HRP (Cat#sc2020) secondary antibody were from Santa Cruz Biotechnology (Santa Cruz, CA, USA), goat anti-mouse HRP (Cat#31430) was from Thermo Scientific. Alexafluor antibodies were from Molecular Probes (Burlington, ON, Canada).

FBS, dextromethorphan and tetracycline were from Sigma Aldrich (St. Louis, MO, USA), sodium butyrate was from Alfa Aesar (Ward Hill, MA, USA). Synthetic peptides were purchased from GenScript (Piscataway, NJ, USA) . Protease inhibitors and common chemicals were purchased from Fisher Scientific (Toronto, ON, Canada) or Sigma Aldrich.

DMEM and DMEM/F12 high glucose media were purchased from Gibco, Invitrogen (Burlington, ON, Canada). Other culture supplies were from VWR

International, BD Biosciences (Mississauga, ON, Canada), and Corning Life Sciences (Lowell, MA, USA).

Restriction enzymes and DNA modification enzymes were from New England Biolabs (Ipswich, MA, USA) and Invitrogen. Plasmid pcDNA3.1 was from Invitrogen. The T2R1 gene, in plasmid pcDNA3.1 and with 38 AA mouse rhodopsin tag at the N-terminus, was a kind gift from Dr. Kenji Maehashi, Tokyo University of Agriculture, Japan. Codon-optimized T2R1 gene with rho-1D4 tag at the C-terminus was synthesized commercially (GenScript). The epitope for rho-1D4, the octapeptide corresponding to the C-terminal sequence of rhodopsin, was prepared by the Massachusetts Institute of Technology Biopolymer laboratory (Cambridge, Massachusetts, USA). 96-well black-walled clear-bottom microtiter plates were from BD Biosciences, dispensing black tips and Flexstation 3 were from Molecular devices (Sunnyvale, CA, USA). 96-well compound plates were from Greiner (Mississauga, ON). Fluo 4-NW dye was from Invitrogen.

Electrophoresis apparatus was from Bio-Rad Laboratories (Mississauga, ON), ECL substrate was from Pierce, Thermo Fischer Scientific (Nepean, ON), Prolong Anti-fade Gold, Hoechst 33342 were purchased from Molecular Probes, Glass coverslips, mounting slides, Biomax-OMAT Kodak films were from Thermo Fisher Scientific.

2.2. Media and buffer compositions

Media

[A] LB media : 10 g/l Tryptone, 5 g/l Yeast extract.

<superscript>B</superscript> SOB media : 2% Bacto-Tryptone, 0.5% Yeast extract, 10 mM NaCl, 2.5 mM KCl (pH 7.0). 10 mM $MgCl_2$ added before use.

<superscript>C</superscript> $2 \times$ YT: 8 g/l Bacto-tryptone, 5 g/l Bacto-yeast extract, 2.5 g NaCl, pH 7.0.

<superscript>D</superscript> DMEM/F12 : Ham's F-12/DMEM High Glucose (1:1, Gibco, Invitrogen) supplemented with 10% FBS, 2 mM L-glutamine, 100 mg/ml Pencillin, 100 mg/ml Streptomycin.

<superscript>E</superscript>DMEM: Dulbecco's modified Eagle's Medium D-Glucose (4.5 g/l, Gibco, Invitrogen) supplemented with 10% heat inactivated (55°C for 1 hour) FBS, 2 mM L-glutamine, 100 mg/ml Pencillin, 100 mg/ml Streptomycin.

<superscript>F</superscript> DMEM : DMEM High Glucose (Gibco, Invitrogen).

Buffers

<superscript>G</superscript> Transformation buffer (TB) : 10 mM Hepes, 250 mM KCl, 15 mM $CaCl_2$, 55 mM $MnCl_2.4H_2O$ (pH 6.7).

<superscript>H</superscript> PBS : 137 mM NaCl, 2.7 mM KCl, 1.8 mM KH_2PO_4, 10 mM Na_2HPO_4.

<superscript>I</superscript> Storage buffer : 50 mM Tris, 12.5 mM $MgCl_2.6H_2O$, pH 7.4, containing protease inhibitors 1 mM EDTA, 10 µg/ml benzamidine, 20 µg/ml trypsin inhibitor, and 0.2 mM phenylmethylsulfonyl fluoride.

<superscript>J</superscript> Lysis buffer : 10 mM Tris-HCl (pH 7.4) containing protease inhibitors 1 mM EDTA, 10 µg/ml benzamidine, 20 µg/ml trypsin inhibitor, and 0.2 mM phenylmethylsulfonyl fluoride.

<superscript>K</superscript> Acidified alcohol: 197 ml of 95% ethanol, 52 ml of ddH_2O, 1.5 ml concentrated HCl to make 250 ml.

<superscript>L</superscript> 3.7% Paraformaldehyde / 1×PBS.

<superscript>M</superscript> 0.05% Triton X-100 / 1×PBS

<superscript>N</superscript> 2% BSA / 1×PBS.

<superscript>O</superscript> 1.5 M Tris, pH 8.8.

<superscript>P</superscript> 1.5 M Tris, pH 6.8.

[Q] 0.5 M Tris-HCl (pH 6.8), 8% SDS, 60% glycerol, 80 µg/ml bromophenol blue, 8% β-mercaptoethanol.

[R] 0.25 M Tris, 1.92 M glycine, 1% SDS.

[S] Transfer buffer: 25 mM Tris, 192 mM glycine, 20% methanol.

[T] 5% milk powder and 0.05% Tween-20 in 1×PBS.

[U] 0.1 M Potassium phosphate, pH 7.4.

[V] 0.5% skim milk and 0.1% Triton X-100 / 1 × PBS.

[W] TAE (Tris Acetate-EDTA): 4.84 g Tris, 2 ml 0.5 M Na_2EDTA (pH 8.0), 1.1 ml glacial acetic acid, and water to make 1 litre.

[X] Agarose loading buffer : 25 mg bromophenol blue, 3.3 ml 150 mM Tris, pH 7.6, 6 ml glycerol, 0.7 ml water to make 10 ml.

2.3. Methods

2.3.1. Preparation of LB (Luria-Bertani)-ampicillin plates

Petri plates for growth of *E. coli* were prepared by dissolving 20 g of LB-agar in 500 ml of distilled water using a 1L flask and autoclaved for 45 min. Following autoclaving, it was allowed to cool for approximately 30 min at RT with constant stirring at a slow speed on a stirrer/hot plate (Corning PC-420D). 500 µl of 100 mg/ml stock solution of ampicillin was added, the LB-Agar was poured into sterile petri dishes (20-25 ml/plate), and allowed to solidify for 4-5 hours at RT. The plates were stored at 4°C until use.

2.3.2. Preparation of competent *E. coli* cells

Competent *E. coli* cells were made following the Inoue method (Inoue et al, 1990). Briefly, DH5α cells from frozen stock (in LB/50% glycerol) were grown ON in

tubes containing 5 ml of media A at 37°C. 100 µl of the saturated *E.coli* DH5α culture was inoculated in 100 ml of media B or media C in a 1 litre flask, and grown to an A_{600} of 0.6 at 22°C for 18 hours with vigorous shaking (200-250 rpm). The flask was removed from the shaker and placed on ice for 10 min. The culture was transferred to 50 ml falcon tubes and the cells harvested by centrifugation at $2500 \times$ g (4100 rpm) for 10 min at 4°C using SLA 1500 rotor in Sorvall RC 6 Centrifuge. The cell pellet was resuspended gently in 32 ml of ice-cold buffer G, incubated on ice for 10 min, and again centrifuged as above. The cell pellet was resuspended gently in 8 ml of ice-cold buffer G. DMSO was added with gentle swirling to a final concentration of 7% (0.6 ml for 8 ml buffer G). After incubating on ice for 10 min, the cell suspension was aliquoted into 200 µl per eppendorf tube and stored at -80° C.

2.3.3. Transformation of competent *E. coli*

For transformation with different plasmids, a vial of frozen competent *E. coli* cells was thawed on ice. 50 µl of the cells were transferred to a 1.5 ml eppendorf tube and 0.1 µg (1-5 µl) of the plasmid was added to the tube. The mixture was incubated on ice for 35 min. The cells were then incubated at 42°C for 30 seconds, cooled on ice for 2 min and fed with 1 ml of media A. The tube was placed in a 37°C incubator and shaken gently for 1 hour. A momentary spin was given and 100 µl of the mixture was spread-plated on LB plates containing 100 µg/ml ampicillin and colonies allowed to form ON at 37°C. For plasmid miniprep, a select few colonies were inoculated in 5 ml of media A containing 5 µl of 100 mg/ml ampicillin stock solution and allowed to grow ON at 37°C with vigorous shaking (175 rpm) in an Orbital shaker, Forma Scientific.

DNA fragments to be ligated were excised from agarose gel and purified using the gel purification kit from Qiagen according to manufacturer's instructions. The purified DNA was mixed in a ratio of 1:2 of vector to insert in 10 µl volumes, containing 1 unit of T4 DNA ligase mix (Takara Bio. Inc.). Ligation mixtures were incubated for 30 min at 16°C. A sample with no insert DNA added was used as the control.

2.3.4. Recombinant T2R1 genes

The sequence encoding the human T2R1 gene (NCBI Accession # NM_019599) consists of 1469 bp, of which 897 bp encode T2R1, and has been cloned into the *KpnI-NotI* cloning sites of vector pcDNA3.1. The cDNA fragment encoding the first 38 amino acids of mouse rhodopsin have been placed at the N-terminus of human T2R1 to generate the expression vector pcDNA3.1/mRho/hT2R1 (Maehashi et al, 2007). Henceforth, this construct will be referred to as T2R1-rho38 (Figure 7).

Previously, codon-optimization for GPCRs has been shown to increase their expression in mammalian cells (Bradel-Tretheway et al, 2003; Babcock et al, 2001; Farrens et al, 2002; Chelikani et al, 2006). As a means to increase the gene expression, codon usage was optimized for the DNA sequence encoding T2R1. The gene was optimized for mammalian codon usage by utilizing the codons predicted to occur frequently in highly expressed genes of mammals (Nakamura et al, 2000). The synthetic T2R1 gene consists of 954 bp (Figure 8) and to facilitate future cloning into expression vectors, has evenly spaced unique restriction sites. Other salient features of this gene include, (i) a Kozak consensus sequence (**GCCACC<u>ATGG</u>**) 5' to the ATG start codon, (ii) a bovine rhodopsin octapeptide epitope tag (**ETSQVAPA**) immediately 5' to the

natural stop codon of T2R1, to facilitate detection and purification of the protein using the monoclonal antibody rho-1D4, (iii) restriction sites for EcoRI at the 5' end and NotI at the 3' end.

2.3.5. Construction of plasmids

2.3.5.1. Construction of plasmid containing synthetic codon-optimized T2R1 gene in vector pACMVtetO

The codon-optimized T2R1 gene, in plasmid pMT4, was digested with enzyme *EcoRI* and the vector pACMVtetO (Figure 10, Reeves et al, 2002) with enzyme *KpnI* as follows.: (i) 5 µg T2R1, 2 µl BSA (10 ×), 2 µl NEB 2 buffer, 2 µl *EcoRI* (20,000U/ml), and reaction volume made up to 20 µl with water, and (ii) 10 µg pACMVtetO, 2 µl BSA (10 ×), 4 µl NEB 2 buffer, 6 µl *KpnI* (10,000U/ml), and reaction volume made up to 40 µl with water. The restriction digests were incubated for 1.5 hour at 37°C. The linearized plasmid and gene were treated for enzymatic removal using Qiagen Gel Extraction kit (enzyme removal protocol) and eluted in a total volume of 20 µl water. The 5'-overhangs produced by the restriction enzymes were end-repaired using *E.coli* DNA Polymerase I Klenow fragment. The following reaction mixtures were incubated at 22°C for 30 min: 20 µl DNA (around 10 µg), 3 µl NEB 2 buffer, 1 µl DNA Polymerase I (5000U/ml), 1.5 µl of 10 mM dNTP mix (0.5 mM), and water added up to 30 µl reaction volume. The DNA was treated for enzymatic removal as above and eluted in 20 µl water. The DNA was next digested with enzyme *NotI* (10,000U/ml) as follows:

FIGURE 7. Nucleotide and protein sequence of the recombinant T2R1-rho38 construct (Maehashi et al, 2007). Transmembrane helices (depicted in bold) and the intra- and extracellular loops are shown above the sequence. The first 38 AA of mouse rhodopsin have been cloned 5' to the original start codon of the native human T2R1 gene sequence.

```
ttctcccagctgtctgaaggtgtctgattccattatttgcctgtgatgactttgaaagct


ggtaaacctgtaaaatgcaaaagccatcaataagaagcaaattgatgctagagtatctcc

tccttatttgactgtctcagaactaaatagagaaagcagtgacataaacaaatgtacacc


accttcctgccccatgcctttattgttagtcttcttccccagaggagtcctgatctaatt


gaagagcgtgaacaacccaacctgtccaaaactttataacttcattattttttaagtaaa

                                                      TM I
taatttttattcctaaaatgctagagtctcacctcattatctattttcttcttgcagtg
                M   L   E   S   H   L   I   I   Y   F   L   L   A   V


atacaatttcttcttgggattttcacaaatggcatcattgtggtggtgaatggcattgac
 I   Q   F   L   L   G   I   F   T   N   G   I   I   V   V   V   N   G   I   D

                            ICL I
ttgatcaagcacagaaaaatggctccgctggatctccttctttcttgtctggcagtttct
 L   I   K   H   R   K   M   A   P   L   D   L   L   L   S   C   L   A   V   S

                            TM II
agaatttttctgcagttgttcatcttctacgttaatgtgattgttatcttcttcatagaa
 R   I   F   L   Q   L   F   I   F   Y   V   N   V   I   V   I   F   F   I   E

                    ECL I                              TM III
ttcatcatgtgttctgcgaattgtgcaattctcttatttataaatgaattggaactttgg
 F   I   M   C   S   A   N   C   A   I   L   L   F   I   N   E   L   E   L   W


cttgccacatggctcggcgttttctattgtgccaaggttgccagcgtccgtcacccactc
 L   A   T   W   L   G   V   F   Y   C   A   K   V   A   S   V   R   H   P   L

                ICL II
ttcatctggttgaagatgaggatatccaagctggtcccatggatgatcctggggtctctg
 F   I   W   L   K   M   R   I   S   K   L   V   P   W   M   I   L   G   S   L
                                            TM IV
ctatatgtatctatgatttgtgttttccatagcaaatatgcagggtttatggtcccatac
 L   Y   V   S   M   I   C   V   F   H   S   K   Y   A   G   F   M   V   P   Y
```

```
ttcctaaggaaattttctcccaaaatgccacaattcaaaaagaagatacactggctata
 F  L  R  K  F  F  S  Q  N  A  T  I  Q  K  E  D  T  L  A  I
```

TM V
```
cagattttctcttttgttgctgagttctcagtgccattgcttatcttcctttttgctgtt
 Q  I  F  S  F  V  A  E  F  S  V  P  L  L  I  F  L  F  A  V
```

ICL III
```
ttgctcttgatttctctctggggaggcacacccggcaaatgagaaacacagtggccggc
 L  L  L  I  F  S  L  G  R  H  T  R  Q  M  R  N  T  V  A  G
```

TM VI
```
agcagggttcctggcaggggtgcacccatcagcgcgttgctgtctatcctgtccttcctg
 S  R  V  P  G  R  G  A  P  I  S  A  L  L  S  I  L  S  F  L
```

```
atcctctacttctcccactgcatgataaaagtttttctctcttctctaaagtttcacatc
 I  L  Y  F  S  H  C  M  I  K  V  F  L  S  S  L  K  F  H  I
```

ECL III   TM VII
```
agaaggttcatctttctgttcttcatccttgtgattggtatatacccttctggacactct
 R  R  F  I  F  L  F  F  I  L  V  I  G  I  Y  P  S  G  H  S
```

```
ctcatcttaattttaggaaatcctaaattgaaacaaaatgcaaaaaagttcctcctccac
 L  I  L  I  L  G  N  P  K  L  K  Q  N  A  K  K  F  L  L  H
```

```
agtaagtgctgtcagtgagagagaagttggatcagttcaaagaacccatgattcaatgat
 S  K  C  C  Q
```

```
ttacccatgcctgccacacttccctcagccagacaaagcagcctgttcataaatatacaa
```

```
catgtccccttcaggcctgtttatccagcctgag
```

FIGURE 8. Nucleotide sequence of the codon-optimized T2R1-rho1D4 construct, and the corresponding amino acid sequence. The locations of the *EcoRI-NotI* restriction sites are shown above the DNA sequence. Transmembrane helices (depicted in bold) and intra- and extracellular loops are also shown. The synthetic gene contains at its C-terminus the rhodopsin C-terminal octapeptide sequence (underlined) to facilitate detection and purification of the protein using the mouse monoclonal antibody rho-1D4.

```
   EcoRI                                                  TM I
ttccggaattcgccaccatgggcgagagccatctgatcatttatttcctgctggccgtga
                     M  G  E  S  H  L  I  I  Y  F  L  L  A  V


cagtttctgctgggcattttcactaacgggatcattgtggtggtgaacggcatcgatctg
 Q  F  L  L  G  I  F  T  N  G  I  I  V  V  V  N  G  I  D  L

                              ICL I
atcaagcaccggaaaatggccccgctcgatctcctgctgtcttgtctggctgtgtctcgg
 I  K  H  R  K  M  A  P  L  D  L  L  L  S  C  L  A  V  S  R

                         TM II
atcttcctgcagctgttttatattctacgtgaatgtgattgtgatctttttcatcgagttt
 I  F  L  Q  L  F  I  F  Y  V  N  V  I  V  I  F  F  I  E  F

               ECL I                       TM III
attatgtgcagcgccaattgcgccatcctgctctttatcaacgagctggagctgtggctg
 I  M  C  S  A  N  C  A  I  L  L  F  I  N  E  L  E  L  W  L


gccacctggctgggggtcttctactgcgccaaggtggccagcgtgagacacccctgtttt
 A  T  W  L  G  V  F  Y  C  A  K  V  A  S  V  R  H  P  L  F

      ICL II                                TM IV
atctggctgaagatgcggatcagcaagctcgtgccttggatgatcctgggcagcctgctc
 I  W  L  K  M  R  I  S  K  L  V  P  W  M  I  L  G  S  L  L


tacgtgagcatgatctgcgtgtttcacagcaagtacgccggctttatggtcccctatttc
 Y  V  S  M  I  C  V  F  H  S  K  Y  A  G  F  M  V  P  Y  F
                        ECL II
ctgcggaagttcttctcacagaatgccaccatccagaaggaggatacccttggccattcaa
 L  R  K  F  F  S  Q  N  A  T  I  Q  K  E  D  T  L  A  I  Q

                        TM V
atcttcagcttcgtggcagagtttccgttccctgctcatctttctgtttgctgtgctg
 I  F  S  F  V  A  E  F  S  V  P  L  L  I  F  L  F  A  V  L
```

```
                                                    ICL III
ctcctgatcttcagcctgggccggcacactagacagatgcgcaacacagtggccggcagc
 L   L   I   F   S   L   G   R   H   T   R   Q   M   R   N   T   V   A   G   S

                                                 TM VI
cgcgtgcctggtagaggcgcccccatttctgccctgctctccattctgtcctttctgata
 R   V   P   G   R   G   A   P   I   S   A   L   L   S   I   L   S   F   L   I


ctgtactttagccactgtatgattaaggtgtttctgagctccctgaagtttcatatccgg
 L   Y   F   S   H   C   M   I   K   V   F   L   S   S   L   K   F   H   I   R

   ECL III                                  TM VII
cggtttattttcctcttctttatcctggtcatcggcatatacccaagcggccacagtctg
 R   F   I   F   L   F   F   I   L   V   I   G   I   Y   P   S   G   H   S   L


atcctaatcctggggaatccgaaactgaaacagaatgccaagaagttcctcctgcactcc
 I   L   I   L   G   N   P   K   L   K   Q   N   A   K   K   F   L   L   H   S


aagtgttgccaagagaccagccaggtggctccggcctgagcggccgcaatct
 K   C   C   Q   E   T   S   Q   V   A   P   A           NotI
```

FIGURE 9. Nucleotide sequence alignment of the synthetic T2R1-rho1D4 (optimized) construct and T2R1-rho38 (non-optimized, Maehashi et al, 2007) recombinant gene. The alignment was done using Emboss-Align tool.

```
Opt         0  --------------------------------------------------      0
Nonopt      1  TTCTCCCAGCTGTCTGAAGGTGTCTGATTCCATTATTTGCCTGTGATGAC     50

Opt         0  --------------------------------------------------      0
Nonopt     51  TTTGAAAGCTAGGTAAACCTGTAAAATGCAAAAGCCATCAATAAGAAGCA    100

Opt         0  --------------------------------------------------      0
Nonopt    101  AATTGATGCTAGAGTATCTCCTCCTTATTTGACTGTCTCAGAACTAAATA    150

Opt         0  --------------------------------------------------      0
Nonopt    151  GAGAAAGCAGTGACATAAACAAATGTACACCACCTTCCTGCCCCATGCCT    200

Opt         0  --------------------------------------------------      0
Nonopt    201  TTATTGTTAGTCTTCTTCCCCAGAGGAGTCCTGATCTAATTGAAGAGCGT    250

Opt         0  --------------------------------------------------      0
Nonopt    251  GAACAACCCAACCTGTCCAAAACTTTATAACTTCATTATTTTTTAAGTAA    300

Opt         1  ---TTCCGGAATTCGCCACCATGGGCGAGAGCCATCTGATCATTTATTTC     47
               .|.....|||| |.|..||...|||...||.||.||.||.|||||.
Nonopt    301  ATAATTTTTTATTC-CTAAAATGCTAGAGTCTCACCTCATTATCTATTTT    349

Opt        48  CTGCTGGCCGTGATCCAGTTTCTGCTGGGCATTTTCACTAACGGGATCAT     97
               ||.||.||.|||||.||.|||||.||.||.|||||||||.||.||.|||||
Nonopt    350  CTTCTTGCAGTGATACAATTTCTTCTTGGGATTTTCACAAATGGCATCAT    399

Opt        98  TGTGGTGGTGAACGGCATCGATCTGATCAAGCACCGGAAAATGGCCCCGC    147
               |||||||||||||.|||||.||..|||||||||||.|.||||||||.||||
Nonopt    400  TGTGGTGGTGAATGGCATTGACTTGATCAAGCACAGAAAAATGGCTCCGC    449

Opt       148  TCGATCTCCTGCTGTCTTGTCTGGCTGTGTCTCGGATCTTCCTGCAGCTG    197
               |.|||||||||.||.||||||||||.||.|||.|.||.||.||.|||||||.||
Nonopt    450  TGGATCTCCTTCTTTCTTGTCTGGCAGTTTCTAGAATTTTTCTGCAGTTG    499

Opt       198  TTTATATTCTACGTGAATGTGATTGTGATCTTTTTCATCGAGTTTATTAT    247
               ||.||.|||||||||.||||||||||.|||||.|||||.||.||.||.||
Nonopt    500  TTCATCTTCTACGTTAATGTGATTGTTATCTTCTTCATAGAATTCATCAT    549

Opt       248  GTGCAGCGCCAATTGCGCCATCCTGCTCTTTATCAACGAGCTGGAGCTGT    297
               |||....||.|||||.||.||.||...|.|||||.||.||..|||||.||.|
Nonopt    550  GTGTTCTGCGAATTGTGCAATTCTCTTATTTATAAATGAATTGGAACTTT    599

Opt       298  GGCTGGCCACCTGGCTGGGGGTCTTCTACTGCGCCAAGGTGGCCAGCGTG    347
               |||||.||||||.|||||.||.||.||.||||||.||.|||||||||.||||||||.
Nonopt    600  GGCTTGCCACATGGCTCGGCGTTTTCTATTGTGCCAAGGTTGCCAGCGTC    649

Opt       348  AGACACCCCCTGTTTATCTGGCTGAAGATGCGGATCAGCAAGCTCGTGCC    397
               .|.||||||.||.||.|.|||||.|||||||||.||||...|||||.||.||
Nonopt    650  CGTCACCCACTCTTCATCTGGTTGAAGATGAGGATATCCAAGCTGGTCCC    699
```

```
Opt      398  TTGGATGATCCTGGGCAGCCTGCTCTACGTGAGCATGATCTGCGTGTTTC     447
              .||||||||||||||||....|||||.||.||....|||||.||.||.||.|
Nonopt   700  ATGGATGATCCTGGGGTCTCTGCTATATGTATCTATGATTTGTGTTTTCC     749

Opt      448  ACAGCAAGTACGCCGGCTTTATGGTCCCCTATTTCCTGCGGAAGTTCTTC     497
              |.||||||.||.||.||.||||||||||||.||.||||||..|||||.||.|||
Nonopt   750  ATAGCAAATATGCAGGGTTTATGGTCCCATACTTCCTAAGGAAATTTTTC     799

Opt      498  TCACAGAATGCCACCATCCAGAAGGAGGATACCCTGGCCATTCAAATCTT     547
              ||.||.|||||||||.||.||.||.||.|||||.|||||.||.||.||.||
Nonopt   800  TCCCAAAATGCCACAATTCAAAAGAAGATACACTGGCTATACAGATTTT     849

Opt      548  CAGCTTCGTGGCAGAGTTTTCCGTTCCCCTGCTCATCTTTCTGTTTGCTG     597
              |...||.||.||.|||||.||.||.||..|||||.|||||.||.||||||||
Nonopt   850  CTCTTTTGTTGCTGAGTTCTCAGTGCCATTGCTTATCTTCCTTTTTGCTG     899

Opt      598  TGCTGCTCCTGATCTTCAGCCTGGGCCGGCACACTAGACAGATGCGCAAC     647
              |..|||||.|||||.|||...|||||..|||||||||..|.||.|||.|.|||
Nonopt   900  TTTTGCTCTTGATTTTCTCTCTGGGGAGGCACACCCGGCAAATGAGAAAC     949

Opt      648  ACAGTGGCCGGCAGCCGCGTGCCTGGTAGAGGCGCCCCCATTTCTGCCCT     697
              ||||||||||||||||.|.||.||||||.||.||.||.|||||...||..|
Nonopt   950  ACAGTGGCCGGCAGCAGGGTTCCTGGCAGGGGTGCACCCATCAGCGCGTT     999

Opt      698  GCTCTCCATTCTGTCCTTTCTGATACTGTACTTTAGCCACTGTATGATTA     747
              |||.||.||.|||||||||.|||||.||.|||||...|||||.|||||.|
Nonopt  1000  GCTGTCTATCCTGTCCTTCCTGATCCTCTACTTCTCCCACTGCATGATAA    1049

Opt      748  AGGTGTTTCTGAGCTCCCTGAAGTTTCATATCCGGCGGTTTATTTTCCTC     797
              |.||.||||||....||.||.|||||||||.|||.|..|||||.||.||.
Nonopt  1050  AAGTTTTTCTCTCTTCTCTAAAGTTTCACATCAGAAGGTTCATCTTTCTG    1099

Opt      798  TTCTTTATCCTGGTCATCGGCATATACCCAAGCGGCCACAGTCTGATCCT     847
              |||||.|||||.||.||.||.||.||||||||....||.|||..|||.||||.|
Nonopt  1100  TTCTTCATCCTTGTGATTGGTATATACCCTTCTGGACACTCTCTCATCTT    1149

Opt      848  AATCCTGGGGAATCCGAAACTGAAACAGAATGCCAAGAAGTTCCTCCTGC     897
              |||..|.||.|||||.|||.||||||||||.|||||.||.|||||||||||.|
Nonopt  1150  AATTTTAGGAAATCCTAAATTGAAACAAAATGCAAAAAAGTTCCTCCTCC    1199

Opt      898  ACTCCAAGTGTTGCCAAGAGACCAGCCAGGTGGCTCCGGCCTGAGCGGCC     947
              ||...|||||.||.| ||.||.....||.||||.||.|...|..||...||
Nonopt  1200  ACAGTAAGTGCTGTC-AGTGAGAGAGAAGTTGGATCAGTTCAAAGAACCC   1248

Opt      948  GCAATCT--------------------------------------------     954
              ...||..
Nonopt  1249  ATGATTCAATGATTTACCCATGCCTGCCACACTTCCCTCAGCCAGACAAA   1298

Opt      954  --------------------------------------------------     954

Nonopt  1299  GCAGCCTGTTCATAAATATACAACATGTCCCCTTCAGGCCTGTTTATCCA   1348

Opt      954  -------     954

Nonopt  1349  GCCTGAG     1355
```

20 μl DNA (around 10 μg), 2 μl BSA (10 ×), 2.5 μl NEB 3 buffer, 2 μl *NotI* (10,000

U/ml), and water added upto 30 μl, and reaction mixture incubated at 37°C for 1.5 hour.

The *EcoRI(blunt)-NotI* and *KpnI-NotI* fragments of T2R1 gene and plasmid

pACMVtetO respectively were purified by 1% agarose gel electrophoresis using Qiagen

gel purification kit and eluted in 20 μl water. To prevent re-circularization of the end-

repaired vector and to remove 5'-phosphate groups, the vector DNA was treated with calf

intestinal alkaline phosphatase (CIP) in the following reaction mixture: 20 μl DNA

(around 10 μg), 3 μl dephosphorylating buffer (10 ×), 1.5 μl of CIP (10,000U/ml), and

water adding to 30 μl reaction volume. The mixture was incubated for 30 min at 37°C.

The purified T2R1 gene was ligated into the vector pACMVtetO to generate

pACMVtetO-T2R1 construct and the ligation mixture was used directly for

transformation of competent *E. coli* DH5α as described earlier.

Isolated colonies from the previous step were picked and used to inoculate 5 ml

of media A containing 100 μg/ml ampicillin. After growth at 37°C for 16-18 hours, DNA

was purified from the cultures using Qiagen DNA purification miniprep kit. The DNA

was eluted in 20 μl sterile water and restriction digest was done by incubating the

following reaction mixture at 37°C for 1.5 hour: 2 μg DNA, 1 μl BSA (10 ×), 1 μl EcoRI

buffer (NEB), 1 μl *EcoRI* (20,000U/ml), 1 μl *NotI*, and water added upto 10 μl. The

samples were analyzed by gel electrophoresis on a 1% agarose gel. The isolates showing

the correct banding pattern were sequence confirmed (Robarts Research Institute,

London, ON).

2.3.5.2. Construction of plasmid containing T2R1 gene in expression vector pcDNA3.1

The T2R1 gene, codon-optimized and with rho-1D4 tag, in plasmid pMT4 was digested with *EcoRI* and *NotI* enzymes as described before on page 29. The following reaction mixtures were incubated at 37°C for 1.5 hr: 1 µg plasmid DNA, 1 µl BSA (10 ×), 1 µl EcoRI buffer (NEB), 1 µl *NotI* (10,000U/ml), 0.5 µl *EcoRI* (20,000U/ml), and water added to 10 µl final volume. The enzymes were removed using the Qiagen gel extraction kit. The *EcoRI-NotI* fragments were purified by gel electrophoresis using 1% agarose gel, and the T2R1 DNA was extracted from the gel using the Qiagen gel extraction kit in a total volume of 20 µl. The T2R1 gene was then ligated into the plasmid pcDNA3.1 and the ligation mixtures were used for transformation of competent *E.coli*.

2.3.6. Expression of T2R1 in Human Embryonic Kidney (HEK293) cells

2.3.6.1. Construction of Tetracycline-inducible HEK293S stable cell lines expressing codon-optimized T2R1 receptor

Frozen HEK293S-tetR cells were revived and the plasmid pACMVtetO-T2R1 was then transfected into three 10 cm plates of HEK293S-tetR cells (10 µg plasmid/ plate) which had reached 70-80% confluency. Transfection was carried out with Lipofectamine 2000 using media D. An untransfected 10 cm plate of HEK293S-TetR cells was grown at 37°C, 5% CO_2 as a negative control. After transfection for 44-48 hours, the cells were split at a dilution ratio of 1:15, 1:100 and 1:500 (in duplicates) using media D supplemented with 20% conditioned medium (Reeves et al, 2002a), and the untransfected plate was split 1:15 only. The next day, medium was replaced with buffer

D media containing 20% conditioned media and G418 (1 mg/ml). The cells were re-fed every three days with fresh medium containing G418 until large isolated colonies formed (about 2 weeks). Cells in the untransfected control plate died after a week.

Colony formation was observed in 7-10 days. A few isolated colonies were selected and circled with a marker at bottom of the plate, and the medium from the plate was removed. Using sterile forceps, the bottom of the sterile glass cloning rings was given a touch of vacuum grease and placed around the colony. 75 µl of $1 \times$ trypsin was added to each colony enclosed in the cloning rings. After 1 min, 50 µl of media D was added to each cloning ring. The solution was pipetted up and down before being transferred to 24-well dishes containing 1 ml complete media/well with G418 (1 mg/ml). On reaching confluence, the cells in each well were split into 3 wells and the latter incubated until the cells reached confluence. One well of cells was frozen for storage, while the cells in the second well were fed with media D containing both tetracycline (1 µg/ml) and sodium butyrate (7.5 mM). The cells in the third well were not induced, and used as the control. After induction for 44-48 hours, the cells were harvested in 1 ml of 1 $\times$ buffer H by pipetting up and down. The cells in buffer H were transferred to 1.5 ml eppendorf tubes and centrifuged at 6000 rpm for 1 min at 4°C. The supernatant was aspirated and the cell pellet was frozen at -80°C.

2.3.6.2. Screening of selected clones by slot blot

The best clones were selected after screening them using the slot blot apparatus containing a nitrocellulose membrane. The screening was done as follows. The frozen cell pellet from the above step was thawed on ice and solubilized in 200 μl buffer I containing 1% DM at 4°C as described on page 43. 100 μl of the solubilized supernatant from the tetracycline and sodium butyrate-induced clones was transferred to the first slot on the left column on slot blot apparatus containing a nitrocellulose membrane, whereas the same volume of uninduced clones was added to the first slot on the right. Serial dilutions of 1:5 were created in total of 3 dilutions, by removing 20 μl of each sample and adding to the next. This was mixed with 80 μl of $1 \times$ buffer H, 20 μl was removed and added to the next slot. The same was repeated for the uninduced samples. After addition of samples to all the slots, vacuum was applied. Each slot was washed twice with 100 μl of cold buffer H using a multichannel pipetter. The nitrocellulose membrane was removed and allowed to dry for 5 min, and blocked overnight in 100 ml buffer H containing 5% milk powder and 0.05% Tween-20. The membrane was developed as described in 'western blot' section. The clones being expressed the most in induced samples but the least in uninduced samples were selected for future work.

2.3.7. Expression of T2R1 genes by transient transfection in rat C6 glioma cells

Frozen stocks (-136°C) of C6 glioma cells were thawed quickly by placing the vials in a 37°C water bath. The cells were slowly transferred to a 10-cm tissue culture

treated plate containing 10 ml of media E and incubated at 37°C, 5% CO_2 in

ThermoScientific, Steri-Cycle Hepa Class 100 incubator. The media was changed the

following day. Alternatively, the cells from the cryovial were transferred to a 15 ml

Falcon tube containing 10 ml of media. The cells were pelleted at $100 \times g$ for 2 min, the

supernatant was aspirated and 10 ml of fresh media was added. The cells were

resuspended and transferred to a 10-cm tissue culture dish and incubated at 37°C, 5%

CO_2. Cells were fed every two to three days, until 80-90% confluence was reached.

On reaching 90% confluence, the cells were split. Prior to trypsinization, the 10-

cm plates were washed with 10 ml of buffer H. 1 ml of $1 \times$ trypsin (prepared from a 10

$\times$ stock solution 5 g/l trypsin and 2 g/l EDTA in buffer H) was added to the cells and the

plate was incubated at 37°C for 2 min or until the cells detached from the surface. 9 ml of

media E was added to inactivate trypsin. Cells were removed from the plates by pipetting

up and down and transferred to new plates in appropriate ratios.

For long-term storage of cells, 80-90% confluent 10-cm plates were trypsinized as

described above. After centrifugation at $700 \times g$ for 5 min., the supernatant was aspirated

and the cell pellet was resuspended in 10 ml media F containing 10% DMSO and

supplemented with 20% FBS. 1 ml aliquots were prepared in cryovials and kept at -80°C

ON where the cooling rate was 1°C/min. The following day, the vials were transferred to

liquid nitrogen.

The cells were split into four plates and on reaching 70-80% confluence, they were

transiently transfected with the T2R1 genes using Lipofectamine 2000. 10 µg plasmid-

DNA per 10-cm plate was diluted in 1 ml of opti-MEM I reduced-serum medium in a 15

ml Falcon tube, and 20 µl of Lipofectamine 2000 per 10-cm plate was diluted in 1 ml of

opti-MEM I in another 15 ml tube. For transfecting cells in 6-well plates, 4 µg plasmid-

DNA per well was diluted in 250 µl opti-MEM I and 10 µl of Lipofectamine 2000 diluted

in 250 µl opti-MEM I. After incubating at RT for 5 min, the complexes were gently

mixed and incubated for another 20 min. The DNA complexes were then added to the

cells in 10 cm plates or in 6-well plates containing 8 ml or 1.5 ml of media F respectively.

2.3.8. Preparation of cell membranes containing the T2R1 genes

The culture media was removed 44-48 hours post-transfection or post-induction

for stable cell lines, and the cells in four 10 cm dishes were rinsed with ice-cold buffer

H. 5 ml of buffer J was added to the first dish and the cells were harvested using a cell

scraper and the cell suspension transferred to the second, third and fourth dish and then to

a 15 ml falcon tube on ice. 5 ml of buffer J was again added to the first dish and the

process was repeated. The cells from the 15 ml tube were poured into a 15 ml glass

dounce tissue homogenizer, and homogenized with 25 strokes. The cell lysate was

transferred back to 15 ml tube and centrifuged at $700 \times g$ (2150 rpm) for 10 min at 4°C

using SLA 1500 rotor (Sorvall RC 6 Centrifuge). The pellet was discarded and the

supernatant was transferred to an ice cold high speed centrifuge tube and centrifuged at

$45450 \times g$ (19500 rpm) for 20 min at 4°C using SS 34 rotor. The resulting pellet was

resuspended in 1 ml buffer I by pipetting up and down to obtain a uniform suspension.

Aliquots of the suspension were snap-frozen and stored at -80°C until further use.

2.3.9. Solubilization of cell membranes

For solubilization of cell membranes expressing T2R1, 50 µl of cell membranes was added to 450 µl buffer I containing 1% DM (dodecyl-n-maltoside). The membranes were end-over-end mixed for 1 hour at 4°C. The unsolubilized material was removed by centrifugation for 30 min at 4°C, 50,000 rpm using Ti 70 rotor and Beckman UltraCentrifuge L8-M. The supernatant was transferred to a fresh eppendorf tube and the protein concentration was measured as described later.

2.3.10. Polymerase Chain Reaction (PCR)

2.3.10.1. RNA isolation

Total RNA was isolated from untransfected cells (to be used as control) and 24 hours post-transfected cells using RNeasy mini kit (Qiagen) according to the manufacturer's instructions. The media from the 6-well was aspirated, and 600 µl/well of RLT buffer (contains guanidine thiocyanate) was added to the well to lyse the cells. β-mercaptoethanol (β-ME, 10 µl/ml) was added to RLT buffer before use. The lysate was collected by pipetting into a 1.5 ml microcentrifuge tube and it was ensured that no cell clumps were visible. One volume of 70% ethanol was added to the lysate, and mixed thoroughly by pipetting. Upto 700 µl of the sample was transferred to RNeasy spin columns placed in 2 ml collection tubes, and centrifuged for 30 sec at 10,000 rpm. The flow-through was discarded. To wash the spin column membranes, 700 µl of buffer RW1 (contains ethanol) was added to the spin columns and centrifuged for 30 sec at 10,000 rpm, and the flow-through was discarded. Then 500 µl of buffer RPE (contains guanidine

hydrochloride) was added to the spin columns and centrifuged for 30 sec at 10,000 rpm. To ensure that no ethanol was carried over during RNA elution, 500 µl of buffer RPE was again added to the spin columns and centrifuged for 2 min at 10,000 rpm. The RNeasy spin columns were placed in new 2 ml collection tubes, and centrifuged for 1 min at 13,000 rpm. The spin columns were placed in new 1.5 ml collection tubes. 50 µl RNase-free water was directly added to the spin column membranes, and centrifuged for 75 sec at 10,000 rpm to elute the RNA.

2.3.10.2. DNase I Treatment

To remove genomic DNA contamination, the RNA samples were treated with DNase I. Total RNA (10 µg) was resuspended in $1 \times$ DNase I Reaction Buffer (10 mM Tris-HCl, 2.5 mM $MgCl_2$, 0.5 mM $CaCl_2$, pH 7.6) to a final volume of 100 µl. 4 units of DNase I (2000 units/ml) were added, mixed thoroughly and incubated at 37°C for 30 min. To stop the reaction, 1 µl of 0.5 M EDTA (to a final concentration of 5 mM) was added and heat inactivated at 75°C for 10 min.

RNACleanup: RNA was again purified using the RNA Cleanup protocol in RNeasy mini-kit. RLT buffer (350 µl) was added to the samples followed by 250 µl ethanol (96-100%) and mixed gently by pipetting. The samples were transferred to RNeasy minispin columns placed in 2 ml collection tubes and centrifuged for 30 sec at 10,000 rpm. The flow-through was discarded, and 500 µl of buffer RPE was added to the spin columns and the rest of the procedure was same as described for total RNA isolation. The purified RNA was eluted in 50 µl of RNase-free water. The optical density of RNA was measured in a glass cuvette at A_{260} and A_{280}.

2.3.10.3. cDNA Synthesis

For a 20 µl reaction volume, 0.25-1 µg RNA was added to a nuclease-free microcentrifuge tube and mixed with 1 µl of oligo $(dT)_{20}$ primer (50 µM), 1 µl 10 mM dNTP mix (10 mM each dATP, dGTP, dCTP and dTTP at neutral pH), and sterile distilled water. The mixture was heated to 65°C for 5 min and incubated on ice for at least 1 min. The contents of the tube were collected by brief centrifugation and 4 µl 5X first-strand buffer (Invitrogen), 1 µl 0.1 M DTT, and 1 µl of superscript III reverse transcriptase (200 units/µl) were added to the tube. The mixture was mixed by pipetting gently up and down, and incubated at 50°C for 30 min. The reaction was inactivated by heating at 70°C for 15 min. All incubation steps were carried out in a thermocycler (MJ mini cycler, Bio rad). Samples without the addition of superscript III reverse-transcriptase were kept as controls. The cDNA synthesized was used as template for amplification in PCR.

2.3.10.4. Reverse-Transcriptase Polymerase Chain Reaction (RT-PCR)

Partial length T2R coding sequences were amplified from rat C6 cells cDNA using synthetic oligonucleotide primers designed for hT2R1. The primer sequences used for PCR analysis of hT2R1 expression have been listed in table II. PCR reaction was set up in a total volume of 20 µl containing 14.2 µl sterile water, 2 µl of 10 X DyNAzyme^{TM} II Hot start reaction buffer (final $1 \times$ reaction concentration of buffer contains 15 mM Tris-HCl, pH 8.2 at 25°C, 2.5 mM $MgCl_2$, 30 mM KCl, 5 mM $[NH_4]_2SO_4$ and 0.02% bovine serum albumin), 0.4 µl of 10 mM dNTP mix (200 µM each), 1 µl each of forward and reverse primers (0.5 µM), 1 µl of reverse-transcribed cDNA, and 0.4 µl of

TABLE II.   Primer sequences used for PCR analysis of GAPDH and hT2R1 expression in rat C6 glial cells.

Gene	Species	Gene length (bp)	PCR primers (5'-3')	Amplicon size (bp)
GAPDH	Rat	1307	F-ATGACTCTACCCACGGCAAG R-GATCTCGCTCCTGGAAGATG	105
T2R1-rho38[1]	Human	1469	F-CCGTCACCCACTCTTCATCT R-GGGACCATAAACCCTGCATA	129
T2R1-rho1D4[2]	Human	954	F-AGAATGCCACCATCCAGAAG R-AGGCTGAAGATCAGGAGCAG	118
T2R1	Rat	1008	F-CTCATTGTGGTTGTCCATGC R-GCCAGGCAAAATAGAAGCAG	80

[1] Corresponds to T2R1 gene with the mouse rhodopsin 38 AA tag at the N-terminal.
[2] Corresponds to codon-optimized T2R1 gene with bovine rhodopsin 8 AA tag at the C-terminal.
  Abbreviation: F, forward; R, reverse.

DyNAzyme^{TM} II Hot Start DNA Polymerase (0.04 U/µl). The mixture was mixed by

pipetting gently up and down. The cycling conditions consisted of an initial denaturation

step of 94ºC for 10 min, followed by 45 cycles of denaturation at 94ºC for 20 sec,

annealing at 58ºC for 20 sec and extension at 72ºC for 20 sec, with a final extension at

72ºC for 2 min on a thermocycler (MJ mini cycler, Biorad). The housekeeping gene

GAPDH was used as a control in the PCR reactions. A reagent blank without cDNA was

used as an internal control. All PCR products were separated on 2% agarose gels stained

with ethidium bromide. Gel images were recorded and photographed under UV light.

2.4. Analytical Procedures

2.4.1. DNA Sequencing

DNA sequences were confirmed by automated DNA sequencing (Robarts

Research Institute, London, ON). The synthetic oligonucleotide primers used for

sequencing were designed using the primer design software (Invitrogen), and were

purchased from Invitrogen. The primer sequences used for DNA sequencing are listed in

table III.

2.4.2. Protein Quantification

Protein concentration of the resuspended membrane pellet was determined using

a modified DC protein assay kit from Bio-Rad Laboratories. DC protein assay is a

colorimetric assay for protein concentration following detergent solubilization. A

TABLE III. DNA Sequencing Primers

Gene/Plasmid	Gene size (bp)	Oligonucleotide sequencing primers (5'-3')
T2R1-rho38/pcDNA3.1[1]	1469	Forward - ATTAATACGACTCACTATAG Reverse - GCCTCGACTGTGCCTTCTAG
T2R1-rho1D4/pcDNA3.1[2]	954	Forward - GACAATGACATCCACTTTGCC Reverse - TAGGATTGCCGTCAAGTTTGG
T2R1-rho1D4/pMT4[2]	954	Forward - AGCAGAGCTCGTTTAGTGAACC Reverse - AGTGAAAATGCCCAGCAGAAA
T2R1-rho1D4/pACMVtetO[2]	954	Forward- GCAGAGCTCGTTTAGTGAACCG

[1] Corresponds to T2R1 gene with the mouse rhodopsin 38 AA tag at the N-terminal.
[2] Corresponds to codon-optimized T2R1 gene with bovine rhodopsin 8 AA tag at the C-terminal.

standard curve was obtained by preparing six dilutions of a 1.44 mg/ml stock of bovine

serum albumin (BSA) by mixing 0.1, 0.2, 0.4, 0.6, 0.8 and 1 mg/ml with buffer I

containing 1% DM in 13 × 100 mm test tubes such that the final volume was 100 µl. The

sample solutions were also adjusted to 100 µl at appropriate dilutions. Then 500 µl of

reagent A (an alkaline copper tartarate solution) was added to each test tube and mixed by

vortexing. Then 4 ml of reagent B (a dilute Folin reagent) was added to each tube and

vortexed immediately. After 15 min of incubation at RT, absorbance was read at 750 nm

using a glass cuvette and the spectrophotometer (Amersham, Ultrospec 4300). The

concentration was determined using the bovine serum albumin standard curve.

2.4.3. DNA, RNA Quantification

DNA/RNA was quantified using the spectrophotometer (Ultrospec 4300 pro,

Amersham,). A 1:50 dilution of the purified DNA/RNA was prepared by adding 10 µl to

490 µl of water. Around 500 µl of water was used as blank (reference). Absorbance was

measured at 260 nm and 280 nm using a glass cuvette. The purity of DNA/RNA was

given by the ratio of A_{260} and A_{280}. The concentration of DNA was calculated as the A_{260}

of dilution × 50* × dilution factor (i.e. 50) µg/ml.

*Concentration of 1 A_{260} unit of dsDNA = 50 µg/ml H_2O.

The concentration of RNA was calculated as the A_{260} of dilution × 44* × dilution factor

*Concentration of 1 A_{260} unit of ssRNA = 44 µg/ml H_2O.

2.4.4. Sub-cellular localization of T2R1 in C6 glioma cells using immunofluorescence microcopy

Preparation of glass coverslips

Round glass coverslips (size 25CIR, thickness # 1, Fischer Thermo Scientific) were dipped overnight in buffer K. The next day they were rinsed thoroughly with distilled water, transferred to a fresh beaker containing double distilled water and autoclaved for 1 hour. On cooling, the coverslips were dried in the fumehood on an autoclaved filter paper. Once dry, they were coated with poly-L-lysine (Sigma), again dried and transferred to 6-well tissue culture dish using sterile forceps.

A day before transfection, rat C6 glioma cells were split into a 6-well tissue-culture plate containing glass coverslips. This was followed by transient transfection with T2R1 gene using Lipofectamine 2000 and media D or E. 24 hours post-transfection, the cells were washed with $1 \times$ buffer H and fixed in buffer L for 15 min at RT. The cells were immediately permeabilized with buffer M for 10 min. After washing with $1 \times$ buffer H, the cells were blocked for 1 hour in buffer N in a humidified chamber. The primary antibody dilutions of mouse monoclonal anti-rho-1D4 (1:500) and plasma membrane marker rabbit polyclonal anti-cadherin (1:100) were prepared as a cocktail in buffer N, and the cells were incubated ON at 4°C in a humidified chamber. The coverslips were gently washed 4×15 min with $1 \times$ buffer H. Secondary antibody incubations consisted of goat anti-mouse Alexafluor 594 (1:500) which recognizes mouse rho-1D4 antibody, and goat anti-rabbit Alexafluor 488 (1:300) which recognizes rabbit anti-cadherin, and incubation times were for 1 hour at RT in a humidified chamber. All steps during and after secondary antibody incubation were carried out in the dark. After washing the

coverslips 4 × 15 min with 1 × buffer H, the cells were stained with nuclear stain Hoescht 33342 (1:1000) for 15 seconds. This was followed by 4 × 5 min washes with sterile water, and drying the coverslips for 30 min in the dark. The cover slips were mounted on glass slides using 30 µl Prolong Anti-fade Gold, allowed to dry and the edges sealed with nail paint. The slides were visualized under B X 61 Olympus microscope using ImagePro software (Media Cybernetics).

2.4.5. Agarose gel electrophoresis

Agarose gels (1% or 2%) were prepared by dissolving 0.5 g or 1 g of agarose respectively in 50 ml buffer W and heating for 1 min in microwave oven. The agarose was allowed to cool for 5 min to about 60°C and 1 µl of ethidium bromide (10 mg/ml) was added and swirled to mix before pouring in the Bio-Rad Mini Sub Cell horizontal electrophoresis tray. The comb was inserted and the gel was left to set for at least 30 min. Samples of 10 µl volume were mixed with 1µl of buffer X and loaded on the gel. Low molecular weight DNA Ladder or 1 kb plus DNA Ladder (New England Biolabs) were used as molecular weight size standards. Electrophoresis was carried out at 70 V, usually until the bromophenol dye front had migrated two-thirds of the length of the gel. Following electrophoresis, DNA bands were visualized with ultraviolet light using a Bio-Rad Gel Doc.

2.4.6. SDS PAGE Analysis

Polyacrylamide gels were cast as vertical slabs of dimensions 10 cm × 10 cm and 0.5 mm thickness (mini gels). Resolving gels (12%) were poured after mixing 1.65

ml of water, 2 ml of 30% acrylamide, 1.25 ml of buffer O, 50 µl of SDS (10%), 50 µl

APS (10%) and 5 µl TEMED. Stacking gels (3.75%) were poured after mixing 1.25 ml

of water, 0.25 ml of 30% acrylamide, 0.5 ml of buffer P, 25 µl of SDS (10%), 25 µl APS

(10%), and 2.5 µl TEMED. Protein samples were mixed with 4 × sample buffer Q and 4

µl of 100 mM DTT and were run in buffer R at 150 V constant voltage in a Bio-Rad Mini

Protean electrophoresis system. Staining of the fractionated proteins was with 45%

methanol, 9% acetic acid, 0.2% Coomassie blue for 45 min with shaking. Destaining was

with 15% methanol and 7.5% acetic acid in water. The final rinse destain solution was

made up of 10% methanol, 7.5% acetic acid and 3% glycerol in water.

2.4.7. Western Blotting

DM-solubilized T2R1 cell membranes (10-40 µg) were mixed with 4 µl of 100

mM DTT and 4 µl of buffer Q and loaded on the polyacrylamide gel. The proteins on the

gel were transferred to a 0.45 µm nitrocellulose membrane in buffer S for 45 min, 100V

at 4°C using BioRad transblot electrophoretic transfer apparatus. The polyacrylamide gel

was then stained with Coomassie blue and destained to confirm the complete transfer of

proteins to the nitrocellulose membrane. The membrane was removed and blocked

overnight in 100 ml buffer T. After ON incubation, buffer T was removed and the

membrane washed twice with 1 × buffer H. Primary antibody reaction buffer (Magic

block) was prepared by dissolving 0.25% BSA, 0.5% gelatin, 0.2% sodium azide, and

1000 µg of rho-1D4 monoclonal antibody (345 µl of a 2.9 mg/ml stock solution, 1:1000

dilution) in 100 ml of buffer U and 1:200 dilution for rho-S17 goat polyclonal antibody.
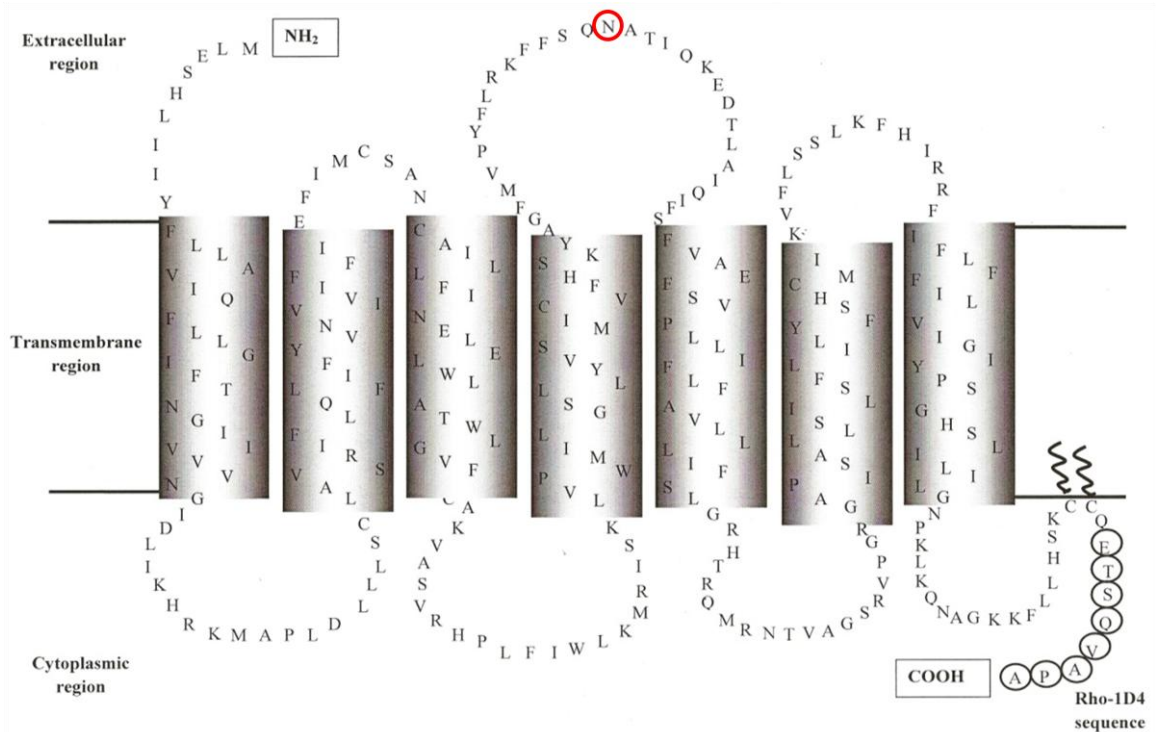
FIGURE 10. Predicted secondary structure model of the primary amino acid sequence of T2R1 showing the seven TM helices, three extracellular loops, three intracellular loops and the rho-1D4 epitope tag at the C-terminus. The protein comprises of 299 amino acids. The Asn-x-Ser/Thr consensus sequence present on the second extracellular loop is N-glycosylated (circled) and conserved across the T2R family.

The membrane was submerged in magic block and incubated for 3-4 hours at RT with slow shaking. The magic block was removed and transferred into a 50ml falcon tube for reuse and stored at 4°C. The membrane was washed 4×15 min with buffer V and then incubated with 5 µl of secondary antibody goat anti-mouse IgG (H+L), peroxidase conjugated in 25 ml of buffer V (1:5000 dilution for rho-1D4, 1:2000 for rhoS17) for 1 hour at RT with slow shaking. The secondary antibody was removed and the membrane washed 4×15 min with buffer V. The membrane was then transferred to a saran wrap containing 1 ml of chemiluminesce (ECL, Pierce), incubated for 2-3 min, and then kept in a X-ray cassette and developed on Kodak Biomax Xar film.

2.4.8. Measurement of intracellular calcium

For calcium dose-response functional assays, rat C6 glioma cells were counted from a 10 cm plate using a hemocytometer. Approximately 1.5×10^5 cells /well were seeded and simultaneously transfected with T2R1 genes in 96-well black microtitre BD optilux plates. Empty pcDNA vector transfected cells were used as negative control. The cells were transiently transfected with 200 ng plasmid DNA per well using 500 nl Lipofectamine 2000 per well and 25 µl opti-MEM I reduced serum medium per well in media F according to the procedure described previously. After 24-26 hours of transfection, the media from the 96-well plate was removed and 100 µl (per well) of calcium-sensitive Fluo-4 NW dye (Invitrogen) was added. The cells were incubated with the dye for 30 min at 37°C and another 30 min at RT. Probenecid, an inhibitor of organic anion transport, was added at a concentration of 2.5 mM, minimizing the loss of the

calcium indicator dye from the cells. A 96-well plate (assay compound plate) was prepared with different concentrations of synthetic peptides. Receptor activation was determined by measuring changes in intracellular calcium after application of synthetic peptides using Flexstation 3 fluorescence plate reader (Molecular Devices, CA) at 525 nm following excitation at 494nm. Dose-response curves were constructed and EC_{50} values calculated by nonlinear regression using Graphpad Prism software. Bar plots were plotted using Microsoft Excel.

2.4.9. Molecular modeling

T2R1 receptor models were built by homology modeling using the crystal structure of active opsin in complex with a C-terminal peptide of transducin (3DQB) as template. The transmembrane domains were predicted using different hydrophobicity scales. T2R1 sequence was then aligned with the sequences of opsin and rhodopsin. The similarity of the whole sequence was ~20%, and that of residues in the transmembrane regions was higher, at ~25-30%.

The transmembrane regions of T2R1 were modeled by MODELLER 9V7 (Sali et al, 1995). The loops of the receptor were modeled using loop database of ModLoop software (Fiser et al, 2000). Side chains of the molecule were refined with SCWRL4 database (Krivov et al, 2009). The whole molecule was minimized by 1000 steps of steepest descent (SD) and 1000 steps of conjugate gradients by using SPDBV 4.0.1. The modeled structure (Figure 11) was further refined by molecular dynamics (MD) using Open MM Zephyr (Friedrichs et al, 2009). In MD simulations, the structure was minimized, followed by solvation in water. The simulations were then run for 10 ps a total of 5000 steps at room temperature (22°C) using Amber 96 force field. The quality of

model was verified using PROCHEK (Laskowski et al, 1993) available at NIH server. This model was docked with different peptides.

Molecular docking studies were performed by using AutoDock Vina (Trott et al, 2009). The binding site for the peptides on T2R1 was defined by forming a cube with the dimensions 60 x 70 x 70 around the protein with a grid point spacing 0.375Å and center grid boxes -15.241, 0.715 and 0.519 in X, Y and Z dimensions respectively. For each peptide 50 genetic algorithm runs were performed, and for each run the best pose was saved. Finally all the best poses of each run were superimposed and the most frequent orientation of the ligand was taken as the final pose. Then the protein-ligand complex was minimized by using 2000 steps of conjugate gradients. These minimized structures were used as the active forms for further study.
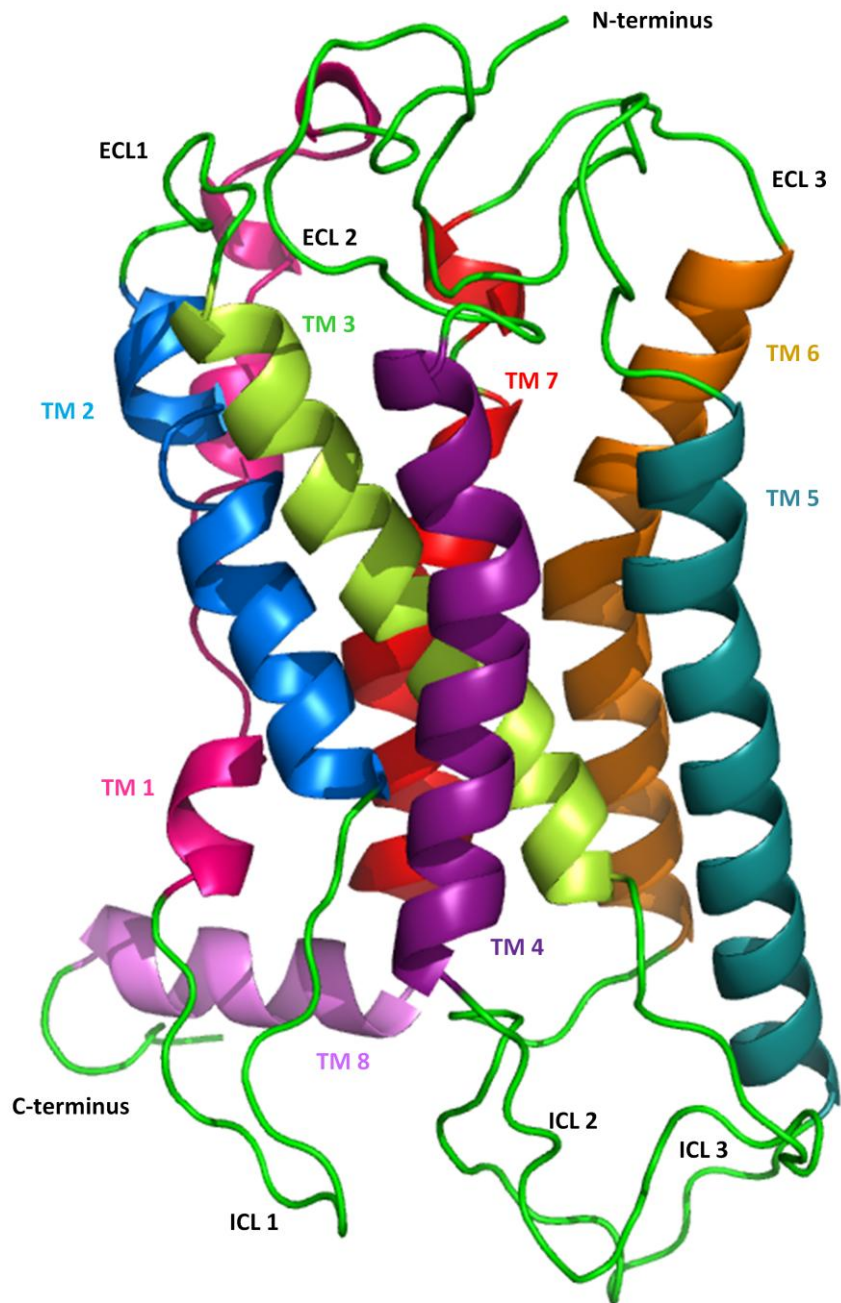
FIGURE 11. Three-dimensional structure of T2R1 receptor. Each transmembrane helix is shown in its respective color code. The loops near the N-terminus represent the extracellular loops (ECLs) and the loops near the C-terminus represent the intracellular loops (ICLs). The homology-derived model was built using the crystal structure of active opsin in complex with a C-terminal peptide of transducin (3DQB) as template. The transmembrane regions were modeled by MODELLER 9V7 and the loops were modeled using loop database of ModLoop software. The 3D structure was built using Pymol software.

CHAPTER THREE

RESULTS

3.1. Overexpression of T2R1-rho1D4 in HEK293S-TetR stable cell line

3.1.1. Sub-cellular localization

The sub-cellular localization of T2R1 expressed in the tetracycline-inducible

HEK293S stable cell line was determined by immunofluorescence using fluorescence

microscopy. The sub-cellular distribution of T2R1 in the HEK293S-TetR cells was

examined, before and after induction with tetracycline and sodium butyrate, using anti-

rho1D4 antibody for staining. The overexpressed T2R1 was found mainly localized at the

cell surface (Figure 12A). This localization is a strong indication of correct folding of

T2R1 because misfolded membrane proteins are retained in the endoplasmic reticulum

(ER) by the highly effective ER quality control system (Ellgaard et al, 2003). Owing to

the tight repression by tetR protein, in the absence of inducers, tetracycline and sodium

butyrate, HEK293S-TetR cells containing the T2R1 gene did not show any detectable

fluorescent signal (Figure 12B).

3.1.2. Western blot analysis of the expressed receptor

Western blot analysis of T2R1-rho1D4 expressed stably in tetracycline-

inducible HEK293S cells showed that T2R1 consisted of three major protein bands with

an apparent molecular mass in the range of 28-34 kDa (Figure 13). The three bands,

A.
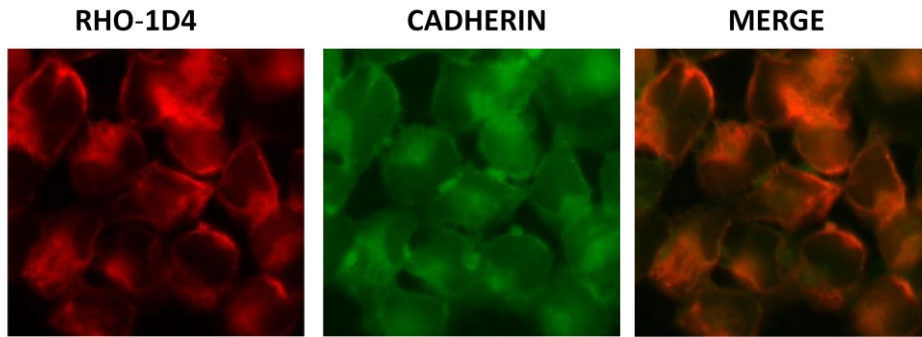
B.
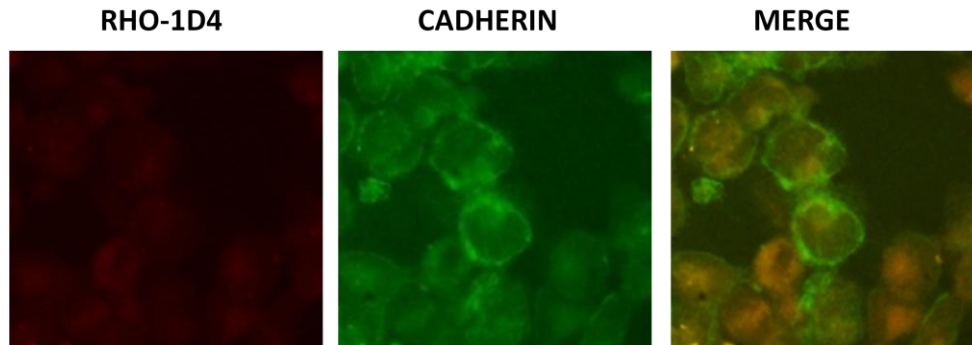
FIGURE 12. Localization of T2R1 overexpressed in HEK293S-TetR cell line. Dual-immunofluorescence was performed using mouse anti-rho1D4 antibody and rabbit anti-cadherin antibody (plasma membrane marker). Mouse rho-1D4 was visualized with goat anti-mouse Alexa 594 antibody (red) and rabbit anti-cadherin antibody was visualized with goat anti-rabbit Alexa 488 antibody (green). Following induction with tetracycline and sodium butyrate, T2R1 was expressed and localized at the plasma membrane (**A**), while T2R1 localization was not detected in the uninduced cells (**B**).

presumably, represent distinct heterogenous N-glycosylation states of the receptor (monomeric forms), with the higher band of 34 kDa corresponding to a fully N-glycosylated receptor. The upper band at around 64 kDa range probably represents the dimeric form of the receptor.

The complex N-glycans in the expressed integral membrane proteins (GPCRs) are reported to be extremely heterogenous in nature, which can pose a problem for biochemical and biophysical studies. To overcome this drawback, a HEK293 mutant expression system was developed in which N-glycan formation is restricted and homogenous (Reeves et al, 2002b). This cell line is resistant to ricin as a consequence of loss of N-acetylglucosamine transferase I (GnTI⁻) activity. Use of this cell line enabled the crystallization of a few integral membrane proteins. To remove the heterogeneously glycosylated protein bands, T2R1-rho1D4 was transiently expressed in HEK293S (GnTI⁻) cell line. T2R1, as expressed in this cell line, showed homogenous glycosylation pattern and migrated predominantly as a single band with an apparent molecular mass of ~34 kDa, and as a dimer which was observed at ~64 kDa (Figure 13). The observed molecular weight of 34 kDa is, thus, in agreement with the theoretically predicted molecular mass of 34.3 kDa for T2R1.

3.1.3. Quantitation of T2R1 receptor from western blot

The total amount of T2R1 receptor obtained after overexpression in tetracycline-inducible HEK293S cell line was determined by using quantitative
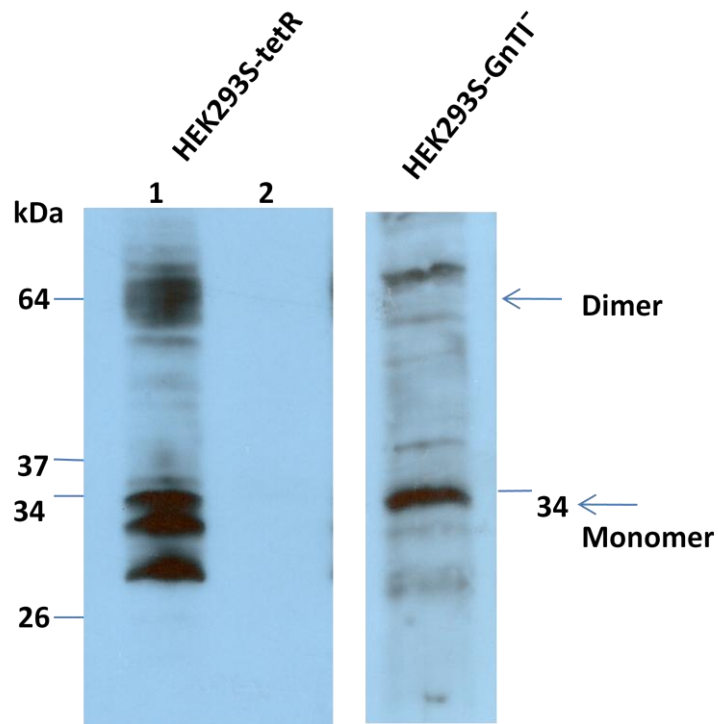
FIGURE 13. Western blot analysis of T2R1-rho1D4 using the monoclonal antibody rho-1D4. T2R1 stably expressed in HEK293S-tetR cell line, after induction with tetracycline and sodium butyrate, showed heterogenous glycosylation pattern (lane 1), whereas uninduced T2R1 did not show any detectable expression (lane 2). By using a HEK293S (GnTI⁻) cell line defective in N-acetylglucosamine transferase I, T2R1 was transiently expressed with restricted and homogenous N-glycosylation. 10 µg of DM-solubilized membrane protein was loaded in lanes 1 and 2 (HEK293S-tetR cells), while 40 µg of membrane protein was loaded from transiently transfected HEK293S-GnTI⁻ cells. Mobility of molecular weight standards is indicated on the left of the gel.

western blot analysis. For these assays, known amounts of purified bovine rhodopsin (200, 400, 600, 800 and 1000 pg) were used to generate a standard curve (Figure 14). The bovine rhodopsin was purified and western blot prepared by Dr. Chelikani according to previously published methods (Takayama et al, 2008). The pixel density of the protein bands was determined using Scion Image for Windows (Scion Corporation, Frederick, MD). The data were fit using a linear regression algorithm in Sigma plot v10.0 (SPSS Science, Chicago, IL). Quantitation of the western blot indicated that the expression levels for T2R1-rho1D4 expressed in HEK293S-tetR cells was ~ 60-70 ng/10 cm tissue culture plate.

3.2. Expression and functional characterization of T2R1-rho1D4 and T2R1-rho38 in rat glial cells

3.2.1. T2R1-rho1D4 and T2R1-rho38 genes

GPCRs, with the exception of light-sensitive opsins found in bacteria and in the retinae of higher organisms, occur at very low levels (Khorana, 1992). There are very few expression systems, except for rhodopsin, that yield reproducible levels of GPCRs. Studies have shown that many GPCRs, in particular sensory receptors, require specific chaperones for maturation and cell surface targeting (Baker et al, 1994; Dwyer et al, 1998). Chimeric receptors consisting of the first 20 amino acids of rhodopsin attached in-frame to the N-termini of various rodent olfactory receptors, enabled these receptors to be successfully targeted to the plasma membrane in HEK293 cells (Krautwurst et al, 1998).

During recent years, enormous progress in the deorphanization of hT2Rs has been achieved by functional heterologous expression of the receptors in mammalian cell lines. The first 39 amino acids of bovine rhodopsin were found to be very effective in targeting T2Rs to the plasma membrane of HEK293 cells (Chandrashekhar et al, 2000). The necessity to add amino-terminal 'export-tags' for proper functional expression at the cell surface indicates that, like most GPCRs, hT2Rs are expressed at very low levels in mammalian cells.

The T2R1-rho38 construct used in this study was a gift from Dr Kenji Maehashi, Tokyo University of Agriculture, Tokyo and contains the cDNA fragment encoding the first 38 amino acids of mouse rhodopsin in-frame with the 5'-end of human T2R1 coding cDNA sequence. The rhodopsin fragment was amplified from mouse cDNA, which was made by reverse transcriptase-PCR (RT-PCR) from total RNA extracted from mouse retina (Maehashi et al, 2008).

Codon-optimization has previously been shown to provide a means to increase the expression of genes (Bradel-Tretheway et al, 2003; Babcock et al, 2001; Farrens et al, 2002; Chelikani et al, 2006). To investigate if optimizing the codon usage could provide an alternate means of increasing the expression level of hT2R1, the second construct used in this study, T2R1 rho1-D4, was codon-optimized and tagged with a C-terminal octapeptide bovine rhodopsin epitope at the C-terminus. This epitope helps in detection of the protein by mouse monoclonal rho-1D4 antibody. Furthermore, the addition of a Kozak consensus sequence to T2R1-rho1D4 construct resulted in a change of the second amino acid from leucine to glycine in the coding sequence.

A.
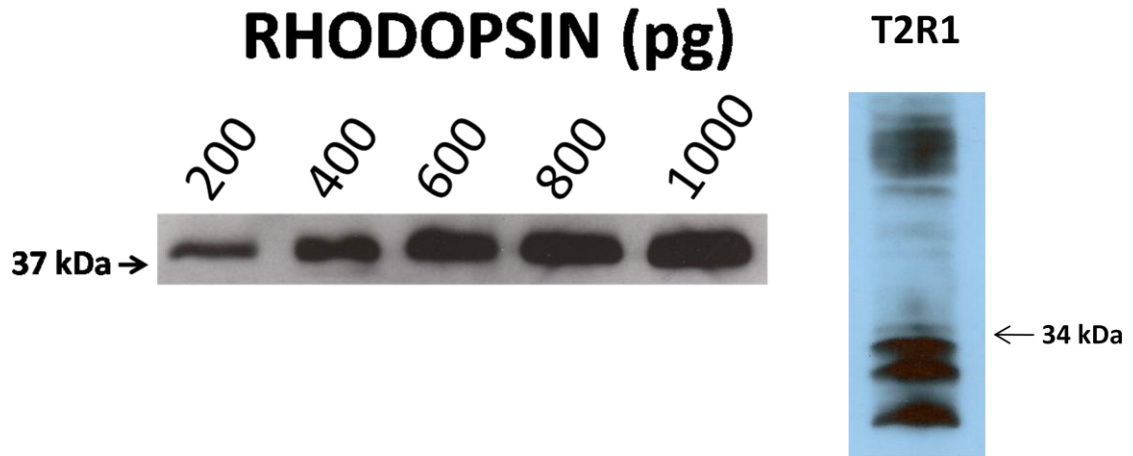
B.
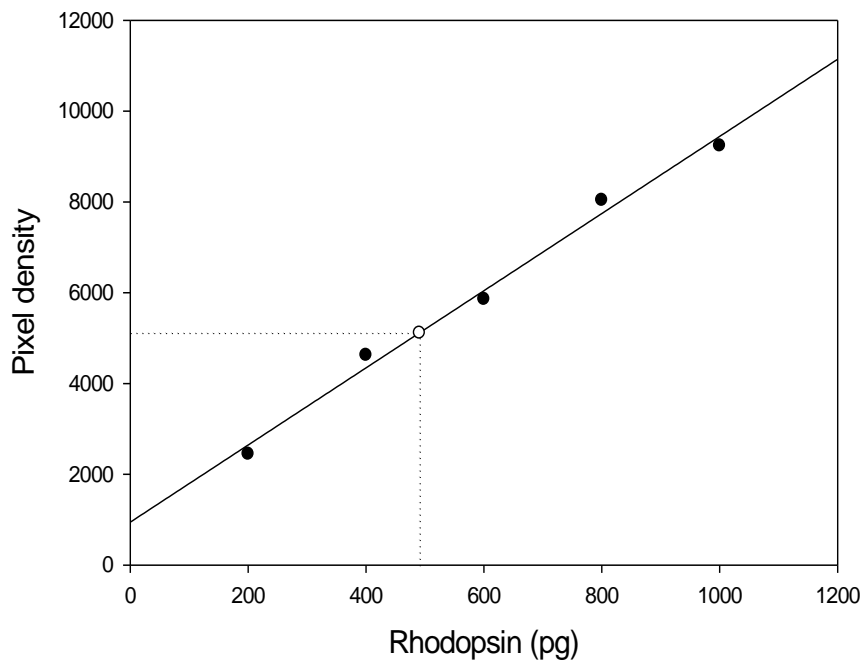
FIGURE 14. Quantitative analysis of T2R1 receptor expressed in HEK293S-TetR stable cell line. **A.** The increasing amounts of rhodopsin standards allow determination of the amount of the expressed T2R1. **B.** Determination of T2R1 expression level from comparison to the rhodopsin standards shown in A. To enable a direct comparison between the two blots, both the blots were exposed for the same amount of time (60 seconds). By this method, the expression level was found to be ~60 ng/10 cm culture dish.
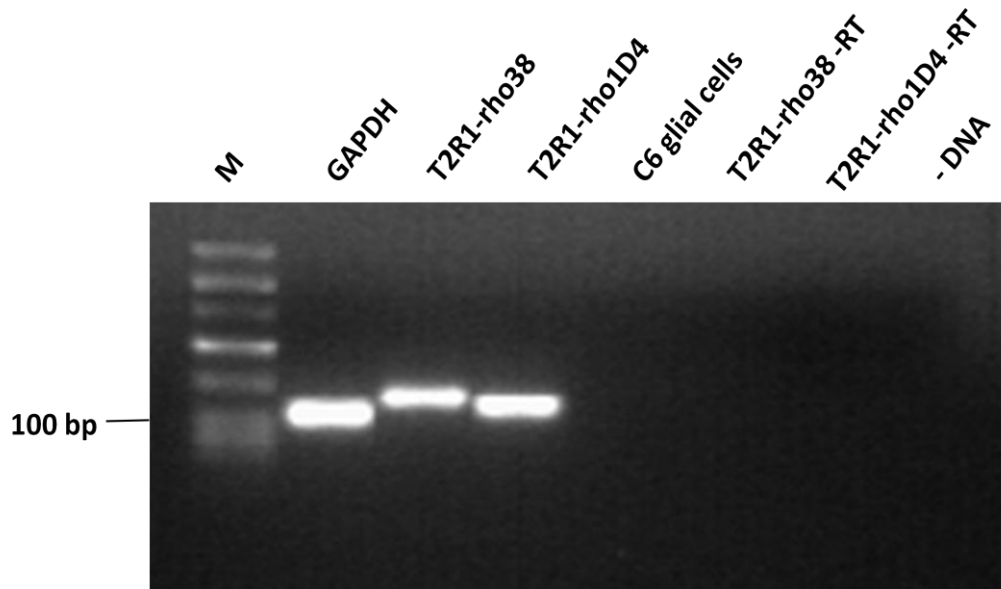
FIGURE 15. Reverse Transcriptase (RT)-PCR analysis of T2R1 expression in rat C6 glial cells. M indicates low molecular weight DNA marker; GAPDH was used as an internal control; untransfected glial cells were used to analyse the expression of endogenous T2R1 receptor; T2R1-rho38−RT and T2R1-rho1D4 −RT indicate that reverse transcriptase was omitted from the reaction to rule out the presence of contaminating genomic DNA; −DNA indicates a negative control with no template present. The amplified products were resolved on 2% agarose gel stained with ethidium bromide and visualized under UV light.

3.2.2. Reverse-Transcriptase (RT)-PCR analysis

RT-PCR was performed with total RNA extracted from T2R1-transfected rat glial cells. Recent studies have shown that T2Rs are also expressed in non-lingual tissues (Finger et al, 2003; Wu et al, 2002; Shah et al, 2009). RT-PCR of untransfected rat glial cells mRNA was done to investigate the expression of endogenous T2R1 receptor, using primers specific for rat and human T2R1 (Table III). The sequence homology between rat and human T2R1 is ~68%. Endogenous T2R1 gene was not detected in glial cells (Figure 15). Both the transfected human T2R1 constructs, T2R1-rho38 and T2R1-rho1D4, migrated on 2% agarose gel at the expected amplicon size of 129 bp and 118 bp respectively. This confirmed the T2R1 gene expression in glial cells following transient transfection. GAPDH was used as an internal control using primers specific for rat GAPDH (Table III). Controls which included omission of the reverse transcriptase were performed to rule out the presence of contaminating genomic DNA. A no template control (without any reverse-transcribed cDNA) was used as a negative control. Thus the expression observed in glial cells in figure 15 is specific for the transfected T2R1 genes.

3.2.3. Sub-cellular localization

Sub-cellular localization of the transiently transfected T2R1-rho1D4 construct in rat glial cells was elucidated by fluorescence microscopy. Immunofluorescence staining of the cells with mouse monoclonal anti-rho1D4 antibody showed that T2R1 was predominantly localized to the plasma membrane (Figure 16A) and was thus properly folded. Untransfected glial cells were used as a negative control and did not show any

A.

RHO-1D4   CADHERIN   MERGE

B.

RHO-1D4   CADHERIN   MERGE
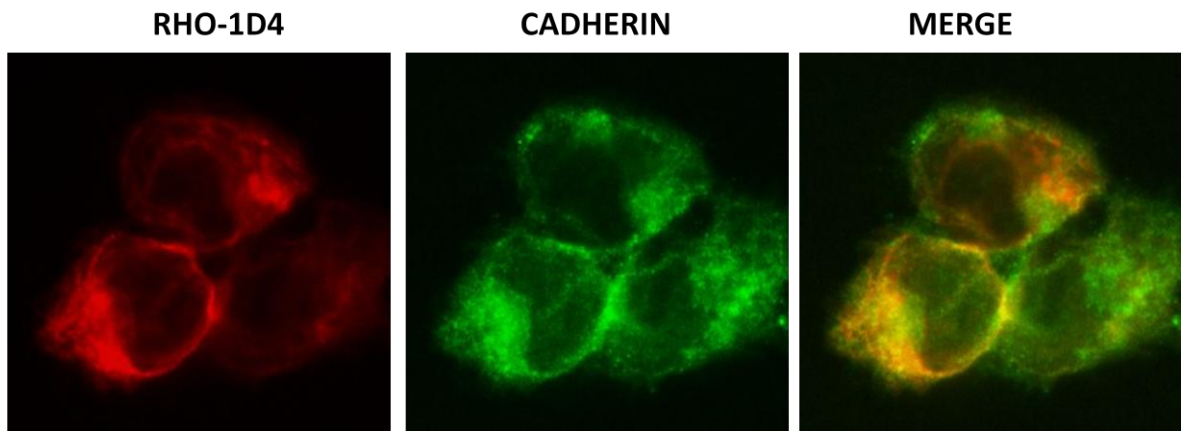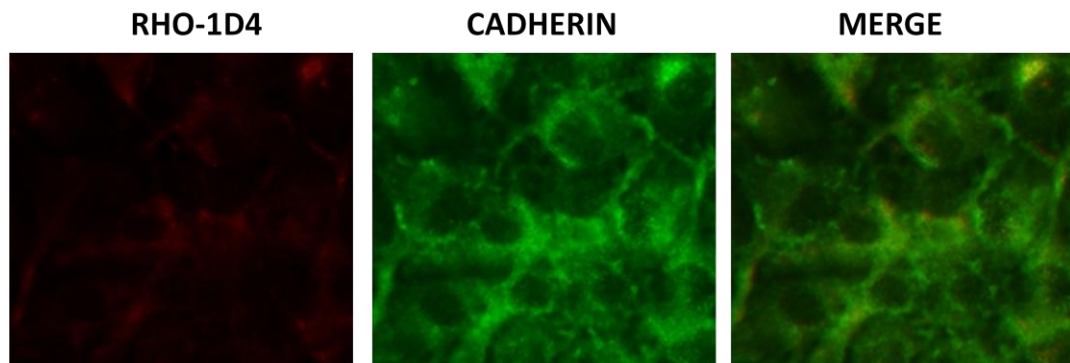
FIGURE 16. Immunofluorescence microscopy in rat C6 glial cells
A. Localization of T2R1-rho1D4 transiently expressed in rat C6 glial cells **B.**
Localization of untransfected glial cells. Dual-immunofluorescence was performed with
mouse anti-rho1D4 antibody and rabbit anti-cadherin antibody, which is localized at the
plasma membrane. Mouse rho-1D4 was visualized with goat anti-mouse Alexa 594
antibody (red) and rabbit anti-cadherin was visualized with goat anti-rabbit Alexa 488
antibody (green). Transiently expressed T2R1 was found localized to the cell membrane
of glial cells (A), whereas no expression of untransfected glial cells was detected with
anti-rho1D4 antibody (B).

staining with anti-rho1D4 antibody (Figure 16B).

3.2.4. Functional characterization of heterologously expressed T2R1

3.2.4.1. Peptide ligands of T2R1

Fermented foods contain numerous peptides which are derived from material proteins by proteolysis during the aging process. As bitterness is frequently generated during enzymatic processes that produce protein hydrolysates (Lovsin-Kukman et al, 1996), it was hypothesized that bitter peptides exist universally in fermented food products. Recent studies have shown that a couple of synthetic dipeptides, GF and GL, could stimulate T2Rs, with T2R1-expressing cells activated the most (Maehashi et al, 2008).

Some peptides in food have various health-related physiological activities, such as antihypertensive (angiotensin I-converting enzyme [ACE] inhibitory), opiod, antioxidative and antimicrobial activities (Yoshikawa et al, 2000). Many bitter dipeptides have been reported to have ACE-inhibitory activity (Pripp et al, 2007; Wu et al, 2007). With the viewpoint that bitterness of peptides could be considered for modification of the bioactive effect of fermented foods, I wanted to investigate whether T2R1 can be activated with synthetic di- and tri-peptides, some of which are reported to have ACE-inhibitory effects. The peptides and compounds used for elucidating the functional expression of T2R1 in rat glial cells are listed in Table IV.

Functional characterization of T2R1 was done by heterologous expression of the T2R1 genes in rat C6 glial cells, followed by measurement of changes in intracellular

68

calcium upon activation of the receptor. Fluorescence was measured from the bottom of

the 96-well plates and intracellular calcium changes were recorded for 200 seconds using

Flexstation 3. The instrument was set-up to read fluorescence as follows. The initial 20

seconds recorded the basal calcium levels of the unstimulated T2R1-expressing cells. The

test compounds were dispensed (50 μl per well) by the built-in 12 channel pipette and

after 20 seconds changes in intracellular calcium levels of the stimulated cells were

recorded in 51 reads at 4 second intervals for the next 180 seconds. Readings were taken

from seven different points in the well and averaged. A multi-channel pipetter was used

for any manual dispensing purposes, so that pipetting errors could be avoided. The

calcium efflux was calculated using the following formula

$$[Ca^{2+}] = K_d \times (F - F_{min}) / (F_{max} - F)$$

where F is the experimentally measured fluorescence intensity; F_{min} is the measured

fluorescence intensity in the absence of Ca^{2+}; F_{max} is the measured fluorescent intensity

of the Ca^{2+}-saturated dye; and K_d is the dissociation constant of the Ca^{2+} indicator. K_d

value of Fluo 4 calcium indicator dye is 345 nM (Takahashi et al, 1999) and its

absorption and emission spectra are in the range of 494 nM and 516 nM. The cutoff filter

option within these wavelengths available for 'Flex mode' was 515 nM, which is very

close to the emission wavelength of the Fluo 4-NW dye. Thus, the readings were taken at

an emission wavelength of 525 nM. Dose-response curves were established by plotting

intracellular calcium release versus log agonist concentration. The half maximal effective

concentrations (EC_{50}) were calculated by nonlinear regression using the equation

$$f(x) = 100/[1 + (EC_{50}/x)^{nH}]$$

where x is the agonist concentration and nH the Hill coefficient. All plots were constructed in Graphpad Prism. All the peptides were dissolved in water, except FFF, which was dissolved in DMSO.

3.2.4.1.1. Activation of T2R1 by synthetic dipeptides

Based on previous studies (Maehashi et al, 2008) and the published sensory bitterness threshold values (Ishibashi et al, 1987a, 1987b; Table IV), responses of T2R1-transfected cells to the three dipeptides, FL, IF and GF, were examined at concentrations ranging from 1 mM to 20 mM. The responses of mock-transfected (i.e. cells transfected with vector only) cells were subtracted from those of T2R1-expressing cells. Each dose-response is from a minimum of four independent experiments done in duplicate. Application of the dipeptides to T2R1-expressing cells elicited transient elevation of intracellular Ca^{2+} concentration.

Calcium release in the range of 70-80 nM was observed from the intracellular stores in glial cells, when T2R1 was stimulated with the dipeptide **FL** (Figure 17A). A robust response was seen with 10 mM and 20 mM of the peptide. A noticeable response was observed with 5 mM concentration, though the lower concentrations elicited weak responses in T2R1 receptor (Figure 17B). The EC_{50} value for FL determined from the dose-response curve was 7.2 ± 0.7 mM.

Stimulation of T2R1 with the dipeptide **IF** produced a calcium release of 60-65 nM (Figure 18A). Noticeable responses were seen with 5-20 mM, whereas at lower concentrations of the dipeptide, T2R1 showed a weaker signal (Figure 18B). The EC_{50} for IF calculated from the FLIPR readings was 7.4 ± 0.9 mM.
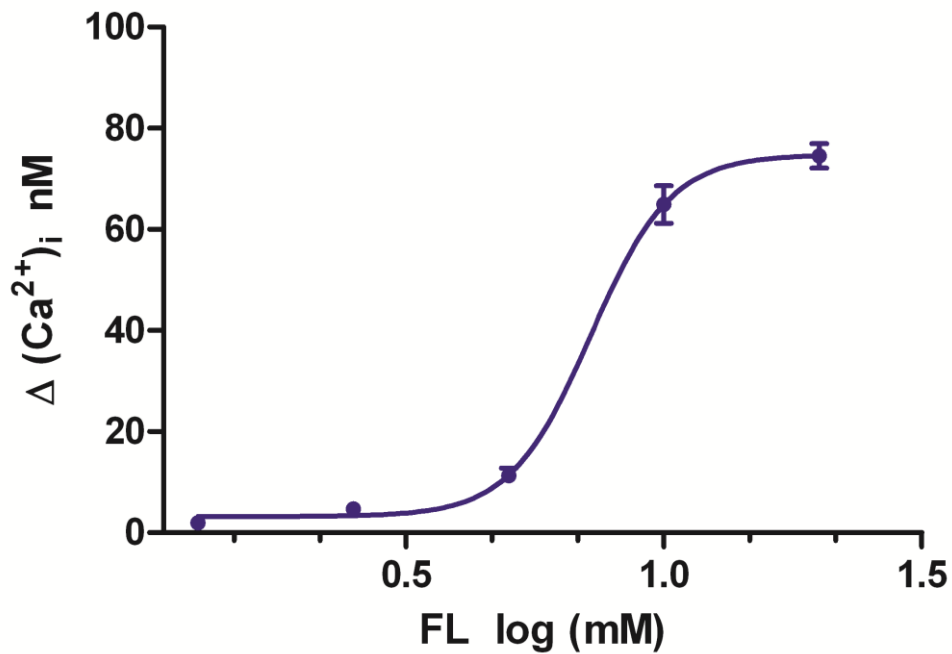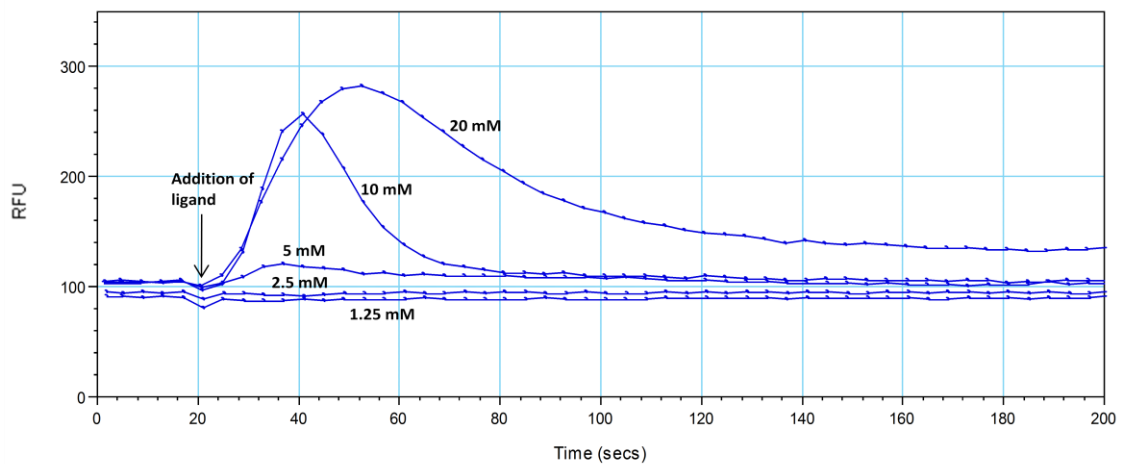
**FIGURE 17. Dose-dependent increases in intracellular calcium [Ca^{2+}] induced by bitter peptide FL in C6 glial cells A.** Dose-response curve of T2R1 stimulated with increasing concentrations of the synthetic di-peptide **FL** after subtraction of the responses of mock-transfected cells. **B.** FLIPR recordings of calcium responses of glial cells expressing T2R1 to the dipeptide FL. The concentrations used are shown next to the plot. The data shown is representative of one experiment. Abbreviation: RFU, relative fluorescent units.
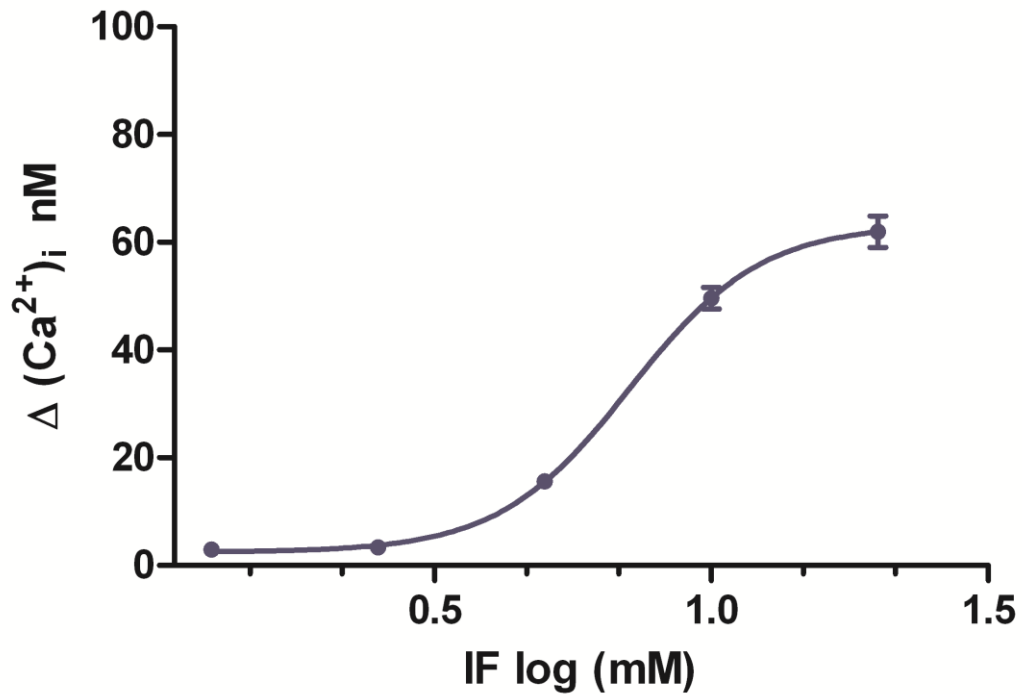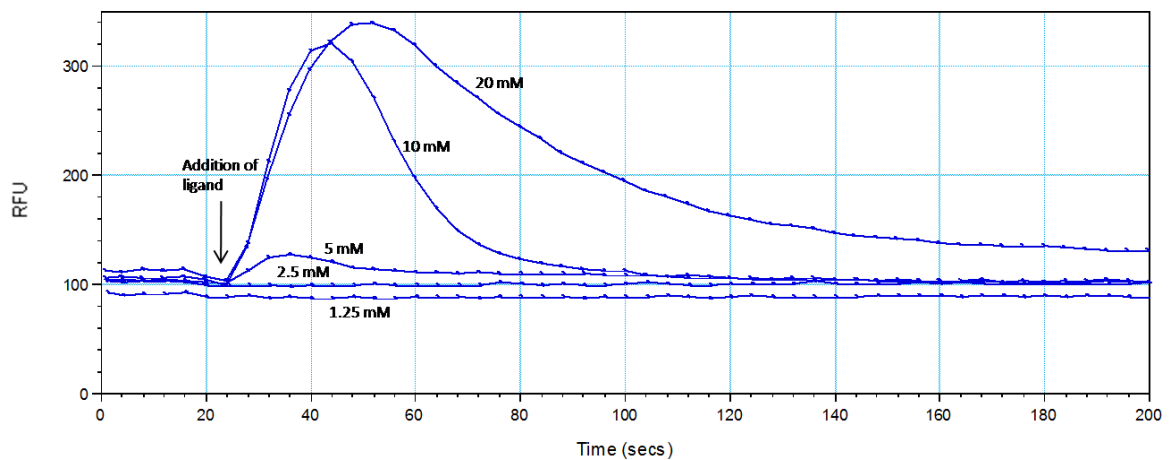
FIGURE 18. Dose-dependent increases in intracellular calcium [Ca^{2+}] induced by bitter peptide IF in C6 glial cells A. Dose-response curve of T2R1 stimulated with increasing concentrations of the synthetic di-peptide **IF** after subtraction of the responses of mock-transfected cells. **B.** FLIPR recordings of calcium responses of glial cells expressing T2R1to dipeptide IF. The concentrations used are shown next to the plot. The data shown is representative of one experiment. Abbreviation: RFU, relative fluorescent units.
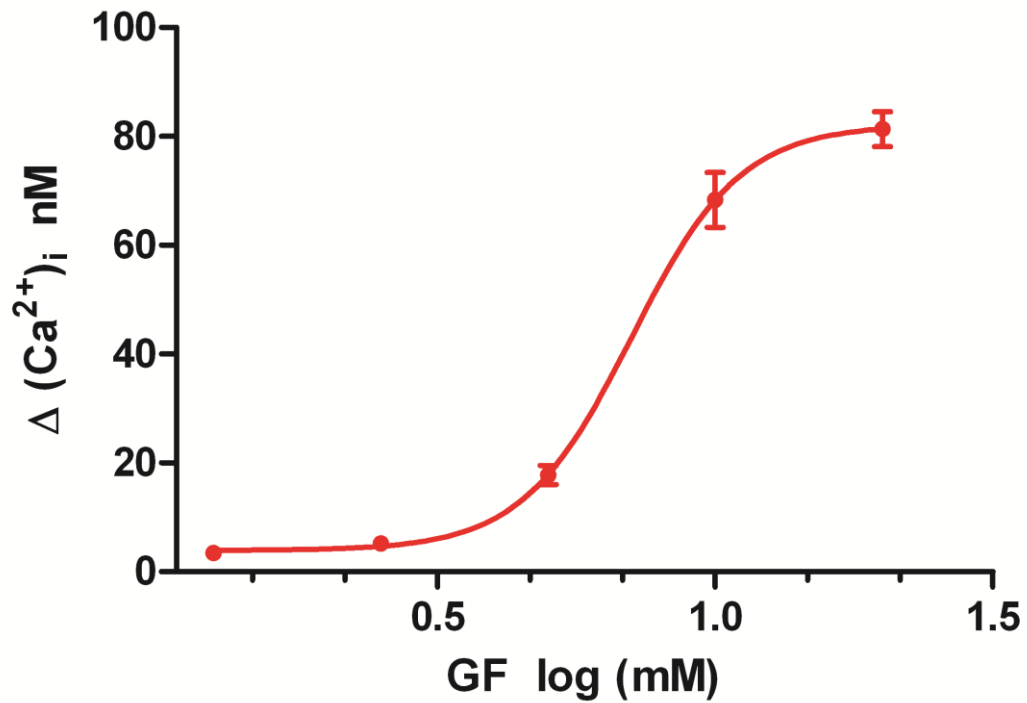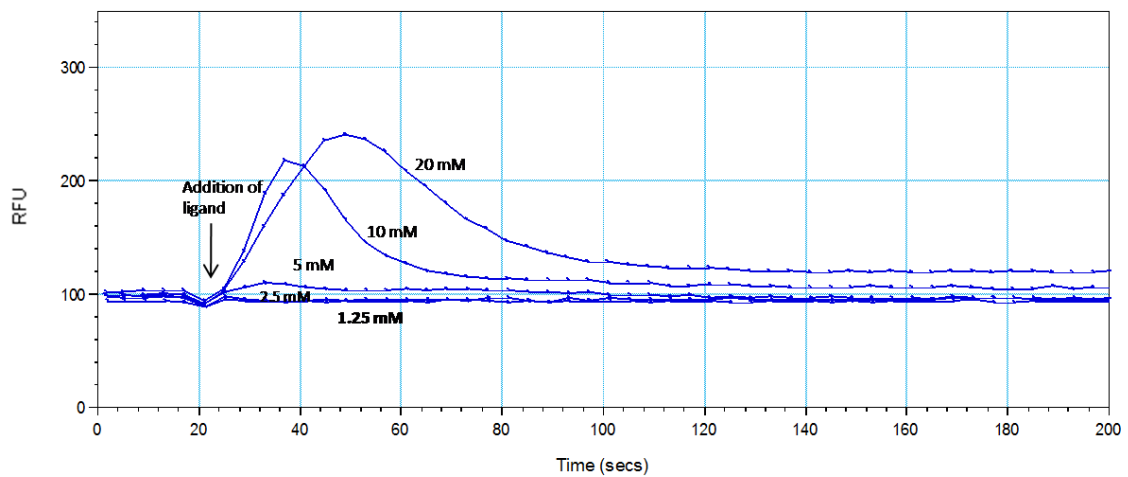
FIGURE 19. Dose-dependent increases in intracellular calcium [Ca^{2+}] induced by bitter peptide GF in C6 glial cells A. Dose-response curve of T2R1 stimulated with increasing concentrations of the synthetic di-peptide **GF** after subtraction of the responses of mock-transfected cells. **B.** FLIPR recordings of calcium responses of glial cells expressing T2R1 to dipeptide GF. The concentrations used are shown next to the plot. The data shown is representative of one experiment. Abbreviation: RFU, relative fluorescent units.

TABLE IV. Summary of the biochemical and sensory properties of synthetic peptide ligands and their ability to activate the human bitter receptor, T2R1

Peptide	Bitterness threshold[a] (mM)	Rcaf[b]	ACE-inhibitory activity[c]	EC$_{50}$[d] (mM)
GF	1.2	0.83	No	7.3 ± 1.1
FL	1.5	0.67	No	7.2 ± 0.7
IF	1.5	0.67	Yes	7.4 ± 0.9
FFF	0.2	5.0	No	$0.37 \pm .11$
GLL	1.5	0.67	No	4.9 ± 0.7
IRW	-	-	Yes	-
IQW	-	-	Yes	6.1 ± 2
LKP	-	-	No	7.6 ± 1.2
Dextromethorphan*	-	-	No	0.031

[a] Published values from sensory test (Ishibashi et al, 1987).
[b] Ratio of bitterness to caffeine (Ishibashi et al, 1987).
[c] Published literature values (Aluko et al, 2006).
[d] Values determined by calcium dose-response functional assays (from this study).
*Bitter compound

Stimulation with the dipeptide GF evoked an intracellular calcium release of 80-90 nM in T2R1-expressing cells (Figure 19A). Robust transient responses were noticed with concentrations of 5-20 mM, with T2R1 responding to GF with an EC_{50} value of 7.3 $\pm$ 1.1 mM.

3.2.4.1.2. Activation of T2R1 by synthetic tripeptides

The relationship between bitterness and the structure of peptides has been studied extensively (Ney et al, 1971; Matoba et al, 1972). There is believed to be an empirical correlation between the hydrophobicity of the peptides and their bitter taste (Guigoz et al, 1976; Lemieux et al, 1992). Matoba et al also proposed that hydrophobic residue in peptides functioned as a bitter taste determinant site.

The presence of the hydrophobic phenylalanine (F) is known to cause the bitter taste in any peptide, this bitterness is enhanced when it forms a dimer or trimer (Ishibashi et al, 1987b). A 100 times greater bitterness than that of phenylalanine (F) has been observed in the taste of tri-phenylalanine (FFF). Based on the bitterness sensory threshold value of 0.2 mM, T2R1 activation in response to the tripeptide FFF was examined at concentrations ranging from 0.0625 mM to 1 mM. T2R1-expressing cells showed calcium responses of 140-150 nM when stimulated with increasing concentrations of FFF (Figure 20A). Noticeable responses were seen with 0.25 mM and 0.5 mM, with signal saturation obtained with 1 mM of the tripeptide. The EC_{50} value determined from the calcium recordings was 0.37 $\pm$ 0.11 mM.

Stimulation with the tripeptide GLL resulted in transient elevation of 40-50 nM

A.
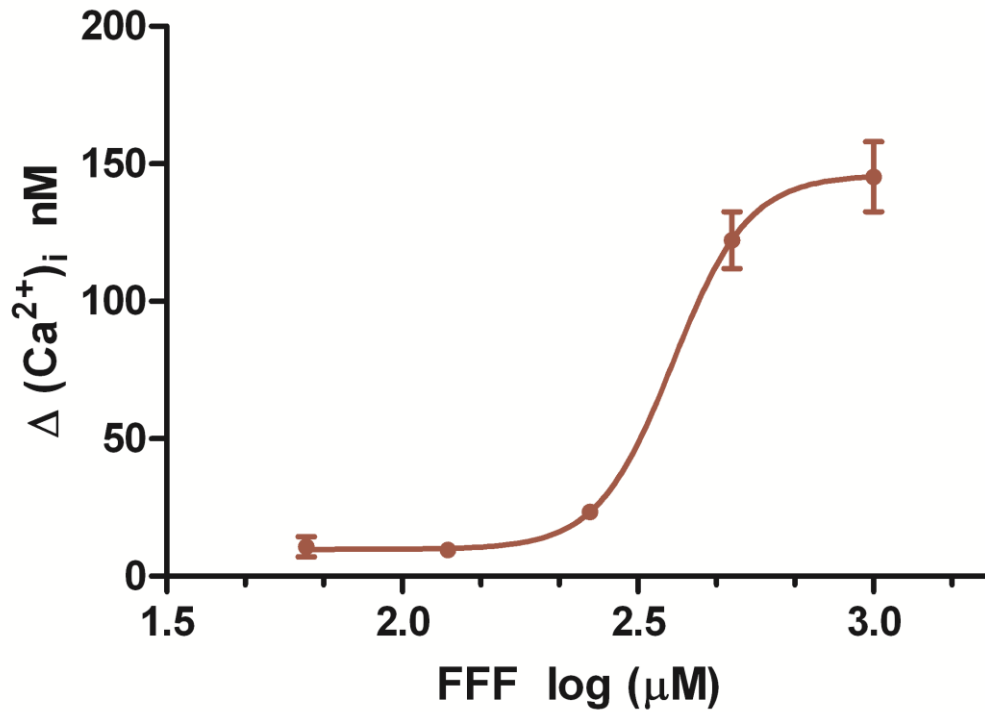
B.
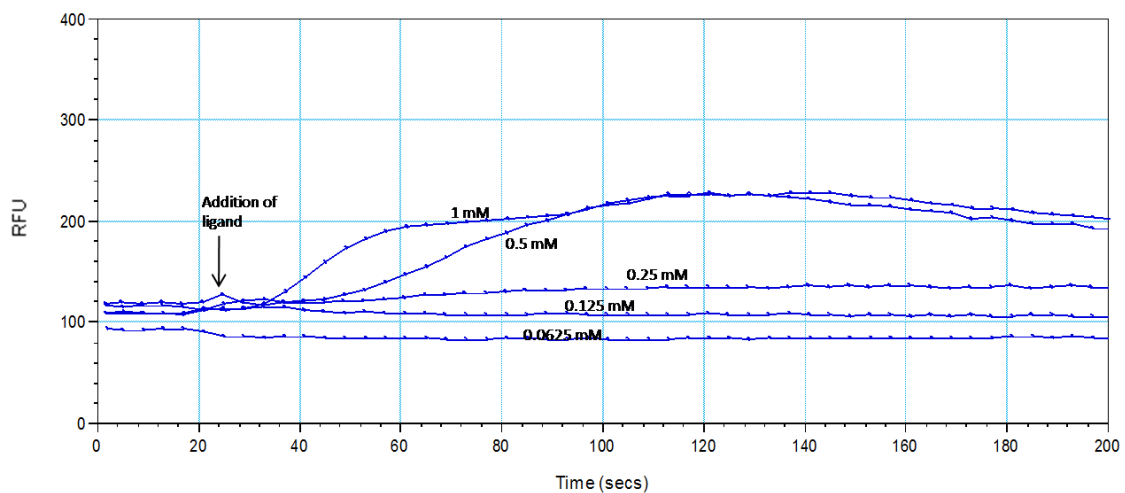
FIGURE 20. Dose-dependent increases in intracellular calcium [Ca^{2+}] induced by bitter peptide FFF in C6 glial cells A. Dose-response curve of T2R1 stimulated with increasing concentrations of the synthetic tri-peptide **FFF** after subtraction of the responses of mock-transfected cells. **B.** FLIPR recordings of calcium responses of glial cells expressing T2R1 to tripeptide FFF. The concentrations used are shown next to the plot. The data shown is representative of one experiment. Abbreviation: RFU, relative fluorescent units.

A.
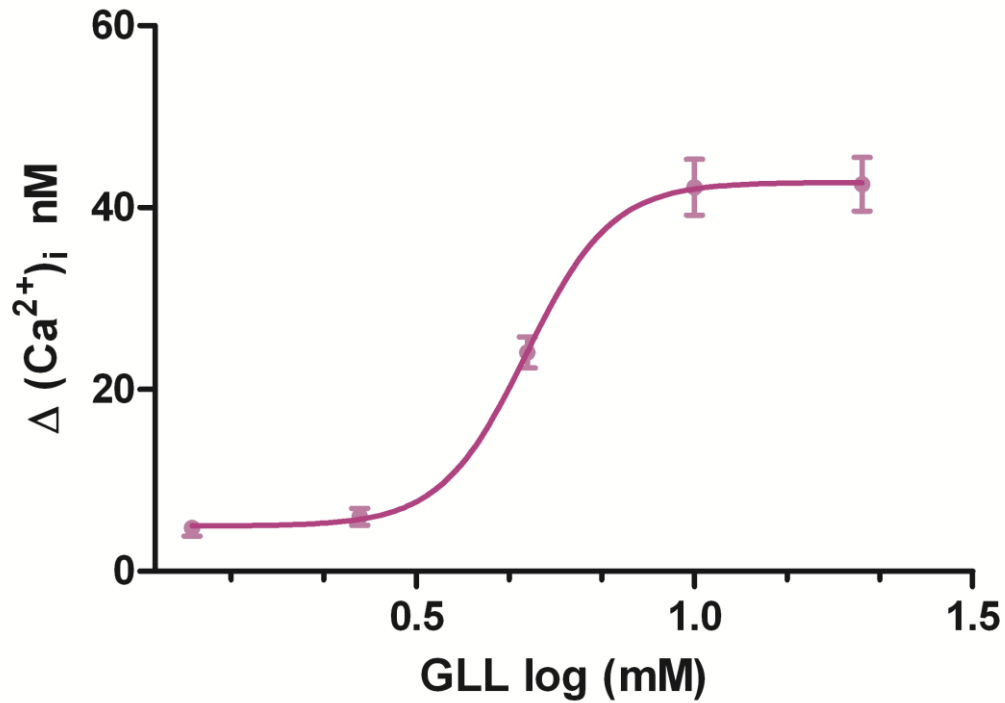
B.
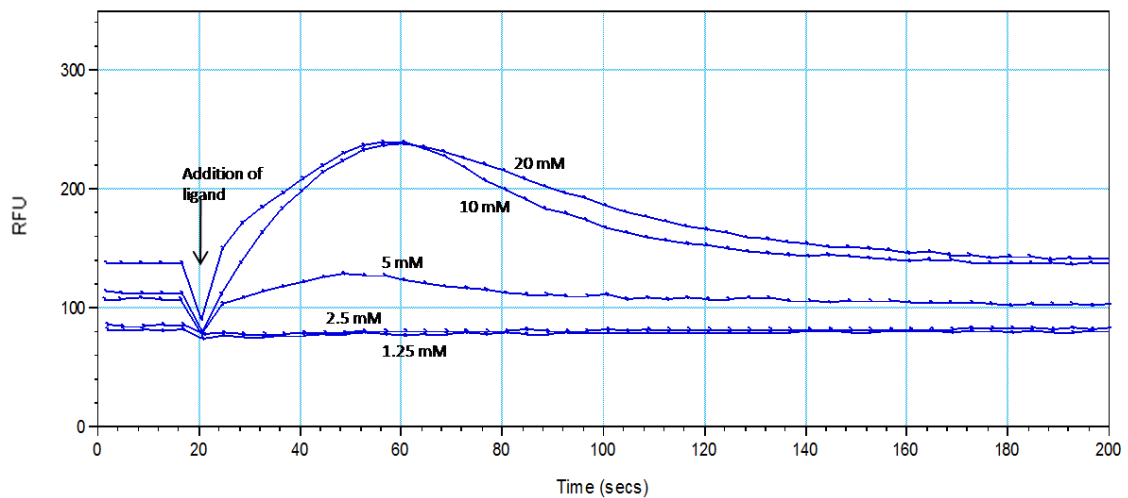
FIGURE 21. Dose-dependent increases in intracellular calcium [Ca^{2+}] induced by bitter peptide GLL in C6 glial cells A. Dose-response curve of T2R1 stimulated with increasing concentrations of the synthetic tri-peptide **GLL** after subtraction of the responses of mock-transfected cells. **B.** FLIPR recordings of calcium responses of glial cells expressing T2R1 to tripeptide GLL. The concentrations used are shown next to the plot. The data shown is representative of one experiment. Abbreviation: RFU, relative fluorescent units.

in intracellular calcium levels (Figure 21A) with receptor saturation seen with 20 mM of the tripeptide. Weak responses were noticed with the lower concentrations. T2R1-expressing cells responded to GLL with an EC_{50} value of 4.9 ± 0.7 mM.

The ACE-inhibitory peptide, IRW, was unable to induce a significant Ca^{2+} response in glial cells expressing T2R1 with upto 5 mM of the tripeptide (Figure 22A). Due to availability of the peptide in limiting amounts and signal saturation not obtained even with 10 mM concentration, determination of EC_{50} was not pursued for IRW.

T2R1 stimulation with IQW, another ACE-inhibitory peptide, evoked intracellular calcium release of approximately 100-120 nM (Figure 23A). Responses were examined with 1.25 mM to 20 mM of the tripeptide. Receptor saturation was reached with 15 mM (Figure 23B), beyond which a reduction in the signal was noticed. Robust elevation of calcium levels was seen with stimulation above 2.5 mM of the peptide and a noticeable response was seen with 5 mM. T2R1 receptor responded to IQW with an EC_{50} value of 6.1 ± 2 mM.

LKP induced an intracellular calcium change of 90-100 nM in T2R1-expressing glial cells (Figure 24A). The concentrations tested ranged from 1 mM to 20 mM, but the highest concentration showed an inhibitory effect on T2R1 activation. Signal saturation was noticed with 15 mM and noticeable responses were seen with 7.5 mM of the tripeptide (Figure 24B). T2R1 showed weak responses with concentrations below 5 mM and it responded to LKP with an EC_{50} value of 7.6 ± 1.2 mM.
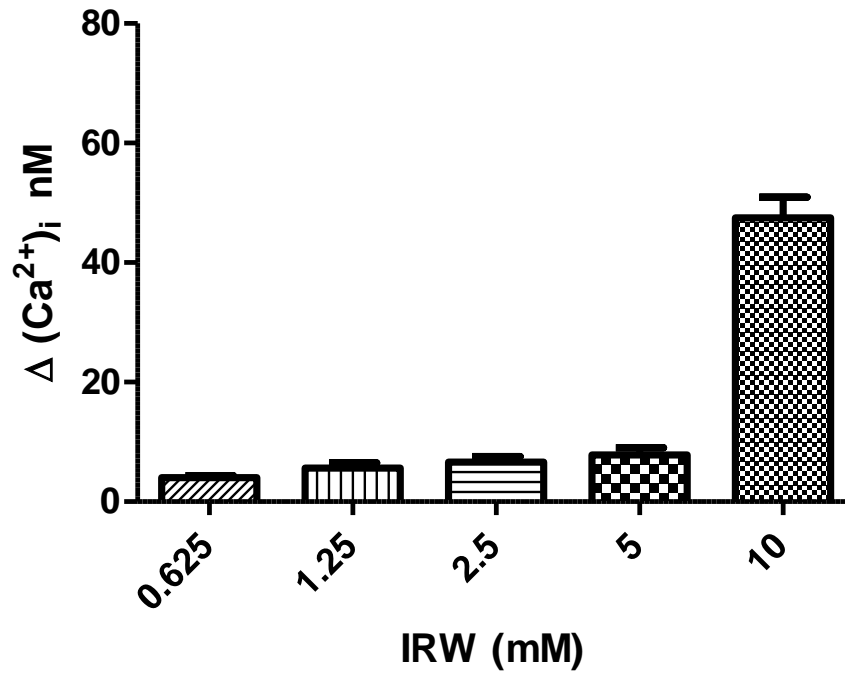
FIGURE 22. Bar plot showing dose-dependent changes in intracellular calcium due to stimulation of T2R1-expressing glial cells with different concentrations of **IRW**, after responses of mock-transfected cells were subtracted.
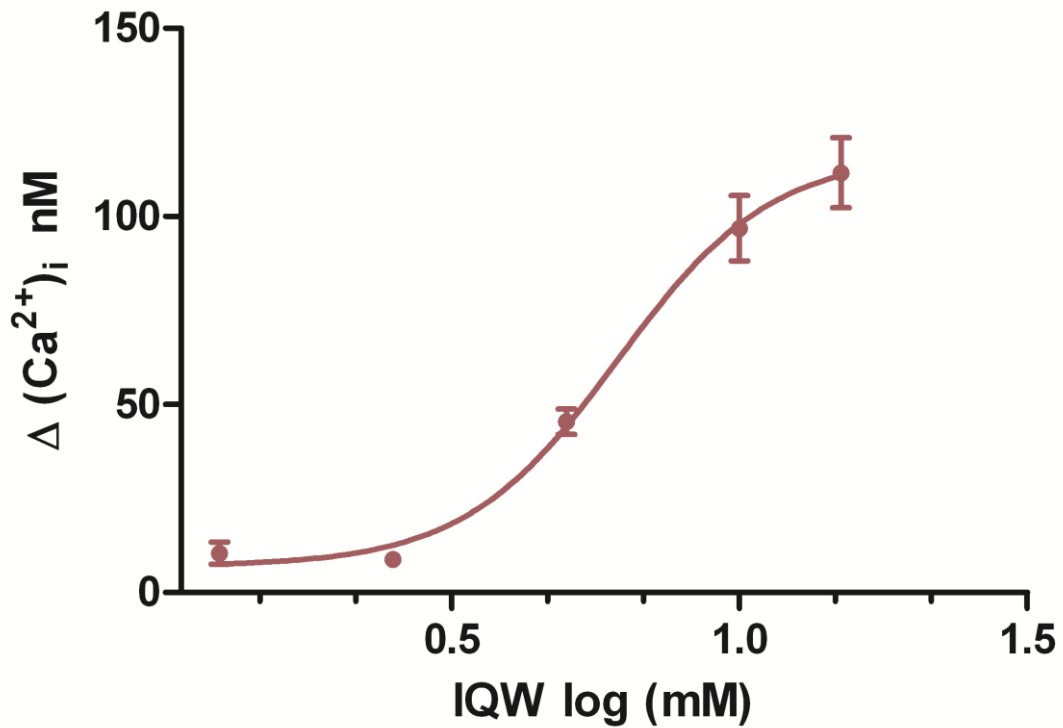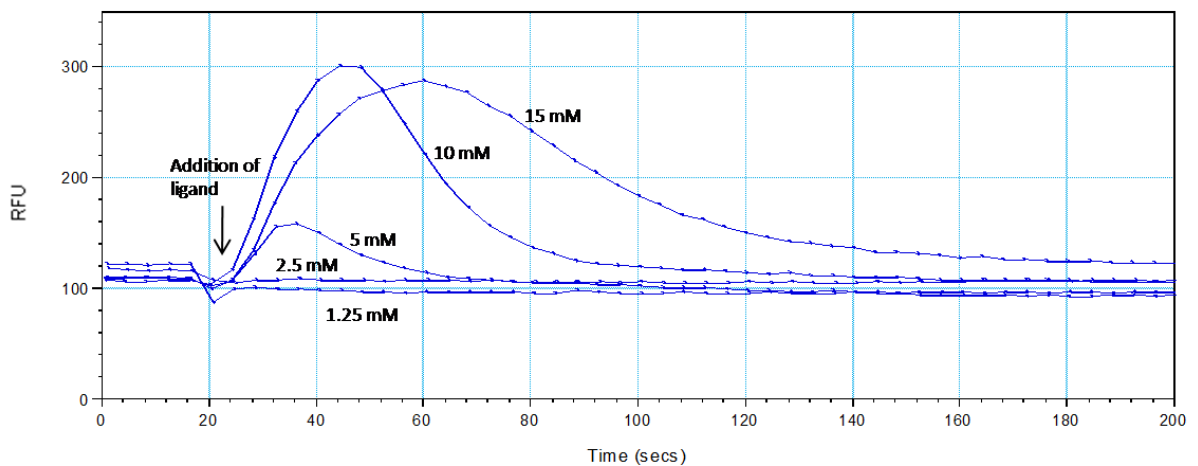
FIGURE 23. Dose-dependent increases in intracellular calcium [Ca^{2+}] induced by bitter peptide IQW in C6 glial cells A. Dose-response curve of T2R1 stimulated with increasing concentrations of the synthetic tri-peptide **IQW** after subtraction of the responses of mock-transfected cells. **B.** FLIPR recordings of calcium responses of glial cells expressing T2R1 to tripeptide IQW. The concentrations used are shown next to the plot. The data shown is representative of one experiment. Abbreviation: RFU, relative fluorescent units.

A.
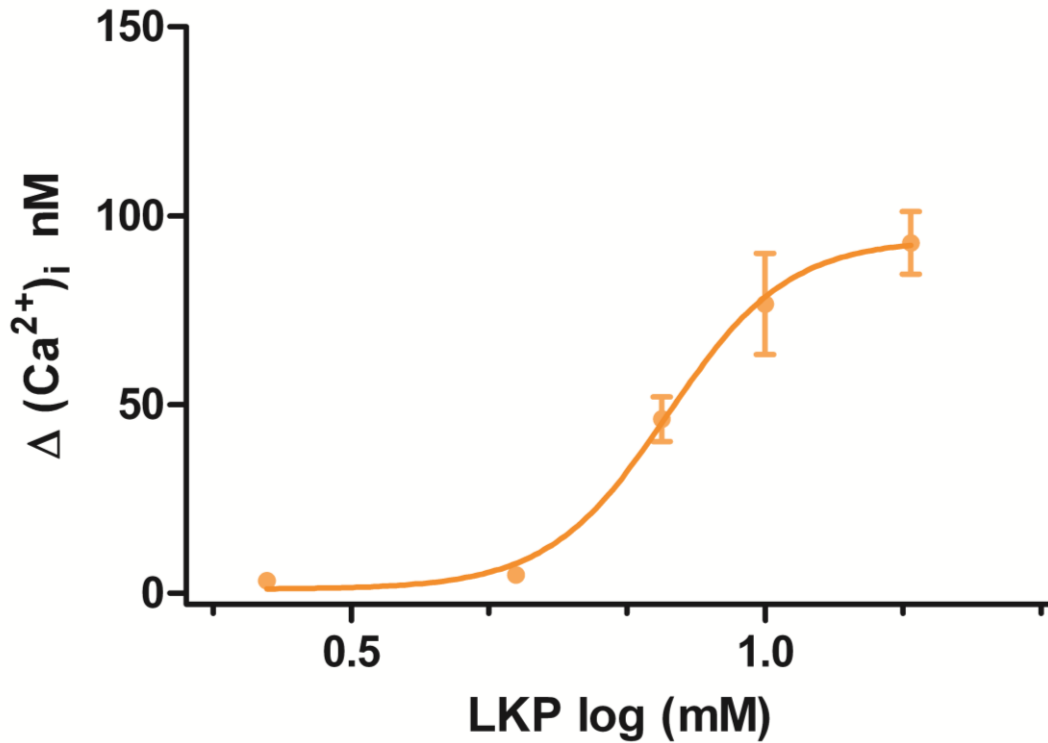
B.
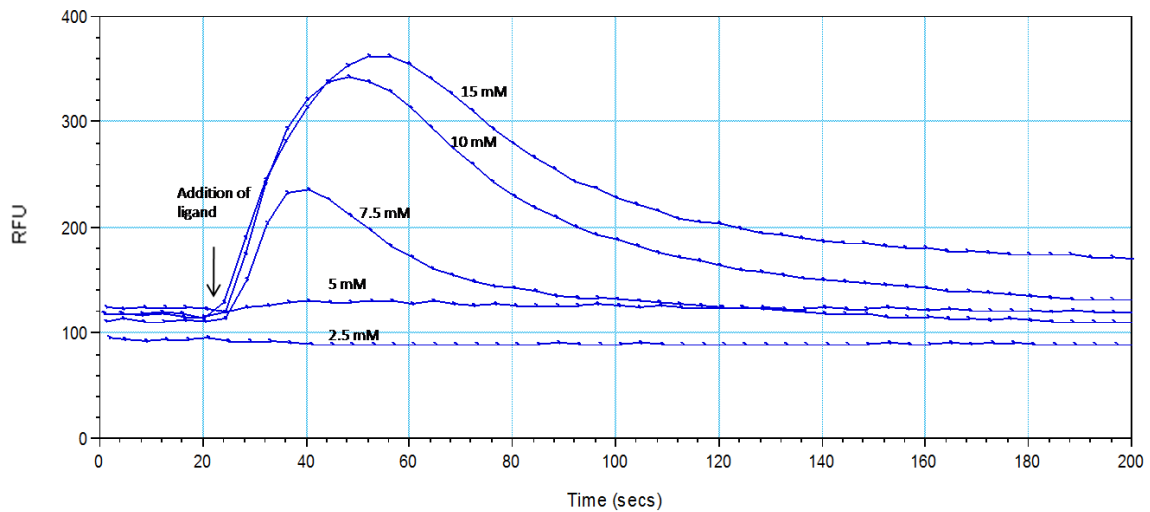
**FIGURE 24. Dose-dependent increases in intracellular calcium [Ca^{2+}] induced by bitter peptide LKP in C6 glial cells A.** Dose-response curve of T2R1 stimulated with increasing concentrations of the synthetic tri-peptide **LKP** after subtraction of the responses of mock-transfected cells. **B.** FLIPR recordings of calcium responses of glial cells expressing T2R1 to tripeptide LKP. The concentrations used are shown next to the plot. The data shown is representative of one experiment. Abbreviation: RFU, relative fluorescent units.

A.
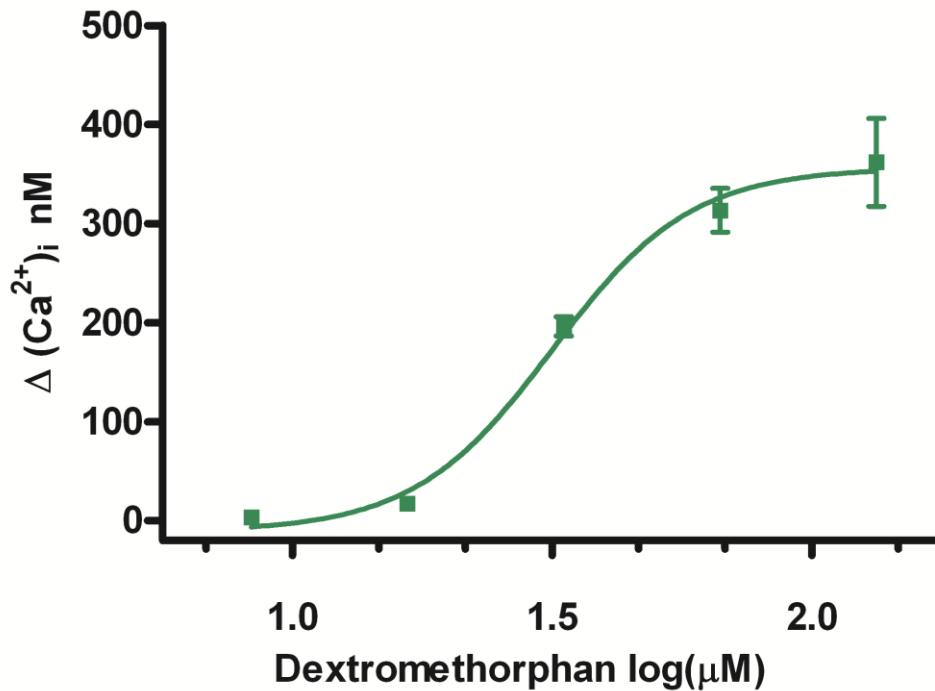
B.
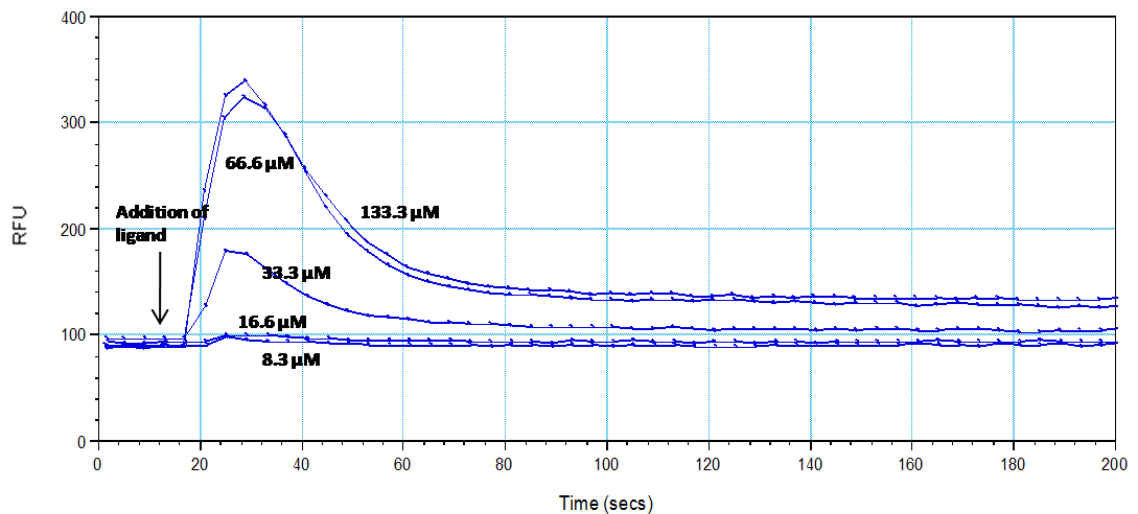
FIGURE 25. Dose-dependent increases in intracellular calcium [Ca^{2+}] induced by bitter compound dextromethorphan in C6 glial cells A. Dose-response curve of T2R1 stimulated with increasing concentrations of dextromethorphan after subtraction of the responses of mock-transfected cells. **B.** FLIPR recordings of calcium responses of glial cells expressing T2R1 to dextromethorphan. The concentrations used are shown next to the plot. The data shown is representative of one experiment. Abbreviation: RFU, relative fluorescent units.
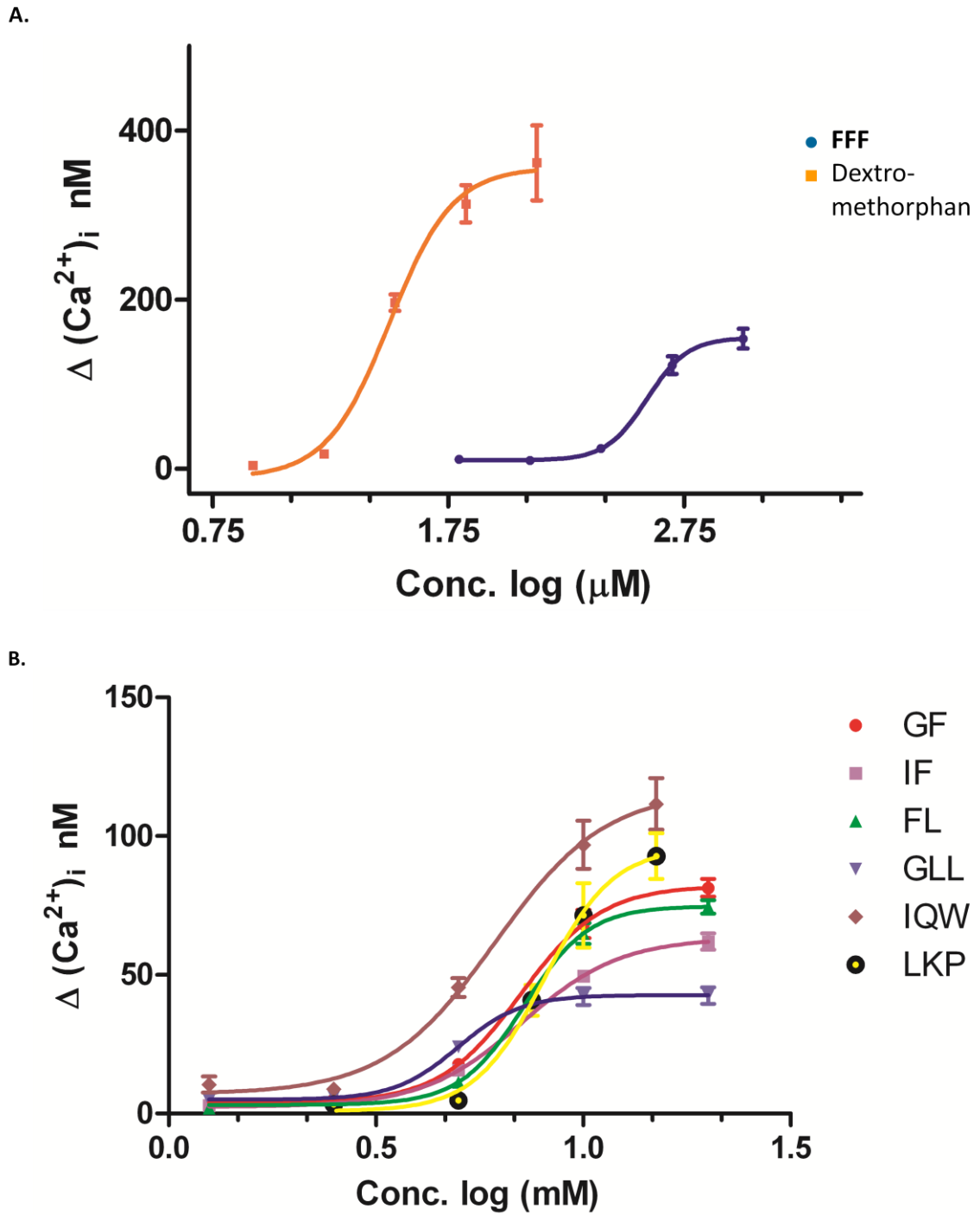
FIGURE 26. Dose-dependent increases in intracellular calcium induced by bitter ligands in C6 glial cells A. Dose-response curve of T2R1 activation in response to increasing concentrations of FFF and the bitter compound dextromethorphan. The responses of mock-transfected cells have been subtracted. **B.** Dose-response curve of T2R1 stimulated with increasing concentrations of different bitter peptides.
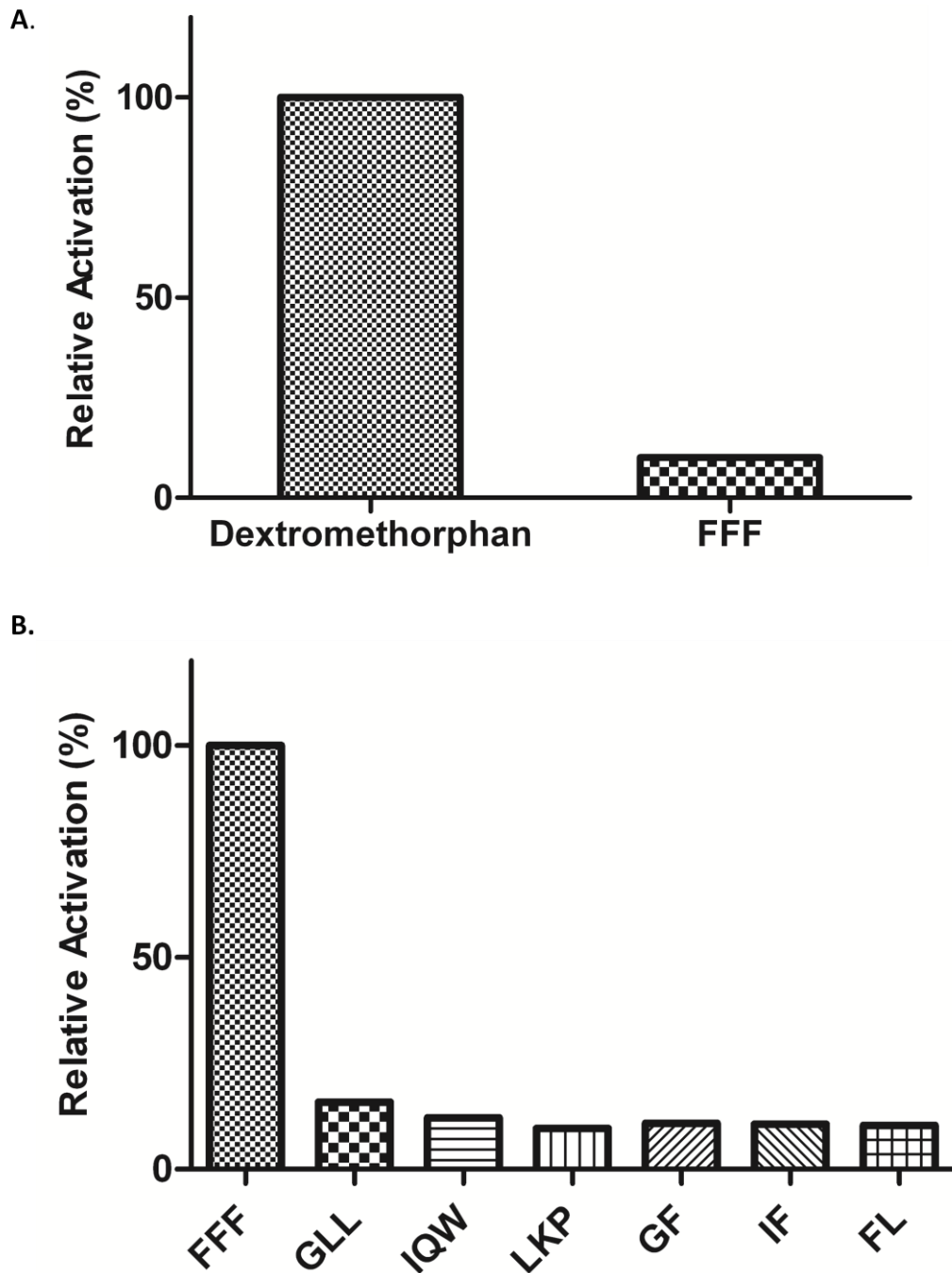
FIGURE 27. Activation rates of T2R1 upon stimulation with bitter ligands A. Relative activation rates of T2R1 in response to stimulation by the tripeptide FFF and the bitter compound dextromethorphan. The activation rates were plotted based on their EC_{50} values. FFF is normalized to the EC_{50} value of dextromethorphan. **B.** Relative activation rates of T2R1 in response to different bitter peptides. All values were normalized to the EC_{50} value of FFF.

3.2.4.2. Activation of T2R1 by dextromethorphan

Application of increasing amounts of dextromethorphan to T2R1-expressing cells elicited robust transient elevation of cytosolic Ca^{2+} concentration of 300-350 nM, with dextromethorphan concentrations between 8 µM to 166 µM (Figure 25A). The tested concentrations were selected based on previous published minimum-threshold value of 10 µM from FLIPR experiments (Meyerhof et al, 2010). Marked responses were seen with concentrations exceeding 16 µM (Figure 25B), and signal saturation was obtained with 166 µM of dextromethorphan. The EC_{50} determined from FLIPR data was 31.68 ± 8.7 µM.

Figure 26A shows the dose-response curves of the effect of increasing concentrations of the tripeptide FFF and the bitter compound dextromethorphan on T2R1 activation. The dose-response curves of T2R1 stimulation in response to different bitter peptides are shown in Figure 26B. The relative activation rates of T2R1 in response to FFF and dextromethorphan, and to different bitter di- and tri-peptides have been shown as bar plots in Figure 27 A and B. The activation rates were plotted based on the EC_{50} values of the ligands. Values were normalized to the EC_{50} of dextromethorphan in Figure 28A, and to the EC_{50} of FFF in Figure 27 B.

3.3. Mapping the ligand-binding pocket of T2R1 by homology modeling

A three-dimensional structure of T2R1 was built by homology modeling using a rhodopsin template and ligands docked to the structure as described in methods section. The predicted site of interaction of the tripeptide FFF with T2R1 receptor is shown in
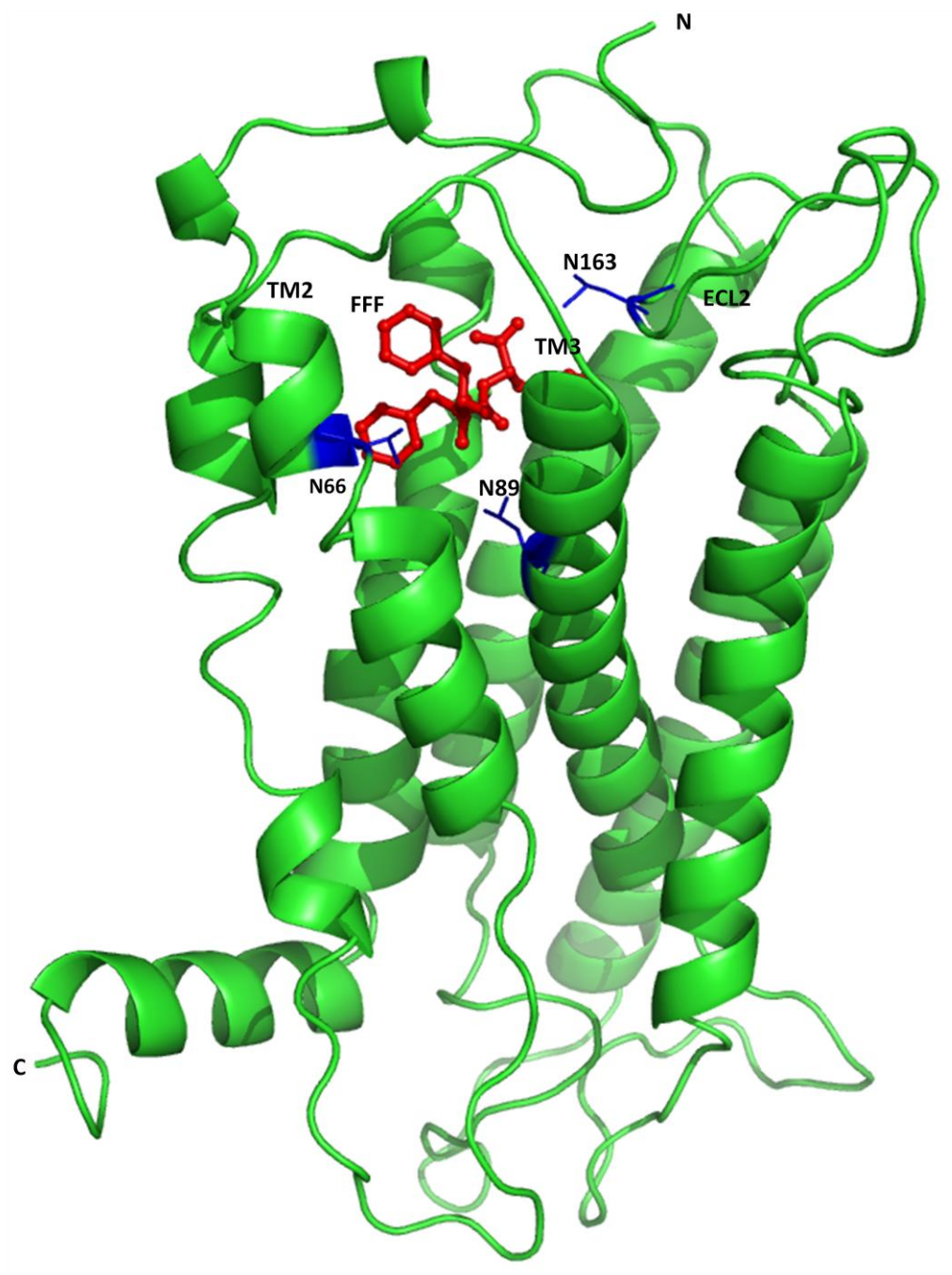
FIGURE 28. Molecular model of T2R1 bound to the tripeptide FFF. FFF was docked to the receptor using AutoDock Vina. The ligand is represented as sticks in red, and the residues in contact, N66 in TM 2, N89 in TM 3 and N163 in ECL2, are shown as lines in blue. N represents the N-terminus and C represents the C-terminus of the receptor.

TABLE V. Amino acid residues lining the ligand-binding pocket of T2R1

No.	Ligand	Predicted binding affinity (kcal/mol)	Amino acids in 4 Å binding pocket of T2R1 (Residues in contact with the ligand are shown in bold)	
			Residues in TMs	Residues in ECLs
1.	FFF	-9.5	I62, **N66**, V69, I70 , L86, **N89**, E90, H240, L260, 261, F262, I263	E74, **N163**
2.	IQW	-8.5	L19, T23, I62, F63, **N66**, V69, I70, L85, L86, N89, **E90,** F261, I263, L264, G267	E74
3.	Dextromet horphan	-8.2	T23, F63, **N66**, I70, F257, F261, I263	
4.	GF	-6.3	F16, **N66**, I70, L86, N89, F257, F261	**E74**
5.	IF	-7.4	F16, L19, F22, T23, I26, I62, F63, **N66**, I70, F261, I263, L264, L264	
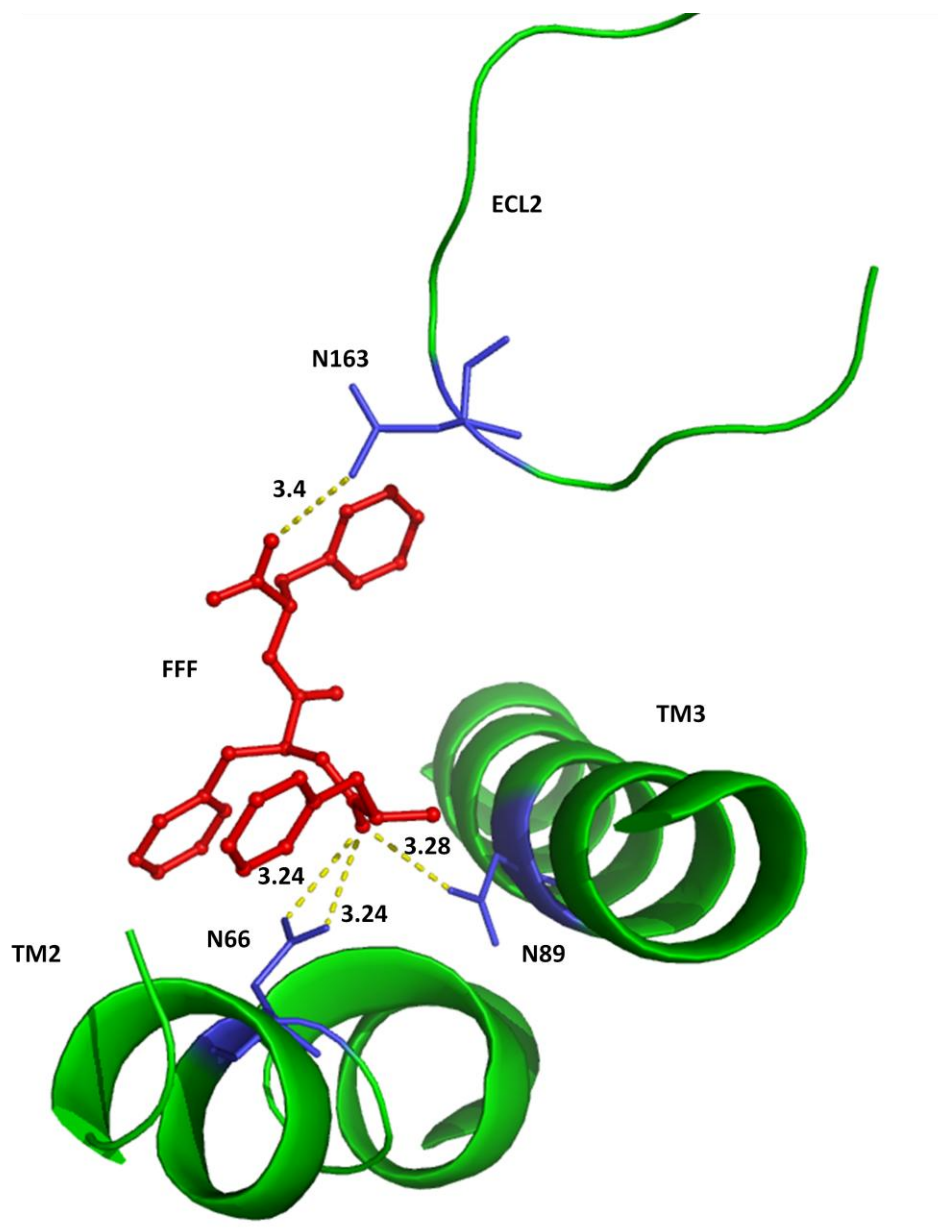
FIGURE 29. Molecular model of T2R1 bound to the tripeptide FFF. The binding-pocket residues within 4 Å distance from FFF, N66 and N89 in TM 2 and TM 3 respectively, and N163 in ECL2 are shown. The ligand FFF is rendered as sticks in red and the amino acid residues are shown as lines in blue. The two hydrogen bonds with N66 residue are at a distance of 3.24 Å each, with N89 residue at a distance of 3.28 Å and the hydrogen bond with N163 is at a distance of 3.4 Å, and shown with dotted yellow lines.
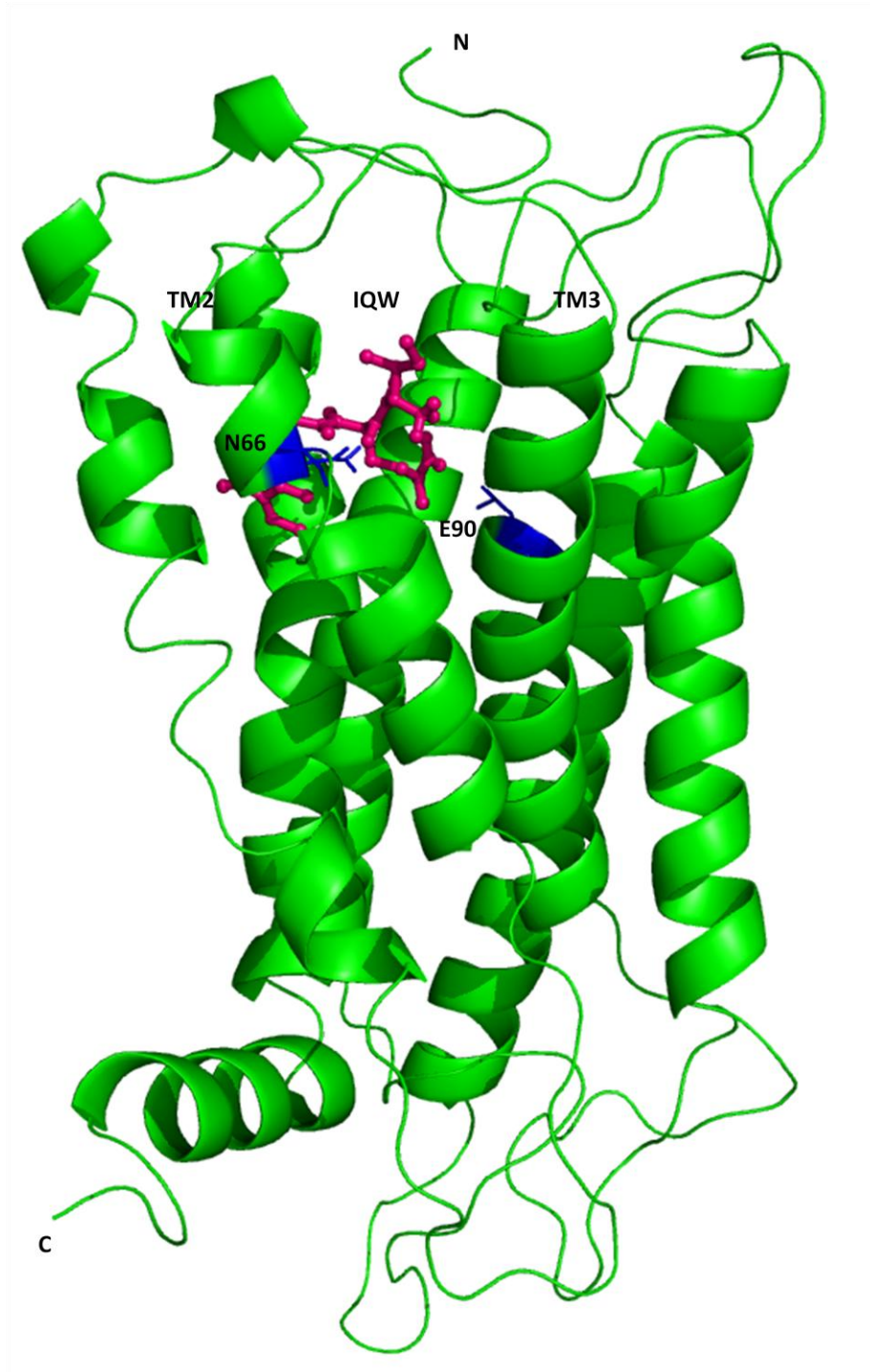
FIGURE 30. Molecular model of T2R1 bound to the tripeptide IQW. IQW was docked to the receptor using AUTODOCK VINA. The ligand is presented as sticks in pink, and the residues in contact, N66 in TM 2 and E90 in TM 3, are shown as lines in blue. N represents the N-terminus and C represents the C-terminus of the receptor.
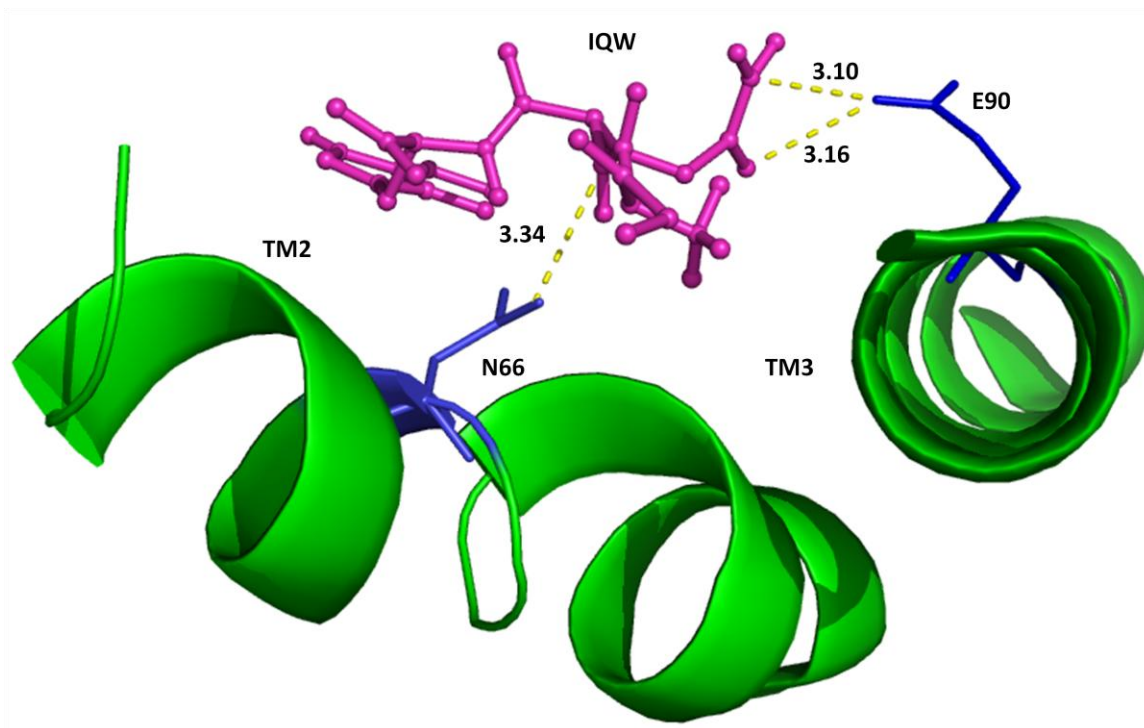
FIGURE 31. Molecular model of T2R1 bound to the tripeptide IQW. The binding-pocket residues within 4 Å distance from IQW, N66 and E90 in TM 2 and TM 3 respectively, are shown. The ligand IQW is rendered as sticks in pink and the residues in contact are shown as lines in blue. The hydrogen bonds are shown with dotted yellow lines. The two hydrogen bonds with E90 residue are at a distance of 3.10 Å and 3.16 Å, and the hydrogen bond with N66 residue is at a distance of 3.34 Å.
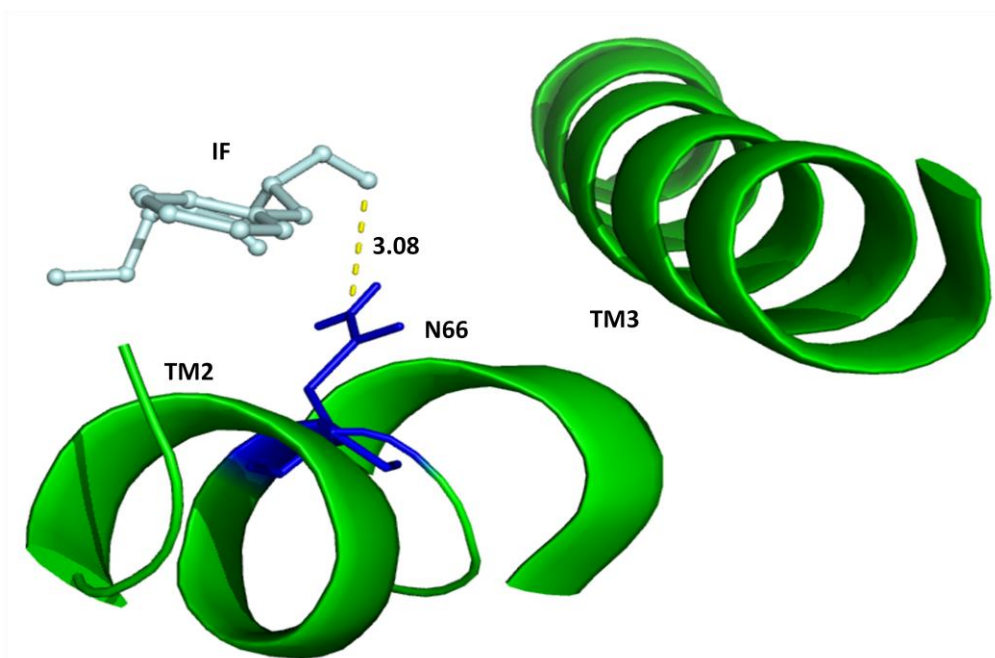
FIGURE 32. Molecular model of T2R1 bound to the dipeptide IF. The binding-pocket residue within 4 Å distance from IF, N66 in TM 2, is shown. The ligand IF is rendered as sticks in light blue and the residue in contact is shown as lines in dark blue. The hydrogen bond with N66 residue which is at a distance of 3.08 Å is shown with dotted yellow lines.
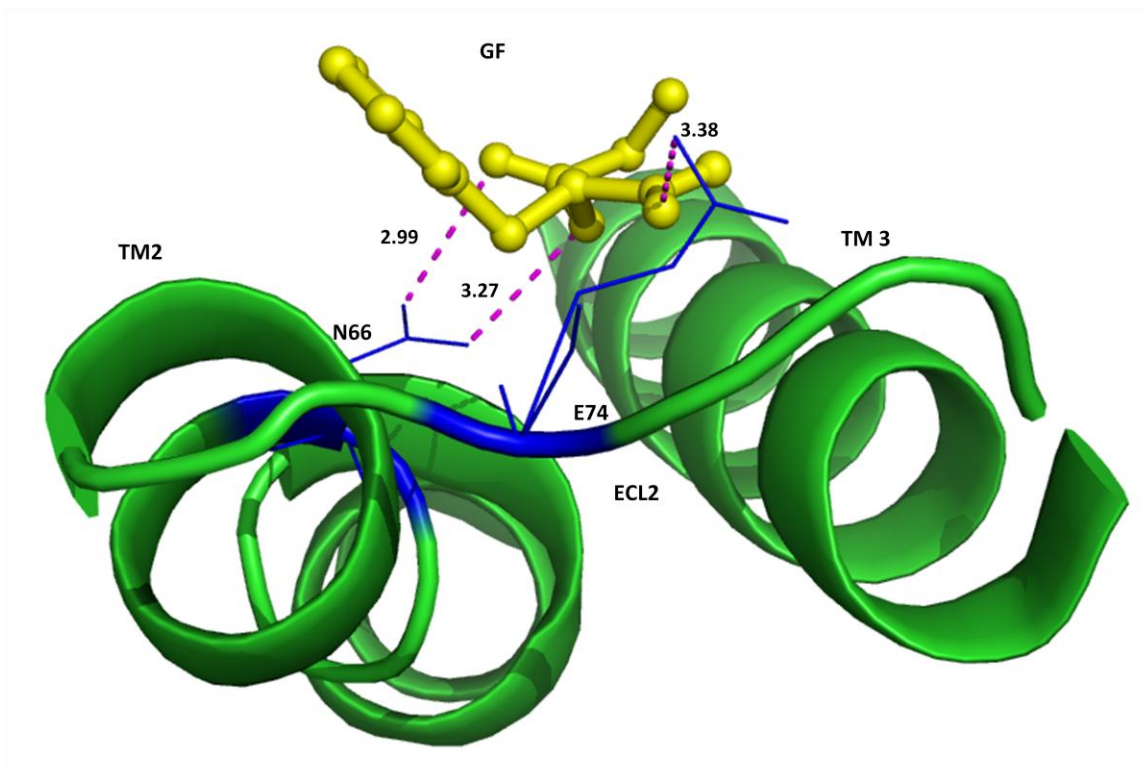
FIGURE 33. Molecular model of T2R1 bound to the dipeptide GF. The binding-pocket residues within 4 Å distance from GF, N66 in TM 2 and E74 in ECL2, are shown. The ligand GF is rendered as sticks in yellow and the residues in contact are shown as lines in blue. The two hydrogen bonds with N66 residue are at a distance of 2.99 Å and 3.27 Å, and the one with E74 is at a distance of 3.38 Å and are shown with dotted lines.
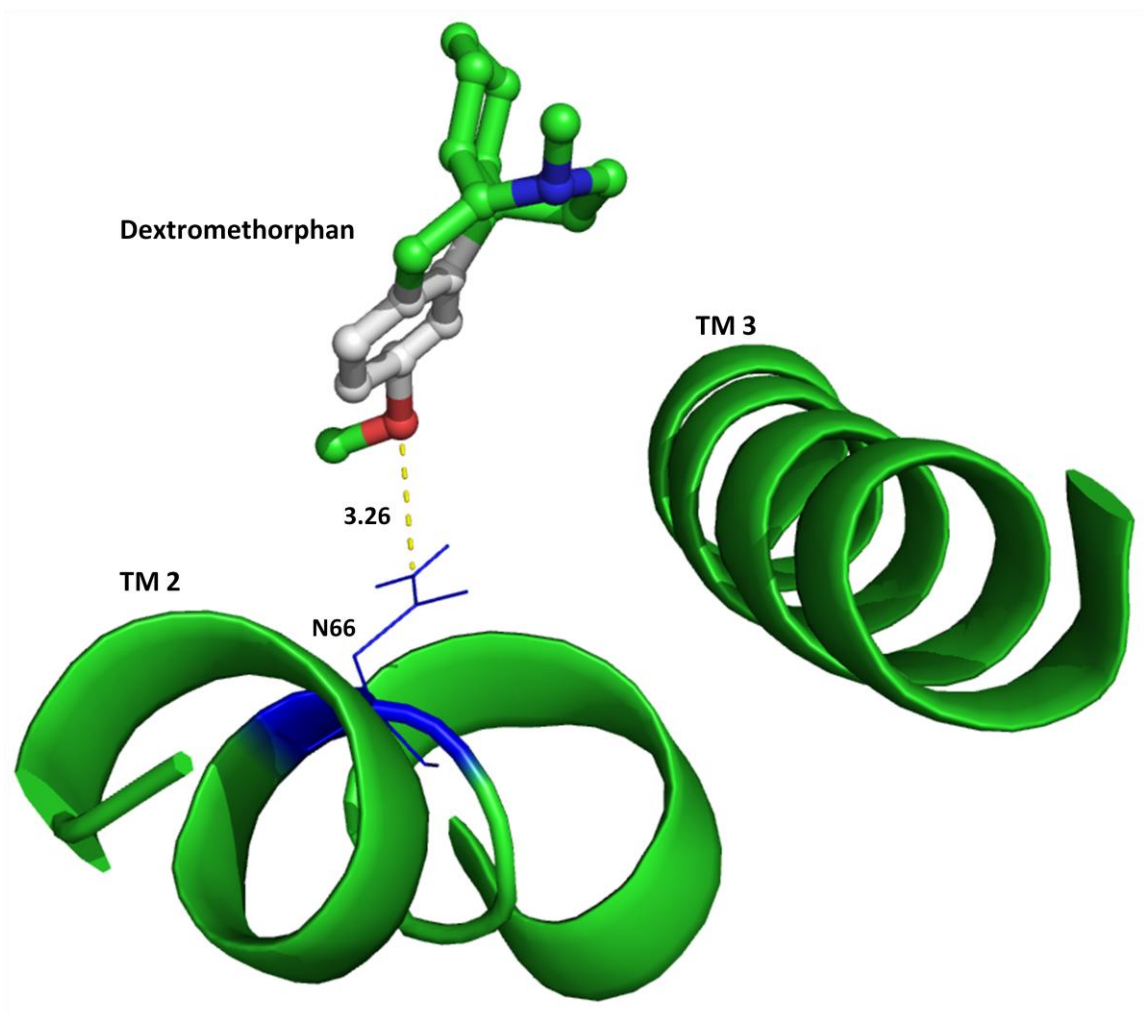
FIGURE 34. Molecular model of T2R1 bound to the bitter compound dextromethorphan. The binding-pocket residue within 4 Å distance from dextromethorphan, N66 in TM 2, is shown here. The ligand is rendered as sticks in green and grey and the residue in contact is shown as lines in blue. The hydrogen bond with N66 residue is at a distance of 3.26 Å and is shown with dotted lines.

Figure 28. The amino acids in the ligand binding pocket in proximity to the ligand within 4 Å are listed in table V. The amino acid residues on T2R1 proposed to be involved in the interaction with FFF are N66 in TM 2, N89 in TM 3 and N163 in ECL2. The two hydrogen bonds with N66 were measured to be at distances of 3.24 Å each, with N89 residue at a distance of 3.28 Å and N163 at a distance of 3.4 Å (Figure 29).

The predicted location of the potential binding site for IQW with T2R1 is shown in Figure 30. Amino acids in proximity to the ligand within 4 Å are listed in table V. The residues proposed to interact with the ligand are N66 in TM 2 and E90 in TM 3. Two hydrogen bonds with E90 residue are at distances of 3.10 Å and 3.16 Å, whereas the hydrogen bond with N66 is at a distance of 3.34 Å (Figure 31).

The only residue in the ligand binding pocket of T2R1 found to interact with the dipeptide IF was N66 in TM 2 (Figure 32). The hydrogen bond formed with this residue was measured to be at a distance of 3.08 Å. The dipeptide GF interacted with residues in TM 2 and ECL2 of the receptor. It formed hydrogen bonds with N66 in TM 2 and with E74 in ECL2 at distances of 2.99 Å, 3.27 Å and 3.38 Å respectively (Figure 33). Dextromethorphan interacted with only N66 residue in TM 2 of the receptor (Figure 34).

CHAPTER FOUR
DISCUSSION

4.1. Expression of T2R1

The localization of T2R1-rho1D4 at the cell surface of HEK293S-tetR and rat C6 glial cells was confirmed by immunofluorescent staining. Immunoblot analysis of T2R1-containing cell membranes showed that it is expressed as three major protein bands, which may be explained by the presence of a positionally conserved consensus site for Asn-linked glycosylation (NXS/T) in the center of the second extracellular loop in all 25 members of the hT2R family (Meyerhof, 2005; Figure 10). This consensus site has been predicted to play an important role in hT2R biosynthesis and/or function (Reichling et al, 2008). Dimer formation, observed at 64 kDa for T2R1, is a characteristic feature of most of the family A GPCRs (Kota et al, 2006; Fotiadis et al, 2003; Liang et al, 2003). Recent studies have shown that like many GPCRs, T2Rs are capable of forming oligomers *in vitro* (Kuhn et al, 2010). Although a physiological significance of the receptor oligomerization is not obvious, it might be considered necessary for receptor function.

To improve the expression level of T2R1-rho1D4 for pursuing biophysical studies such as NMR spectroscopy and protein crystallization, the synthetic gene was expressed in a tetracycline-inducible HEK293S stable cell line. A tetracycline-inducible stable mammalian cell line was selected for overexpression of the gene because the use of

this inducible system for high-level expression of two GPCRs, rhodopsin and β_2-adrenergic receptor, has been reported previously (Reeves et al, 2002; Chelikani et al, 2006). This system is particularly suited for overcoming problems with toxicity either due to the addition of toxic compounds to the growth medium or due to the expressed protein products. Transient expression of the synthetic T2R1 gene in HEK293 cells yielded 9 ng of membrane protein per 10-cm tissue culture plate. Using the HEK293S-tetR stable cell line, after induction with tetracycline and sodium butyrate, T2R1 was expressed at levels of 60-70 ng of membrane protein, which is 7-8 fold higher than the level of protein observed following transient expression of T2R1.

The T2R1-rho38 construct could not be detected by immunoblot and immunofluorescent staining due to poor binding or detection by the available goat polyclonal primary antibody rho-S17, which recognizes the mouse rhodopsin tag at the N-terminus of T2R1.

4.2. Functional characterization of T2R1 expressed in glial cells

Reverse transcriptase-PCR analysis confirmed the expression of the transiently-transfected T2R1 constructs in glial cells, with no expression of native T2R1 receptor observed. In addition, both the transiently transfected genes were expressed at similar levels (Figure 15). Localization of the expressed T2R1 genes at the plasma membrane of glial cells was confirmed by immunofluorescence microscopy (Figure 16). Previous studies involving T2R chimeras with N-terminal rhodopsin export-tags have shown T2Rs to be localized at the plasma membrane (Chandrashekhar et al, 2000; Bufe et al, 2002; Behrens et al, 2004). Though localization of rho38 construct could not be detected by the

goat polyclonal antibody, based on published data, it was assumed to be localized at the cell surface. Having demonstrated that transient transfection of the T2R1 genes was successful and the expressed proteins were localized to the cell surface, I wanted to investigate if these receptors are functional and the addition of peptides induces a functional response in T2R1-expressing glial cells. Stimulation with different synthetic peptides elicited a rapid increase in $[Ca^{2+}]_i$. Both T2R1 constructs showed similar functional responses to the synthetic peptides and dextromethorphan.

Based on their functional potencies, the ligands may be classified into two groups:-

The first group is comprised of ligands which are highly potent in activating T2R1, like phe-phe-phe (FFF) and dextromethorphan. The tripeptide FFF consists of hydrophobic amino acids with phenyl groups which are considered significant for causing bitter taste (Matoba et al, 1972). L-phenylalanine exhibits a slightly bitter taste with a threshold value of 20 mM, while D-phenylalanine exhibits a sweet taste with a threshold value of 2.2 mM. However, a 100 times greater bitterness than that of phenylalanine has been observed in the taste of tri-phenylalanine. The bitter taste of the peptide is more apparent when the hydrophobic amino acid is located at the C-terminus (Ishibashi et al, 1987b). For the tripeptides, the middle amino acid residue is considered more important than both the C- and N-terminal amino acids residues (Wu et al, 2007). Among all the tested peptides, FFF activated T2R1-expressing cells at concentrations (0.125 - 1 mM) that humans also perceive as bitter, with an EC_{50} value of 0.37 mM.

The bitter compound dextromethorphan also falls in the group of high potency bitter ligands that activate T2R1. Previous functional studies showed that T2R1-

expressing HEK293 cells were activated by dextromethorphan at a threshold concentration of 10 µM (Meyerhof et al, 2010). However, Meyerhof et al did not calculate the EC50 value as the calcium responses generated in their control cells were high at high concentrations of the ligand. Glial cells have low basal noise, and thus T2R1 activation could be tested with five different concentrations from 8.6 µM to 133.3 µM, showing half maximal response of the receptor at 31 µM.

The second group encompasses peptides of medium potency, and includes dipeptides GF, FL, IF and tripeptides GLL, LKP and IQW. Tri-peptides have been found to be more potent than the dipeptides which can be explained by the fact that bitterness of peptides is intensified as the number of amino acids in the peptide chain increases (Ishibashi et al, 1987a; 1987b). LKP and IQW peptides saturated the receptor with 10-15 mM, whereas signal saturation with other di- and tri-peptides was observed with 15-20 mM. At concentrations of LKP and IQW above 15 mM, a decrease in the signal was noticed due to a nonspecific inhibitory effect of the peptides in the assay. Alternatively, this might be due to adaptation or desensitization of the receptor with higher concentrations of the peptides. Concentration ranges that span two orders of magnitude are often seen for hT2Rs and their agonists. This was also seen with the peptides used in this study, as T2R1 was half maximally activated by micromolar concentrations of high potency ligands and by millimolar concentrations of medium potency peptides.

Some T2Rs, like T2R4 and T2R54, when expressed in Sf9 cells were shown to have very high basal activity and were found in a constitutively active conformation in Sf9 generated membranes (Pronin et al, 2004). In the absence of any peptide or bitter

compound, T2R1 displayed low basal activity.

Among the tested peptides, FFF was the most potent to activate T2R1. Its bitterness is imparted by the presence of hydrophobic phenyl groups. Based on the functional potencies, FFF was followed by GLL, IQW, LKP and the dipeptides. Glycine residue in GLL is tasteless, thus bitterness of the tripeptide would be imparted by the presence of two hydrophobic residues. Stimulation of T2R1 with GLL showed a calcium release of 40-50 nM with an EC_{50} of 4.9 mM. GLL has similar sensory bitter threshold value as the dipeptides, but the concentration required to induce its half maximal response for T2R1 activation is less. This can be explained by the addition of an extra hydrophobic residue (leucine) at the C-terminus of the peptide. Phenyl groups in phenylalanine (FFF) and the imino rings in proline (LKP) had been recognized as bitter taste determinant sites in bitter peptides (Maehashi et al, 2009). But the role of proline residue in the bitter taste of a peptide is different from that of a hydrophobic amino acid. The most significant role of proline residue proposed in peptide bitterness was conformational alteration of the peptide molecule by folding of the peptide due to the imino ring of the proline residue. This ensured that the peptide molecule could form a suitable conformation for the bitter taste receptor. The bitterness of tripeptides was enhanced when proline was intercalated between two hydrophobic residues (Ishibashi et al, 1988). LKP had a basic amino acid, lysine, intercalated between a hydrophobic residue, leucine, and proline at the C-terminus. The bitterness of such tripeptides was considered to be less intense. This aspect may be compatible with the EC_{50} of 7.6 mM for LKP.

The theoretically calculated binding affinities for high potency ligands, FFF and dextromethorphan, are quite high and almost similar (Figure 35). Their EC_{50} values are in micromolar range and suggest that these ligands are very potent. The binding affinity for IQW is similar to that of high potency ligands, but the EC_{50} falls in millimolar (6mM) range. The two values are not in agreement with each other, which suggests that IQW can be a partial or inverse agonist of T2R1. The low binding energies of the dipeptides can partly explain their EC_{50} values in millimolar concentrations. Although the concentration range for some of the peptides needed for detectable activation of T2R1 in calcium imaging assay is higher than the reported 'bitter threshold' in humans, this discrepancy can be due to the observation that sensory detection thresholds are often much lower than those observed in heterologous assays. For example, the reported bitterness threshold for denatonium to activate T2R4 receptor is 100 µM (Chandrashekhar et al, 2000), which is over two orders of magnitude higher than the human psychophysical threshold for denatonium (Saroli, 1984).

4.3. Mapping the ligand-binding pocket of T2R1

The amino acid residues on T2R1 involved in interaction with some of the tested ligands were proposed (Table V) after docking them using AutoDock Vina software. The ligand-binding pocket of the receptor comprises of TM1, TM2, TM3, TM7, ECL1 and ECL2 regions (Figure 36). The amino acids involved in making polar contacts were in TM2, TM3, ECL1 and ECL2. The amino acid residue N66 in TM2 formed hydrogen bonds with all the docked ligands, FFF, IQW, GF, IF and dextromethorphan. Other
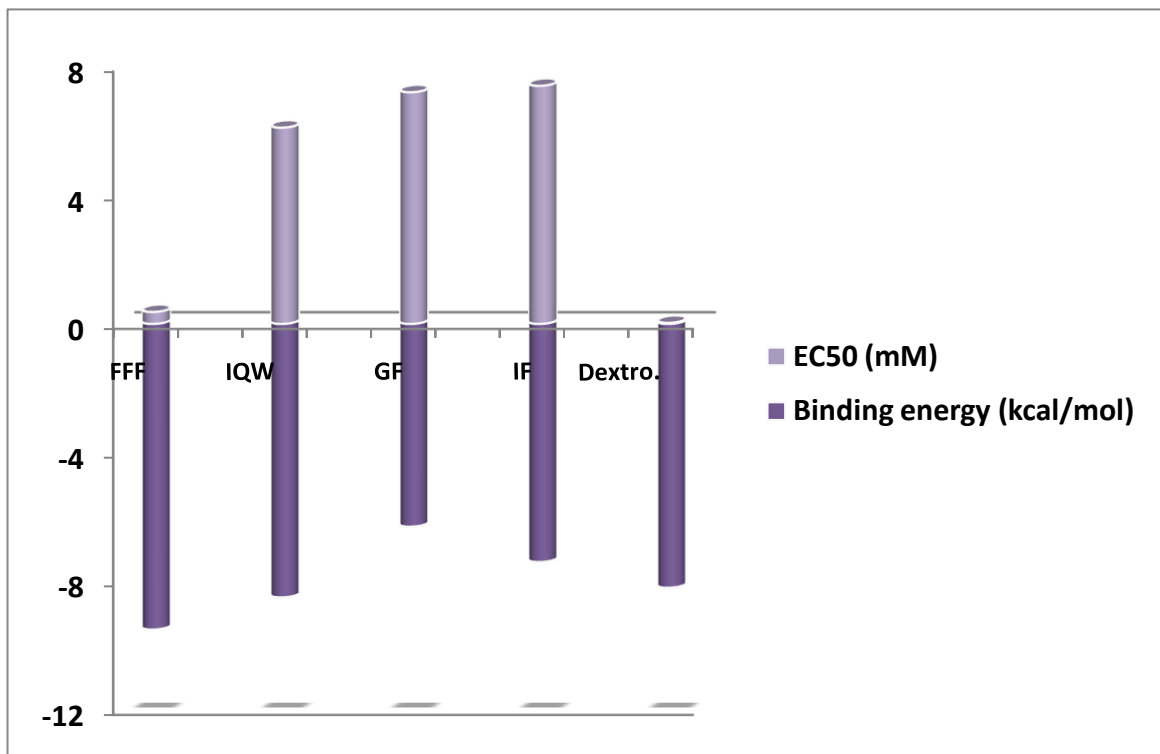
FIGURE 35. Calculated binding affinities (kcal/mol) and EC$_{50}$ values for FFF, IQW, GF, IF and dextromethorphan. The ligands were docked to T2R1 receptor using Autodock Vina. The EC$_{50}$ values were calculated from the calcium dose-response functional assay data using Graphpad Prism 5.0.

residues within 4 Å of the ligand were N89 in TM3 and N163 in ECL2 with FFF, E90 in TM3 with IQW and E74 in ECL1 with GF. Thus results from the modeling studies emphasize the role of TM2 and TM3 in T2R1 receptor function. The majority of studies on the activation mechanisms of 7TM receptors have focussed on TM segments 3 through 7. Structure-activity studies on a range of family A GPCRs suggest that TM2 has important functions for both ligand-dependent and -independent activation of 7TM receptors (Benned-Jensen and Rosenkilde, 2009). The number of residues making contact with the ligand varied depending on the orientation of bound ligand and the chemical structure, hydrophobicity and bulkiness of the peptides. The tripeptide FFF being both bulkier and hydrophobic interacted with residues in ECL2 and TMs 2 and 3. IF and dextromethorphan interacted only with N66 residue in TM2.

4.4. Future studies

A number of opportunities for further experimentation arise from the study presented here. Enormous progress in the deorphanization of hT2R receptors was achieved during recent years, but how these bitter taste receptors interact with bitter tastants is poorly understood. In my study, although the interaction of amino acid residues on TM2, TM3, ECL1 and ECL2 of T2R1 receptor with the bitter ligands is supported by modeling data, the role of these residues in bitter taste receptor-ligand interaction requires more investigation. Thus, targeting the residues, like N66, N89, E90 etc., which have been shown to interact with bitter ligands for site-directed mutational
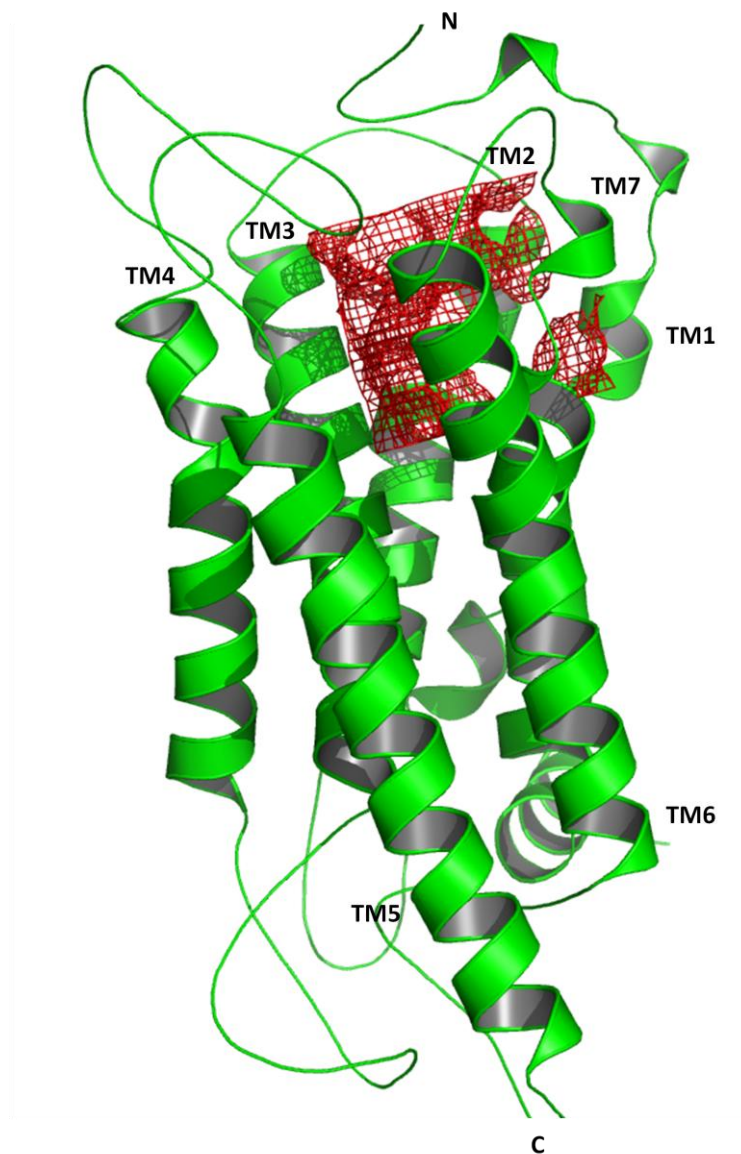
FIGURE 36. The predicted ligand-binding pocket of T2R1 for the bitter peptides, FFF, IQW, GF and IF, and the bitter compound dextromethorphan. The pocket is formed by TMs 1, 2, 3 and 7 and the ECLs 1 and 2, and is presented as a mesh. The binding pocket was predicted by docking the T2R1 receptor with different ligands using AutoDock Vina. For each ligand, 50 genetic algorithm runs were performed, and for each run the best pose was saved. Finally all the best poses of each run were superimposed and the most frequent orientation of the ligand was taken as the final pose.

studies can provide valuable insights into the mechanism of bitter taste perception. Like most GPCRs, the native T2Rs are expressed at very low levels. For proper cell surface functional expression, the first 20 to 38 amino acids of bovine or mouse rhodopsin are placed in frame with 5'-end of the T2R sequence. A second way of improving the expression of GPCRs is optimal usage of the most frequently used codons in mammals, which has been done for the T2R1-rho1D4 construct in my study. To investigate the role of different lengths of these N-terminal export tags in functional expression of T2R1 would be an interesting aspect for further experimentation. Moreover, changes in intracellular calcium upon receptor activation vary from one transfection to another and in part are affected by conditions such as cell viability, transfection efficiency etc. This inconsistency may be reduced if the receptor is expressed in a stable expression system. Thus the construction of CHO-K1 or HEK293 stable cell lines expressing T2R1 might be a useful tool in making the calcium changes between individual functional assays more consistent.

5. LITERATURE REFERENCES:-

Adler, E., Hoon, M.A., Mueller, K.L., Chandrashekhar, J., Ryba, N.J.P., and Zuker, C.S. (2000) A novel family of mammalian taste receptors. *Cell* **100**, 693-702.

Babcock, G.J., Mirzabekov, T., Wojtowicz, W., and Sodroski, J. (2001) Ligand binding characteristics of CXCR4 incorporated into paramagnetic proteo-liposomes. *J. Biol. Chem.* **276**, 38433-38440.

Bachmanov, A.A., and Beauchamp, G.K. (2007) Taste receptor genes. *Annu Rev Nutr* **27**, 389-414.

Baker, E.K., Colley, N.J., and Zuker, C.S. (1994). The cyclophilin homolog NinaA functions as a chaperone, forming a stable complex in vivo with its protein target rhodopsin. *EMBO J.* **13**, 4886–4895.

Behrens, M., Brockhoff, A., Kuhn, C.,Bufe, B., Winnig, M., and Meyerhof, W. (2004) The human taste receptor hTAS2R14 responds to a variety of different bitter compounds. *Biochem. Biophys. Res. Commun.* **319**, 479-85.

Behrens, M., and Meyerhof, W. (2006) Bitter taste receptors and human bitter taste perception. *Cell Mol. Life Sci.* **63**, 1501-9.

Beidler, L.M., and Smallman, R.L. (1965) Renewal of cells within taste buds. *J. Cell. Biol.* **27**, 263-272.

Belitz, H.D., and Wieser H. (1985) Bitter compounds: occurrence and structure-activity relationship. *Food Rev Int.* **1**, 271-354.

Benned-Jensen, T., and Rosenkilde, M.M. (2009) The role of transmembrane segment II in 7TM receptor activation. *Curr Mol Pharmacol* **2**, 140-8.

Biere, A., Marak, H.B., and van Damme, J.M. (2004) Plant chemical defense against herbivores and pathogens: generalized defense or trade offs? *Oecologia* **140**, 430-441.

Bradel-Tretheway, B.G., Zhen, Z., and Dewhurst, S. (2003) Effects of codon-optimization on protein expression by the human herpesvirus 6 and 7 U51 open reading frame. *J. Virol. Methods* **111**, 145-156.

Brockhoff, A., Behrens, M., Appendino, G., Kuhn, C., and Meyerhof, W. (2006) Identification of agonist interaction sites in the human bitter taste receptor hTAS2R46. *Chem. Senses* **31**, E55.

Bufe, B., Hofmann, T., Krautwurst, D., Raguse, J.D., and Mewerhof W. (2002) The human TAS2R16 receptor mediates bitter taste in response to beta-glucopyranosides. *Nat Genet.* **32**, 397-401.

Chandrashekhar, J., Mueller, K.L., Hoon, M.A., Adler, E., Feng, L., Guo, W., Zuker, C.S., and Ryba, N.J. (2000) T2Rs function as bitter taste receptors. *Cell* **100**, 703-11.

Chandrashekhar, J., Hoon, M.A., Ryba, N.J.P., and Zuker, C.S. (2006) The receptors and cells for mammalian taste. *Nature* **444**, 288-294.

Chandrashekhar, J., Yarmolinsky, D., von Buchholtz, L., Oka, Y., Sly, W., Ryba, N.K., and Zuker, C.S. (2009) The taste of carbonation. *Science* **326**, 443-5.

Chaudhari, N., Landin, A.M., and Roper, S.D. (2000) A metabotropic glutamate receptor variant functions as a taste receptor. *Nat. Neurosci.* **3**, 113-119.

Chelikani, P., Reeves, P.J., Rajbhandary, U.L., and Khorana, H.G. (2006) The synthesis and high-level expression of a beta2-adrenergic receptor gene in a tetracycline-inducible stable mammalian cell line. *Protein Sci* **15**, 1433-1440.

Clapp, T.R., Stone, L.M., Margolskee, R.F. and Kinnamon, S.C. (2001) Immunocytochemical evidence for co-expression of Type III IP$_3$ receptor with signalling components of bitter taste transduction. *BMC Neurosci* **2**, 6.

Conte, C., Ebeling, M., Marcuz, A., Nef, P., and Andres-Barquin, P.J. (2002) Identification and characterization of human taste receptor genes belonging to the TAS2R family. *Cytogenet. Genome Res.* **98**, 45-53.

Dwyer, N.D., Troemel, E.R., Sengupta, P., and Bargmann, C.I. (1998). Odorant receptor localization to olfactory cilia is mediated by ODR-4, a novel membrane-associated protein. *Cell* **93**, 455–466.

Ellgaard, L., and Helenius, A. (2003) Quality control in the endoplasmic reticulum. *Nat Rev Mol Cell Biol* **4**, 181-191.

Farrens, D.L., Dunham, T.D., Fay, J.F., Dews, I.C., Caldwell, J., and Nauert, B. (2002) Design, expression, and characterization of a synthetic human cannabinoid receptor and cannabinoid receptor/G-protein fusion protein. *J. Pept. Res.* **60**, 336-347.

Finger, T.E., Bottger, B., Hansen, A., Anderson, K.T., Alimohammadi, H., and Silver, W.L. (2003) Solitary chemoreceptor cells in the nasal cavity serve as sentinels of respiration. *Proc. Natl. Acad. Sci. USA* **100:** 8981–8986.

Finger, T.E. (2005a) Cell types and lineages in taste buds. *Chem Senses* **30**, 54-55.

Finger, T.E., Danilova, V., Barrows, J., Bartel, D.L., Vigers, A.J., Stone, L. (2005b) ATP signaling is crucial for communication from taste buds to gustatory nerves. *Science* **310**, 1495-9.

Fiser, A., Do, R.K., and Sali, A. (2000) Modeling of loops in protein structures. *Protein Sci.* **9**, 1753-73.

Fotiadis, D., Liang, Y., Filipek, S., Saperstein, D.A., Engel, A., and Palczewski, K. (2003) Atomic-force microscopy: Rhodopsin dimers in native disc membranes. *Nature* **421**, 127-128.

Frank, O., and Hofmann, T. (2002). Reinvestigation of the chemical structure of bitter-tasting quinizolate and homoquinizolate and studies on their Maillard-type formation pathways using suitable (13)C-labeling experiments. *J. Agric. Food Chem.* **50**, 6027-6036.

Fredriksson, R., Lagerstrom, M.C., Lundin, L.G., and Schioth, H.B. (2003) The G-protein-coupled receptors in the human genome form five main families. Phylogenetic analysis, paralogon groups, and fingerprints. *Mol. Pharmacol.* **63**, 1256-72.

Friedrichs, M.S., Eastman, P., Vaidyanathan, V., Houston, M., LeGrand, S., Beberg, A.L., Ensign, D.L., Bruns, C.M., and Pande, V.S. (2009) Accelerating molecular dynamic simulation on graphics processing units. *J Comput Chem.* **30**, 864-72.

Gilbertson, T.A., Avenet, P., Kinnamon, S.C., and Roper, S.D. (1992) Proton currents through amiloride-sensitive Na channels in hamster taste cells. Role in acid transduction. *J Gen Physiol* **100**, 803-24.

GPCRDB. *Information system for G protein-coupled receptors (GPCRs)*. Accessed March 27, 2007. GPCRDB Inform. Syst. http://www.gpcr.org/7tm/.

Guigoz, Y., and Solms, J. (1976) Bitter peptides, occurrence and structure. *Chem. Senses Flavor* **2**, 71-84.

Heck, G.L., Mierson, S., and DeSimone, J.A. (1984). Salt taste transduction occurs through an amiloride-sensitive sodium transport pathway. *Science* **223**, 403-405.

Hoon, M.A., Adler, E., Lindemeier, J., Battey, J.F., Ryba, N.J. and Zuker, C.S. (1999). Putative mammalian taste receptors: a class of taste-specific GPCRs with distinct topographic selectivity. *Cell* **96**, 541–551.

Huang, A.L., Chen, X., Hoon, M.A., Chandrashekhar, J., Guo, W., Trankner, D., Ryba, N.J., and Zuker, C.S. (2006) The cells and logic for mammalian sour taste detection. *Nature* **442**, 934-938.

Inoue, H., Nojima, H., and Okayama, H. (1990) High efficiency transformation of Escherichia coli with plasmids. *Gene* **96**, 23-8.

Ishibashi, N., Arita, Y., Kanehisa, H., Kouge, K., Okai, H., and Fukui, S. (1987a) Bitterness of leucine-containing peptides. *Agric. Biol. Chem.* **51**, 2389-2394.

Ishibashi, N., Sadamori, K., Yamamoto, O., Kanehisa, H., Kouge, K., Kikuchi, E., Okai, H., and Fukui, S. (1987b) Bitterness of phenylalanine- and tyrosine-containing peptides. *Agric. Biol. Chem.* **51**, 3309-3313.

Ishibashi, N., Kubo, T., Chino, M., Fukui, H., Shinoda, I., Kikuchi, E., Okai, H., and Fukui, S. (1988) Taste of proline-containing peptides. *Agric Biol Chem* **52**, 95-98.

Iwasaky, K., Kasahara, T., and Sato, M. (1985) Gustatory effectiveness of amino acids in mice: behavioral and neurophysiological studies. *Physiol Behav* **34**, 531-42.

Kawamura, A.A. in *Olfaction and Taste II*, Hayashi, T., Ed. (Pergamon, New York, 1967) pp. 431-437.

Kawamura, Y., and Kare, M. (1987) Introduction to Umami: a basic taste. (New York: Dekker)

Khorana, H.G. (1992) Rhodopsin, photoreceptor of the rod cell. An emerging pattern for structure and function. *J. Biol. Chem.* **267**, 1-4.

Kim, D.J., and Roper, S.D. (1995) Localization of serotonin in taste buds: a comparative study in four vertebrates. *J. Comp.Neurol*. **353**, 364-370.

Kim, U.K., Breslin, P.A., Reed, D., and Drayna,D. (2004) Genetics of human taste perception. *J Dent Res* **83**, 448-453.

Kinnamon, S.C., Dionne, V.E., and Beam, K.G. (1988) Apical localization of K^+ channels in taste cells provides the basis for sour taste transduction. *Proc. Natl. Acad. Sci. USA* **85**, 7023-7027.

Kinnamon, S.C., and Cummings, T.A. (1992) Chemosensory transduction mechanisms in taste. *Annu. Rev. Physiol.* **54**, 715-731.

Kitagawa,M., Kusakabe, Y., Miura, H., Ninomiya, Y, and Hino, A. (2001) Molecular genetic identification of a candidate taste receptor gene for sweet taste. *Biochem. Biophys. Res. Commun.* **283**, 236-42.

Komai, M., Bryant, B.P., Takeda, T., Suzuki, H, Kimura, S. in *Olfaction and Taste XI*, Kurihara, K., Suzuki, N., Ogawa, H., Eds. (Springer-Verlag, Tokyo, 1994) pp. 92.

Kota, P., Reeves, P.J., Rajbhandary, U.L., and Khorana, H.G. (2006) Opsin is present as dimers in COS1 cells: Identification of amino acids at the dimeric interface. *Proc Natl Acad Sci U S A.* **103,** 3054-3059.

Krautwurst, D., Yau, K.W., and Reed, R.R. (1998). Identification of ligands for olfactory receptors by functional expression of a receptor library. *Cell* **95**, 917–926.

Krivov, G.G., Shapovalov, M.V., and Dunbrack, R.L. Jr (2009) Improved prediction of protein side-chain conformations with SCWRL4. *Proteins* **77**, 778-95.

Kuhn, C., Bufe, B., Batram, C., and Meyerhof, W. (2010) Oligomerization of TAS2R bitter taste receptors. *Chem Senses* **35**, 395-406.

Kunishima, N.et al. (2000) Structural basis of glutamate recognition by a dimeric metabotropic glutamate receptor. *Nature* **407**, 971–977.

Lander, E.S., Linton, L.M., Birren, B., Nusbaum, C., Zody, M.C., Baldwin, J., Devon, K., Dewar, K., Doyle, M., FitzHugh, W., et al. (2001) The International Human Genome Sequencing Consortium. Initial sequencing and analysis of the human genome [published erratum appears in *Nature* **412:**565, 2001]. *Nature (Lond)* **409:**860–921.

Laskowski, R.A., MacArthur, M.W., Moss, D.S., Thornton, J.M., (1993) PROCHECK: a program to check the stereochemical quality of protein structures. *J. Appl. Cryst.* **26,** 283-291.

Laugerette, F., Passilly-Degrace, P., Patris, B. et al (2005) CD36 involvement in orosensory detection of dietary lipids, spontaneous fat preference, and digestive secretions. *J Clin Invest* **115**, 3177-3184.

Lawton, D.M., Furness, D.N., Lindemann, B. and Hackney, C.M. (2000) Localization of the glutamate–aspartate transporter, glast, in rat taste buds. *Eur. J. Neurosci.*, **12**, 3163–3171.

Lemieux, L., and Simard, R.E. (1992) Bitter flavour in dairy products. II. A review of bitter peptides from caseins: their formation, isolation and identification, structure masking and inhibition. *Lait* **72**, 335-382.

Liang, Y., Fotiadis, D., Filipek, S., Saperstein, D.A., Palczewski, K., and Engel, A. (2003) Organization of the G protein-coupled receptors rhodopsin and opsin in native membranes. *J. Biol. Chem.* **278**, 21655-21662.

Lindemann, B. (2001) Receptors and transduction in taste. *Nature* **413**, 219-25.

Lovsin-Kukman, I., Zelenik-Blatnik, M., and Abram, V. (1996) Bitterness intensity of soybean protein hydrolysates – chemical and organoleptic characterization, *Lebensm, Z. Unters. Forsch.* **203**, 272-276.

Maehashi, K., Matano, M., Wang, H., Vo, L.A., Yamamoto, Y., and Huang, L. (2008) Bitter peptides activate hTAS2Rs, the human bitter receptors. *Biochem Biophys Res Commun.* **365**, 851-5.

Maehashi, K., and Huang, L. (2009) Bitter peptides and bitter taste receptors. *Cell Mol Life Sci*. **66**, 1661-71.

Matoba, T., and Hata, T. (1972) Relationship between bitterness of peptides and their chemical structures. *Agric. Biol. Chem.* **36**, 1423-1431.

Matsunami, H., Montmayeur, J.P., and Buck, L.B. (2000). A family of candidate taste receptors in human and mouse. *Nature* **404**, 601-604.

Mattes, R.D. (2001a) The taste of fat elevates postprandial triacylglycerol. *Physiol Behav* **74**, 343-8.

Mattes, R.D. (2001b) Oral exposure to butter, but not fat replacers elevates postprandial triacylglycerol concentration in humans. *J Nutr* **131**, 1491-6.

Meyerhof, W. (2005) Elucidation of mammalian bitter taste. *Rev. Physiol. Biochem. Pharmacol.* **154**, 37-72.

Meyerhof, W., Batram, C., Kuhn, C., Brockhoff, A., Chudoba, E., Bufe, B., Appendino, G., and Behrens, M. (2010). The molecular receptive ranges of human TAS2R bitter taste receptors. *Chem Senses* **35**, 157-170.

Miyoshi, M.A., Abe, K. and Emori, Y. (2001). IP(3) receptor type 3 and PLCbeta2 are co-expressed with taste receptors T1R and T2R in rat taste bud cells. *Chem. Senses* **26**, 259–265.

Montmayeur, J.P., Liberles, S.D., Matsunami, H., and Buck, L.B. (2001) A candidate taste receptor gene near a sweet taste locus. *Nat. Neurosci.* **4**, 492-98.

Nakamura, Y., Gojobori, T., and Ikemura, T. (2000) Codon usage tabulated from international DNA sequence databases: status for the year 2000. *Nucleic acids Res.* **28**, 292.

Nelson, G.M. and Finger, T.E. (1993). Immunolocalization of different forms of neural cell adhesion molecule (NCAM) in rat taste buds. *J. Comp. Neurol.* **336,** 507–516.

Nelson, G.M. (1998) Biology of taste buds and the clinical problem of taste loss. *Anat Rec.* **253**, 70-8.

Nelson, G., Hoon, M.A., Chandrashekhar, J., Zhang, Y., Ryba, N.J., Zuker, C.S. (2001) Mammalian sweet taste receptors. *Cell* **106**, 381-90.

Nelson, G., Chandrashekhar, J., Hoon, M.A., Feng, L., Zhao, G., Ryba, N.J., and Zuker, C.S. (2002) An amino-acid taste receptor. *Nature* **416**, 199-202.

Ney, K.H. (1971) Prediction of bitterness of peptides from their amino-acid composition. *Z. Lebensm. Unters. Forsch.* **147**, 64-68.

Pripp, A.H., and Ardo, Y. (2007) Modelling relationship between angiotensin-(I)-converting enzyme inhibition and the bitter taste of peptides. *Food Chem* **102**, 880-888.

Pronin, A.N., Tang, H., Connor, J., and Keung, W. (2004) Identification of ligands for two human bitter T2R receptors. *Chem Senses* **29**, 583-593.

Reeves, P.J., Kim, J.M., and Khorana, H.G. (2002a) Structure and function in rhodopsin: A tetracycline-inducible system in stable mammalian cell lines for high-level expression of opsin mutants. *Proc Natl Acad Sci* **99**, 13413-8.

Reeves, P.J., Callewaert, N., Contreras, R., and Khorana, H.G. (2002b) Structure and function in rhodopsin: High-level expression of rhodopsin with restricted and homogenous N-glycosylation by a tetracycline-inducible N-acetylglucosaminyltransferase I-negative HEK293S stable mammalian cell line. *Proc. Natl. Acad. Sci.* **99**, 13419-13424.

Reichling, C., Meyerhof, W., and Behrens, M. (2008) Functions of human bitter taste receptors depend on N-glycosylation. *J Neurochem.* **106**, 1138-1148.

Sali, A., Potterton, L., Yuan, F., van Vlijmen, H., and Karplus, M. (1995) Evaluation of comparative protein modeling by MODELLER. Proteins **23,** 318-26.

Saroli, A. (1984) Structure-activity relationship of a bitter compound: denatonium chloride. *Naturwissenchaften* **71**, 428-9.

Shah, A.S., Shahar, Y.B., Moninger, T.O., Kline, J.N., and Welsh, M.J. (2009) Motile cilia of human airway epithelia are chemosensory. *Science* **325**, 1131-4.

Smith, J.C., Fisher, E.M., Maleszewski, V., and McClain, B. (2000) Orosensory factors in the ingestion of corn oil/sucrose mixtures by the rat. *Physiol Behav* **69**, 135-46.

Striem, B.J., Pace, U., Zehavi, U., Naim, M., and Lancet, D. (1989) Sweet tastants stimulate adenylate cyclase coupled to GTP-binding protein in rat tongue membranes. *Biochem. J.* **260**, 121-126.

Takahashi, A., Camacho, P., Lechleiter, J.D., and Herman, B. (1999) Measurement of intracellular calcium. *Physiol. Rev*. **79**, 1089-1125.

Takayama, H., Chelikani, P., Reeves, P.J., Zhang, S., and Khorana, H.G. (2008) High-level expression, single-step immunoaffinity purification and characterization of human tetraspanin membrane protein CD81. *Plos One* **3**, e2314.

Takeda, S., Kadowaki, S., Haga, T., Takaesu, H., and Mitaku, S. (2002) Identification of G- protein-coupled receptor genes from the human genome sequence. *FEBS Lett.* **520**, 97-101.

Trefz B. (1972) Immunochemical investigation of the modal specificity of taste. *J Dent Res.* **51**, 1203-11.

Trott, O., Olson, A.J. (2009) AutoDock Vina: improving the speed and accuracy of docking with a new scoring function, efficient optimization and multithreading. *J Comput Chem.* **31**, 455-61.

Venter, J.C., Adams, M.D., Myers, E.W., Li, P.W., Mural, R.J., Sutton, G.G., Smith, H.O., Yandell, M., Evans, C.A., Holt, R.A., et al. (2001) The sequence of the human genome [published erratum appears in *Science (Wash DC)* **292:**1838, 2001]. *Science (Wash DC)* **291:**1304–1351.

Wong, G.T., Gannon, K.S., and Margolskee, R.F. (1996) Transduction of bitter and sweet taste by gustducin. *Nature* **381**, 796-800.

Wu, J., and Aluko, R. (2007) Quantitative structure-activity relationship study of bitter di- and tri-peptides including relationship with angiotensin I-converting enzyme inhibitory activity. *J. Pept. Sci*. **13**, 63-69.

Wu, S. V., Rozengurt, N., Yang, M., Young, S. H., Sinnett-Smith, J. and Rozengurt, E. (2002) Expression of bitter taste receptors of the T2R family in the gastrointestinal tract and enteroendocrine STC-1 cells. *Proc. Natl. Acad. Sci. USA* **99**, 2392–2397.

Yang, R., Tabata, S., Crowley, H.H., Margolskee, R.F. and Kinnamon, J.C. (2000a) Ultrastructural localization of gustducin immunoreactivity in microvilli of Type II taste cells in the rat. *J. Comp. Neurol.* **425**, 139–151.

Yang, R., Crowley, H.H., Rock, M.E. and Kinnamon, J.C. (2000b) Taste cells with synapses in rat circumvallate papillae display Snap-25-like immunoreactivity. *J. Comp. Neurol.* **424**, 205–215.

Yee, C. L., Yang, R., Bottger, B., Finger, T. E. and Kinnamon, J. C. (2001) 'Type III' cells of rat taste buds: immunohistochemical and ultrastructural studies of neuron-specific enolase, protein gene product 9.5, and serotonin. *J. Comp. Neurol.* **440**, 97–108.

Yoshikawa, M., Fujita, H., Matoba, N., Takenaka, Y., Yamamoto, T., Yamauchi, R., Tsuruki, H., and Takahata, Y. (2000) Bioactive peptides derived from food proteins preventing lifestyle-related diseases. *Biofactors* **12**, 143-146.

Zancanaro, C., Sbarbati, A., Bolner, A., Accordini, C., Piemonte, G. and Osculati, F. (1995) Biogenic amines in the taste organ. *Chem. Senses* **20**, 329–335.